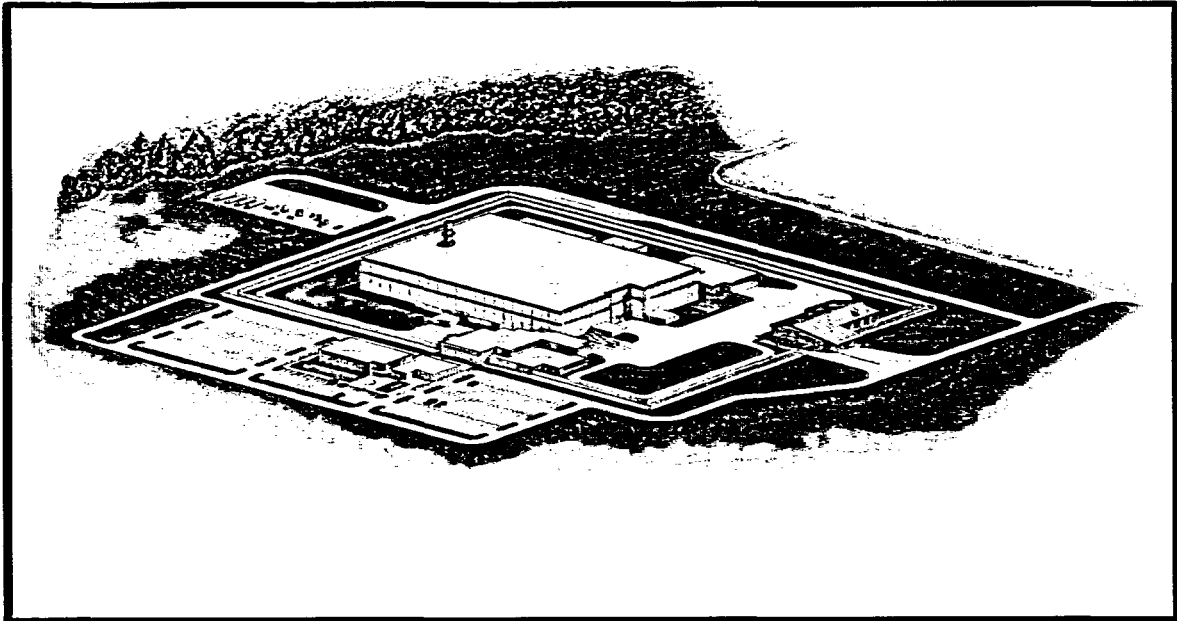


MFFF SITE GEOTECHNICAL REPORT

(DCS01-WRS-DS-NTE-G-00005-E)

June 2003



DUKE COGEMA
STONE & WEBSTER

DOE Contract
DE-AC02-99CH10888
Charlotte, NC



CONFIRMATION REQUIRED

Total Pages: 447

Yes No

MOX FUEL FABRICATION FACILITY
SITE GEOTECHNICAL REPORT

QUALITY LEVEL 1a (IROFS)

DCS01-WRS-DS-NTE-G-00005-E

APPROVALS:

Preparer: William L. Zakely *William L. Zakely* Date: 26 June 2003 Preparer: Samuel Y. Boakye *Samuel Y. Boakye* Date: 27 June 2003

Preparer: Lee Lin *Lee Lin* Date: 26 June 2003 Reviewer: N/A Date:

Discipline Reviewer: Paul J. Trudgian *Paul J. Trudgian* Date: 30 June 2003 Reviewer: N/A Date:

Compliance: N/A Date: Reviewer: N/A Date:

Design Verification Method: Design Verification Review Alternate Calculation Qualification Testing

DV: Thomas Y. Chang *Thomas Y. Chang* Date: 30 June 2003 LDE: John M. McConaghy *John M. McConaghy* Date: 30 June 2003

FDM: Roger Alley *Roger Alley* Date: 30 June 2003 QA Manager: N/A Date:

REVISION DESCRIPTION SHEET

REVISION NUMBER	PAGES REVISED AND DESCRIPTION
"A"	Original Copy.
"B"	All pages revised due to complete revision of table of contents, report text, tables, figures and Attachments to incorporate final test reports, engineering analysis and recommendations.
"C"	<p>Revisions for "C" are identified by the line in the right margin of the text or on the Table and Figure list in the Table of contents.</p> <p>No revisions were made in Attachments 1, 2, 3 and 4.</p>
"D"	<p>Table of Contents, List of Tables and Figures, and Sections 6, 7, and 8 were completely revised. Other revisions for "D" are identified by the line in the right margin of the text.</p> <p>Revision "D" was updated to incorporate data from the 2002 Supplemental Geotechnical Investigation, and with the current structure loads and stiffnesses.</p> <p>TBV – Section 7.2. Confirmation is required since foundation pressures utilized are a result of preliminary structural analysis.</p> <p>See next page for identification of sections prepared by the various preparers.</p>

DISTRIBUTION

Group	Name	Sent	Group	Name	Sent
Doc/Records					

REVISION DESCRIPTION SHEET (CONTINUED)

REVISION NUMBER	PAGES REVISED AND DESCRIPTION
<p>"E" Continued</p>	<p>Section 3 was revised by Samuel Y. Boakye to clarify discussion of the design earthquake. Other minor changes to the geology discussion were made by William L. Zakely.</p> <p>Section 4 was revised by William L. Zakely to enhance the discussion of the results of the 2002 Supplemental Geotechnical Investigation regarding defining extents of the soft zones encountered beneath the site. Additional discussion was added to clarify the numbers of borings and CPTs performed at the MFFF site and the description of the results of the downhole seismic testing that was performed during the 2000 investigation was enhanced.</p> <p>Section 5 was revised by William L. Zakely to clarify the discussion of the relationship between the engineering units and the geology at the MFFF site. Additional information regarding the groundwater regime at the site was also added based on information provided by WSRC.</p> <p>Section 6 was revised by Lee Liu to incorporate the development of the surface response spectra and the cyclic stress ratio profiles based on the individual seismic CPTs.</p> <p>Section 7 was revised by William L. Zakely to include a more thorough description of the Cam-Clay model used in the FLAC analysis and the discussion of the analyses of the postulated collapse of arched soils overlying the soft zones.</p> <p>Section 8 was revised by Samuel L. Boakye to incorporate the liquefaction and post-earthquake settlement analyses based on individual profiles defined by selected seismic CPTs and the discussion regarding surface manifestation of the post-earthquake settlements and differential settlements at the MFFF Building.</p> <p>Section 10 was revised as needed to include additional references identified in the text.</p>

DISTRIBUTION

Group	Name	Sent	Group	Name	Sent
Doc/Records					

TABLE OF CONTENTS

REVISION DESCRIPTION SHEET 2

TABLE OF CONTENTS..... 5

1. EXECUTIVE SUMMARY..... 16

2. INTRODUCTION..... 17

 2.1 PURPOSE AND SCOPE 17

3. GEOLOGY 18

 3.1 REGIONAL GEOLOGY 18

 3.1.1 Atlantic Coastal Plain Stratigraphy 18

 3.2 SOFT ZONES..... 23

 3.3 FAULTING..... 25

 3.4 SEISMOLOGY 25

 3.4.1 Earthquake History of the General Site Region 25

 3.4.2 Paleoseismic Data 26

 3.4.3 Development of the SRS Design Basis Earthquake..... 30

 3.4.4 Selection of MFFF Site Design Earthquake Motion..... 30

4. GEOTECHNICAL EXPLORATION AND TESTING PROGRAMS 32

 4.1 APPROACH 32

 4.2 METHODOLOGY 34

 4.3 SUBSURFACE INVESTIGATIONS..... 35

 4.3.1 General 35

 4.3.2 Exploration Boring Program 35

 4.3.3 Cone Penetration Tests (CPT)..... 35

 4.3.4 Dilatometer Tests 36

 4.3.5 Seismic Downhole Testing..... 36

 4.4 LABORATORY TESTING PROGRAM 37

5. SUBSURFACE CONDITIONS 39

 5.1 ENGINEERING STRATIGRAPHIC UNITS 39

 5.1.1 Subsurface Stratigraphy 39

 5.2 SOFT ZONES AND SOFT MATERIALS..... 41

 5.3 GROUNDWATER CONDITIONS..... 42

TABLE OF CONTENTS (CONTINUED)

5.3.1	Groundwater Aquifers.....	42
5.3.2	Groundwater Quality.....	43
6.	ENGINEERING PROPERTIES	45
6.1	STATIC PROPERTIES	45
6.1.1	General	45
6.1.2	CPT and SPT Field Test Results.....	45
6.1.3	Classification and Physical Property Test Results	46
6.1.4	Strength Test Results.....	46
6.1.5	Consolidation Test Results.....	47
6.1.6	Soft Zone Engineering Properties	48
6.1.7	Engineered Select Structural Fill.....	49
6.2	DYNAMIC PROPERTIES	49
6.2.1	Shear Wave Velocities	49
6.2.2	Dynamic Poisson's Ratio	52
6.2.3	One-Dimensional Free-Field Site Response Analyses.....	53
7.	ENGINEERING EVALUATION.....	59
7.1	FOUNDATION DESIGN CRITERIA.....	59
7.2	FOUNDATION PREPARATION.....	59
7.3	BEARING CAPACITY	60
7.4	SETTLEMENT.....	61
7.4.1	General	61
7.1.2	Conventional Settlement Analysis	62
7.1.3	FLAC Settlement Analysis.....	62
8.	STABILITY OF SUBSURFACE MATERIALS.....	75
8.1	LIQUEFACTION	75
8.1.1	Methodology	75
8.1.2	Liquefaction Results for the Generalized Soil Profile	79
8.1.3	Summary of Liquefaction Analyses for the Generalized Soil Profile.....	84
8.1.4	Liquefaction Results for the Soil Profiles Based on Individual SCPT	84
8.1.5	Summary of Liquefaction Results Based on Individual SCPT	85

TABLE OF CONTENTS (CONTINUED)

8.2	POST-EARTHQUAKE SETTLEMENT	85
8.2.1	Settlement Due to Dissipation of Excess Pore Pressure Buildup from Seismic Loadings	86
8.2.2	Additional Post-Earthquake Settlements for CPT Soundings that Hit Refusal Before Penetrating the ST2 Layer.....	87
8.2.3	Settlement Due to Consolidation of Soft Zone Soils as a Result of Earthquake-Induced Increase in Overburden Pressures.....	87
8.2.4	Results of Post-Earthquake Settlement Analyses for the Generalized Soil Profile.....	89
8.2.5	Results of Post-Earthquake Settlement Analyses for the Individual Soil Profile.....	94
8.2.6	Summary of Post-Earthquake Settlement Analyses.....	94
8.2.7	Static and Post-earthquake Settlement	96
8.3	SOFT ZONE SETTLEMENT	97
8.4	FAULTING.....	98
8.5	SLOPE STABILITY	98
9.	CONCLUSIONS.....	99
10.	REFERENCES.....	101

TABLE OF CONTENTS (CONTINUED)

LISTING OF TABLES

Table 5-1	Correlation of Engineering and Geologic Stratigraphic Units for MFFF Site.....	108
Table 5-2	Top Elevations of Engineering Units	109
Table 5-3	Soft Zones and Soft Materials Found in Borings and CPTs	114
Table 5-4	Groundwater Elevations from CPT Dissipation Tests	116
Table 6-1	Average CPT and SPT Test Results.....	117
Table 6-2	Average Classification and Physical Test Results	118
Table 6-3	Average Strength Test Results	119
Table 6-4	Average Consolidation Test Results	120
Table 6-5	Generalized Subsurface Profile	121
Table 6-6	Seismic CPTs used to Develop Individual Soil Profiles	122
Table 6-7	Statistical Summary of Seismic CPT Shear Wave Velocity Data	122
Table 6-8	Shear Modulus Reduction Values for Use at MFFF Site.....	123
Table 6-9	Damping Ratios Recommended for Use at MFFF Site.....	124
Table 6-10	Seismic CPTs with Pairs of Compression and Shear Wave Velocity Data	125
Table 6-11	Summary of Filtered Dynamic Poisson's Ratios Based on Seismic CPTs	126
Table 6-12	Recommended Values of Dynamic Poisson's Ratio for the MFFF Site.....	126
Table 6-13	Profiles of Low-Strain Shear Wave Velocity, Density, and Dynamic Poisson's Ratio for the MFFF Area	127
Table 6-14	Strain-compatible Shear Wave Velocities, Shear Moduli, and Damping Ratios – PC-3 Rock Motion Scaled Up by 1.25.....	128
Table 6-15	Best-Estimate Strain-compatible Cyclic Stress Ratio, Effective shear Strain, peak shear strain, peak shear stress, and peak ground acceleration – PC-3 Rock Motion Scaled Up by 1.25.....	129
Table 6-16	Best-Estimate Strain-Compatible Cyclic Stress Ratio, Effective Shear Strain, Peak Shear Strain, Peak Shear Stress, and Peak Ground Acceleration – 1886 Charleston (50 th Percentile) Control Motion	130
Table 6-17	Soft Soil Layer Classification And Engineering Properties at MFFF and BEG Building Locations	131
Table 7-1	Summary of Soil Parameters for FLAC Cam-Clay Model	132
Table 7-2	Summary of Soil Parameters for FLAC Mohr-Coulomb Collapse Model	133
Table 7-3	Measured Settlements at S-area Structures	134
Table 8-1	Average Factor of Safety Against Liquefaction by Engineering Unit.....	135
Table 8-2	Summary of Estimated Post-Earthquake Settlements Based on Borings Due to PC-3+ Motion.....	135

TABLE OF CONTENTS (CONTINUED)

Table 8-3	Total Post-earthquake Settlements Based on CPT Data – PC-3+ Motion	136
Table 8-4	Summary of Estimated Post-Earthquake Settlements Based on Borings Due to 1886 Charleston 50 th Percentile Motion.....	141
Table 8-5	Total Post-earthquake Settlements Based on CPT Data – 1886 Charleston 50 th Percentile Motion.....	142
Table 8-6	Summary of Estimated Post-earthquake Settlements - 1886 Charleston 50 th Percentile Motion	147
Table 8-7	Summary of Estimated Total and Differential Settlements of the MFFF Building.....	148

TABLE OF CONTENTS (CONTINUED)

LISTING OF FIGURES

Figure 3-1	Physiography of the SRS Area.....	150
Figure 3-2	Comparison of Chronostratigraphic, Lithostratigraphic, and Hydrostratigraphic Units in the SRS Region	151
Figure 3-3	Location of Type and Reference Wells for Geologic Units at SRS.....	152
Figure 3-4	Regional Scale Faults for SRS and Vicinity	153
Figure 3-5	Location of Sand Blows	154
Figure 3-6	SRS PC-3 Design Basis Surface Response Spectrum (Damped 5%) – Revised 1999	155
Figure 3-7	PC-4 Surface Response Spectra Envelopes	155
Figure 3-8	Comparison of 0.2g Regulatory Guide 1.60 Spectrum to PC-3 and PC- 4 Surface Response Spectra	156
Figure 4-1	Plot Plan and Locations of Geotechnical Investigations.....	157
Figure 5-1	MFFF Building Area, Soft Zone and Material Locations.....	158
Figure 5-2	MFFF Building Area, Geotechnical Section A.....	159
Figure 5-3	MFFF Building Area, Geotechnical Section B	160
Figure 5-4	MFFF Building Area, Geotechnical Section C	161
Figure 5-5	MFFF Building Area, Geotechnical Section D.....	162
Figure 5-6	MFFF Building Area, Geotechnical Section E	163
Figure 5-7	MFFF Building Area, Geotechnical Section F.....	164
Figure 5-8	Groundwater Elevations in F-Area at the SRS.....	165
Figure 6-1	Generalized Subsurface Profile Beneath MFFF Site	166
Figure 6-2	Generalized Profile of Low-Strain Shear Wave Velocity at MFFF Site.....	167
Figure 6-3A	Low-Strain Shear Wave Velocities Measured by SCPT.....	168
Figure 6-3B	Low-Strain Shear Wave Velocities Measured by SCPT.....	169
Figure 6-4	SRS-Recommended Shear Modulus Reduction Curves	170
Figure 6-5	SRS-Recommended Damping Ratio Curves.....	171
Figure 6-6	MFFF Site-Specific and Stokoe-Recommended Shear Modulus Reduction Curves for Sandy Soils	172
Figure 6-7	MFFF Site-Specific and Stokoe-Recommended Damping Ratio Curves for Sandy Soils	173
Figure 6-8	MFFF Site-Specific and Stokoe-Recommended Shear Modulus Reduction Curves for Clayey Soils	174
Figure 6-9	MFFF Site-Specific and Stokoe-Recommended Damping Ratio Curves for Clayey Soils.....	175
Figure 6-10	Response Spectra (Damped 5%) at Rock Used in MFFF Site Response Analyses	176
Figure 6-11	Comparison of Shear Wave Velocities from Seismic CPTs Performed in 2002 vs Those Performed in 2000	177

TABLE OF CONTENTS (CONTINUED)

Figure 6-12	Surface Response Spectra (Damped 5%) – PC-3 Rock Motion Scaled Up by 1.25	178
Figure 6-13	Comparison of Surface Response Spectra – PC-3 Motion Scaled up by 1.25	179
Figure 6-14	Surface Response Spectra (Damped 5%) – 1886 Charleston (50 th Percentile) Control Motion.....	180
Figure 6-15	Profiles of Strain-Compatible Shear Wave Velocities For Generalized MFFF Soil Column	181
Figure 6-16	Profiles of Strain-Compatible Shear Moduli for Generalized MFFF Soil Column.....	182
Figure 6-17	Profiles of Damping Ratio For Generalized MFFF Soil Column	183
Figure 6-18	Variation of Strain Compatible Shear Modulus	184
Figure 6-19	Cyclic Stress Ratio vs Depth – PC-3 Rock Motion Scaled Up by 1.25	185
Figure 6-20	Cyclic Stress Ratio vs Depth – 1886 Charleston (50 th Percentile) Control Motion.....	186
Figure 7-1	Estimated Settlements from Static Loads for MFFF and BEG Buildings Along Section E Based on FLAC Cam-Clay Model.....	187
Figure 7-2	Estimated Ground Pressures from Static Loads for MFFF and BEG Buildings Along Section E (E55,130).....	188
Figure 7-3	Change in Pressure vs Depth from Static Loads for MFFF and BEG Buildings Along Section E (E55,130).....	189
Figure 7-4	Building 221-S Settlement at Monument 13.....	190
Figure 7-5	Building 221-S Settlement at Monument 26.....	191
Figure 7-6	Contour Map – Estimated Settlements from Static Loads for MFFF and BEG Buildings Based on FLAC Cam-Clay Model.....	192
Figure 7-7	Contour Map – Estimated Bearing Pressures from Static Loads for MFFF and BEG Buildings	193
Figure 7-8	Estimated Time of Settlement from Static Loads for MFFF Building	194
Figure 7-9	Contour Map – Coefficients of Subgrade Reaction for Static Loads for MFFF and BEG Buildings Based on FLAC Cam-Clay Model	195
Figure 7-10	Comparison of Estimated Settlements from Static Loads for MFFF and BEG Buildings Along Section E for Cam-Clay and Mohr-Coulomb Collapse Models.....	196
Figure 7-11	Pressure vs Depth from Static Loads for MFFF and BEG Buildings Along Section E for Cam-Clay Model without Structure	197
Figure 7-12	Incremental Settlement vs Depth Along Section E for Cam-Clay Model with Soft Soils but without Structure.....	198
Figure 7-13	Ground Surface Settlements from Mohr-Coulomb Collapse Model	199
Figure 8-1	Factor of Safety Against Liquefaction At CPT-4.....	200
Figure 8-2	Factor of Safety Against Liquefaction at CPT-7.....	201
Figure 8-3	Factor of Safety Against Liquefaction at SCPT-8	202

TABLE OF CONTENTS (CONTINUED)

Figure 8-4	Factor of Safety Against Liquefaction at CPT-9.....	203
Figure 8-5	Factor of Safety Against Liquefaction at SCPT-13	204
Figure 8-6	Factor of Safety Against Liquefaction at CPT-14.....	205
Figure 8-7	Factor of Safety Against Liquefaction at CPT-18.....	206
Figure 8-8	Factor of Safety Against Liquefaction at CPT-21.....	207
Figure 8-9	Factor of Safety Against Liquefaction at CPT-22.....	208
Figure 8-10	Factor of Safety Against Liquefaction at SCPT-23	209
Figure 8-11	Factor of Safety Against Liquefaction at CPT-27.....	210
Figure 8-12	Factor of Safety Against Liquefaction at SCPT-28	211
Figure 8-13	Factor of Safety Against Liquefaction at CPT-29.....	212
Figure 8-14	Factor of Safety Against Liquefaction at CPT-40.....	213
Figure 8-15	Factor of Safety Against Liquefaction at CPT-44.....	214
Figure 8-16	Factor of Safety Against Liquefaction at CPT-45.....	215
Figure 8-17	Factor of Safety Against Liquefaction at CPT-46.....	216
Figure 8-18	Factor of Safety Against Liquefaction at CPT-47.....	217
Figure 8-19	Factor of Safety Against Liquefaction at CPT-48.....	218
Figure 8-20	Factor of Safety Against Liquefaction at CPT-49.....	219
Figure 8-21	Factor of Safety Against Liquefaction at CPT-50.....	220
Figure 8-22	Factor of Safety Against Liquefaction at CPT-51.....	221
Figure 8-23	Factor of Safety Against Liquefaction at CPT-52.....	222
Figure 8-24	Factor of Safety Against Liquefaction at CPT-53.....	223
Figure 8-25	Factor of Safety Against Liquefaction at CPT-54.....	224
Figure 8-26	Factor of Safety Against Liquefaction at CPT-55.....	225
Figure 8-27	Factor of Safety Against Liquefaction at CPT-56.....	226
Figure 8-28	Factor of Safety Against Liquefaction at CPT-57.....	227
Figure 8-29	Factor of Safety Against Liquefaction at CPT-58.....	228
Figure 8-30	Factor of Safety Against Liquefaction at CPT-59.....	229
Figure 8-31	Factor of Safety Against Liquefaction at CPT-60.....	230
Figure 8-32	Factor of Safety Against Liquefaction at CPT-61.....	231
Figure 8-33	Factor of Safety Against Liquefaction at CPT-62.....	232
Figure 8-34	Factor of Safety Against Liquefaction at CPT-63.....	233
Figure 8-35	Factor of Safety Against Liquefaction at CPT-64.....	234
Figure 8-36	Factor of Safety Against Liquefaction at SCPT-65	235
Figure 8-37	Factor of Safety Against Liquefaction at SCPT-66	236
Figure 8-38	Factor of Safety Against Liquefaction at SCPT-67	237
Figure 8-39	Factor of Safety Against Liquefaction at SCPT-68	238
Figure 8-40	Factor of Safety Against Liquefaction at SCPT-69	239
Figure 8-41	Factor of Safety Against Liquefaction at SCPT-70	240
Figure 8-42	Factor of Safety Against Liquefaction at SCPT-71	241
Figure 8-43	Factor of Safety Against Liquefaction at SCPT-72	242
Figure 8-44	Factor of Safety Against Liquefaction at SCPT-73	243

TABLE OF CONTENTS (CONTINUED)

Figure 8-45	Factor of Safety Against Liquefaction at SCPT-74	244
Figure 8-46	Factor of Safety Against Liquefaction at SCPT-75	245
Figure 8-47	Factor of Safety Against Liquefaction at SCPT-76	246
Figure 8-48	Factor of Safety Against Liquefaction at SCPT-77	247
Figure 8-49	Factor of Safety Against Liquefaction at SCPT-78A.....	248
Figure 8-50	Factor of Safety Against Liquefaction at SCPT-79	249
Figure 8-51	Factor of Safety Against Liquefaction at SCPT-80	250
Figure 8-52	Factor of Safety Against Liquefaction at SCPT-81	251
Figure 8-53	Factor of Safety Against Liquefaction at CPT-82.....	252
Figure 8-54	Factor of Safety Against Liquefaction at SCPT-83	253
Figure 8-55	Factor of Safety Against Liquefaction at SCPT-84	254
Figure 8-56	Factor of Safety Against Liquefaction at SCPT-85	255
Figure 8-57	Factor of Safety Against Liquefaction at SCPT-86	256
Figure 8-58	Factor of Safety Against Liquefaction at SCPT-87A.....	257
Figure 8-59	Factor of Safety Against Liquefaction at SCPT-88	258
Figure 8-60	Factor of Safety Against Liquefaction at SCPT-89A.....	259
Figure 8-61	Factor of Safety Against Liquefaction at SCPT-90	260
Figure 8-62	Factor of Safety Against Liquefaction at CPT-91.....	261
Figure 8-63	Factor of Safety Against Liquefaction at CPT-92.....	262
Figure 8-64	Factor of Safety Against Liquefaction at CPT-93.....	263
Figure 8-65	Factor of Safety Against Liquefaction at SCPT-94	264
Figure 8-66	Factor of Safety Against Liquefaction at CPT-95.....	265
Figure 8-67	Factor of Safety Against Liquefaction at SCPT-96	266
Figure 8-68	Factor of Safety Against Liquefaction at SCPT-97	267
Figure 8-69	Factor of Safety Against Liquefaction at CPT-98.....	268
Figure 8-70	Factor of Safety Against Liquefaction at CPT-99.....	269
Figure 8-71	Factor of Safety Against Liquefaction at CPT-100.....	270
Figure 8-72	Factor of Safety Against Liquefaction at CPT-101.....	271
Figure 8-73	Factor of Safety Against Liquefaction at CPT-102.....	272
Figure 8-74	Factor of Safety Against Liquefaction at CPT-103.....	273
Figure 8-75	Factor of Safety Against Liquefaction at CPT-104.....	274
Figure 8-76	Factor of Safety Against Liquefaction at CPT-105.....	275
Figure 8-77	Factor of Safety Against Liquefaction at CPT-106.....	276
Figure 8-78	Factor of Safety Against Liquefaction at CPT-107.....	277
Figure 8-79	Factor of Safety Against Liquefaction at CPT-108.....	278
Figure 8-80	Factor of Safety Against Liquefaction at CPT-109.....	279
Figure 8-81	Factor of Safety Against Liquefaction at CPT-110.....	280
Figure 8-82	Factor of Safety Against Liquefaction at CPT-111.....	281
Figure 8-83	Factor of Safety Against Liquefaction at CPT-112.....	282
Figure 8-84	Factor of Safety Against Liquefaction at CPT-113.....	283
Figure 8-85	Factor of Safety Against Liquefaction at CPT-114.....	284

TABLE OF CONTENTS (CONTINUED)

Figure 8-86	Factor of Safety Against Liquefaction at CPT-115.....	285
Figure 8-87	Factor of Safety Against Liquefaction at CPT-116.....	286
Figure 8-88	Factor of Safety Against Liquefaction at CPT-117.....	287
Figure 8-89	Factor of Safety Against Liquefaction at CPT-118.....	288
Figure 8-90	Factor of Safety Against Liquefaction at CPT-119.....	289
Figure 8-91	Factor of Safety Against Liquefaction at CPT-120.....	290
Figure 8-92	Factor of Safety Against Liquefaction at CPT-121.....	291
Figure 8-93	Factor of Safety Against Liquefaction at CPT-122.....	292
Figure 8-94	Factor of Safety Against Liquefaction at CPT-123.....	293
Figure 8-95	Factor of Safety Against Liquefaction at CPT-124.....	294
Figure 8-96	Average Factor of Safety Against Liquefaction by Engineering Unit.....	295
Figure 8-97	Boundary Curves for Identification of Liquefaction-Induced Damage (Ishihara, 1985)	296
Figure 8-98	Factor of Safety Against Liquefaction at BH-1	297
Figure 8-99	Factor of Safety Against Liquefaction at BH-4	298
Figure 8-100	Factor of Safety Against Liquefaction at BH-7	299
Figure 8-101	Factor of Safety Against Liquefaction at BH-8	300
Figure 8-102	Factor of Safety Against Liquefaction at BH-11	301
Figure 8-103	Factor of Safety Against Liquefaction at BH-12	302
Figure 8-104	Factor of Safety Against Liquefaction at BH-13	303
Figure 8-105	Factor of Safety Against Liquefaction at BH-14	304
Figure 8-106	Factor of Safety Against Liquefaction at BH-15	305
Figure 8-107	Factor of Safety Against Liquefaction at BH-16	306
Figure 8-108	Factor of Safety Against Liquefaction at BH-17	307
Figure 8-109	Factor of Safety Against Liquefaction at BH-18	308
Figure 8-110	Factor of Safety Against Liquefaction at BH-19	309
Figure 8-111	Factor of Safety Against Liquefaction at BH-20	310
Figure 8-112	Factor of Safety Against Liquefaction CPT-67 – 1886 Charleston 50 th Percentile Individual SCPT Profile.....	311
Figure 8-113	Factor of Safety Against Liquefaction CPT-68 – 1886 Charleston 50 th Percentile Individual SCPT Profile.....	312
Figure 8-114	Factor of Safety Against Liquefaction CPT-69 – 1886 Charleston 50 th Percentile Individual SCPT Profile.....	313
Figure 8-115	Factor of Safety Against Liquefaction CPT-70 – 1886 Charleston 50 th Percentile Individual SCPT Profile.....	314
Figure 8-116	Factor of Safety Against Liquefaction CPT-71 and BH-20 – 1886 Charleston 50 th Percentile Individual SCPT Profile.....	315
Figure 8-117	Factor of Safety Against Liquefaction CPT-72 – 1886 Charleston 50 th Percentile Individual SCPT Profile.....	316
Figure 8-118	Factor of Safety Against Liquefaction CPT-73 – 1886 Charleston 50 th Percentile Individual SCPT Profile.....	317

TABLE OF CONTENTS (CONTINUED)

Figure 8-119 Factor of Safety Against Liquefaction CPT-74 – 1886 Charleston 50th
Percentile Individual SCPT Profile 318

Figure 8-120 Factor of Safety Against Liquefaction CPT-75 – 1886 Charleston 50th
Percentile Individual SCPT Profile 319

Figure 8-121 Factor of Safety Against Liquefaction CPT-76 – 1886 Charleston 50th
Percentile Individual SCPT Profile 320

Figure 8-122 Factor of Safety Against Liquefaction CPT-77 – 1886 Charleston 50th
Percentile Individual SCPT Profile 321

Figure 8-123 Factor of Safety Against Liquefaction CPT-78A – 1886 Charleston
50th Percentile Individual SCPT Profile 322

Figure 8-124 Factor of Safety Against Liquefaction CPT-81 and BH-14 – 1886
Charleston 50th Percentile Individual SCPT Profile 323

Figure 8-125 Factor of Safety Against Liquefaction CPT-83 – 1886 Charleston 50th
Percentile Individual SCPT Profile 324

Figure 8-126 Factor of Safety Against Liquefaction CPT-85 – 1886 Charleston 50th
Percentile Individual SCPT Profile 325

Figure 8-127 Factor of Safety Against Liquefaction CPT-86 – 1886 Charleston 50th
Percentile Individual SCPT Profile 326

Figure 8-128 Factor of Safety Against Liquefaction CPT-87A and BH-16 – 1886
Charleston 50th Percentile Individual SCPT Profile 327

Figure 8-129 Factor of Safety Against Liquefaction CPT-97 – 1886 Charleston 50th
Percentile Individual SCPT Profile 328

Figure 8-130 Post-liquefaction Volumetric Strain as a Function of Factor of Safety
with Respect to Liquefaction 329

Figure 8-131 Comparison of CPT Tip Stress Around CPT-106 330

Figure 8-132 Contour Map, Post-Earthquake Settlements – PC-3+ Control Motion 331

Figure 8-133 Post-Earthquake Settlement – 1886 Charleston 50th Percentile Control
Motion 332

Figure 8-134 Bar Chart Showing Percentage of Post-earthquake Settlement in Each
Engineering Unit 333

Figure 8-135 SRS Site-Specific Volumetric Strain vs Factor of Safety with Respect
to Liquefaction 334

Figure 8-136 Static + Post-Earthquake Settlement – 1886 Charleston 50th Control
Motion 335

LISTING OF ATTACHMENTS

ATTACHMENT 1 EXPLORATION BORING PROGRAM AND LOGS OF BORINGS 112 PAGES

1. EXECUTIVE SUMMARY

This report presents the results of the geotechnical assessment of the Mixed Oxide (MOX) Fuel Fabrication Facility (MFFF) site. The results of exploration borings, cone penetration test (CPT) soundings, and laboratory testing of soils at the MFFF site are presented in this report. The results of the static and dynamic laboratory testing of soils, engineering analyses, establishment of final static and dynamic geotechnical design criteria, and site preparation requirements are included in this report.

The results of the field exploration programs, laboratory testing programs, and a detailed assessment of site conditions indicate that subsurface conditions encountered at the MFFF site are consistent with subsurface conditions reported in previous geotechnical investigations for the F-Area at the Savannah River Site (SRS). Regional and SRS site-specific hydrological, geological, tectonic, and seismic conditions described for the Savannah River Site (SRS) in WSRC (2000a) are considered applicable to the MFFF site. No unusual subsurface conditions were encountered at the MFFF site. The geologic, groundwater, and seismic conditions described in SRS reports for F-Area are applicable for the MFFF site.

An assessment of the subsurface conditions encountered at the MFFF site indicates that the site is considered suitable to support the proposed structures. It is anticipated that an engineered select structural fill will be required beneath the MFFF Building (BMF) and Emergency Generator Building (BEG) to properly distribute concentrated edge pressures due to static and seismic loading conditions into the underlying foundation bearing material. Planned foundation preparation and treatment will not have any adverse effects on the existing groundwater conditions at the site.

Some isolated soft soil zones were identified at depth on the MFFF site; however, these are consistent with similar "soft zones" encountered in previous investigations in the F-Area. The exploration borings and CPTs were used to define approximate limits of the soft zones encountered. Critical structures, which include the MOX Fuel Fabrication Building and the Emergency Generator Building, were located on the MFFF site so that only a limited number of smaller, isolated soft zones (≤ 4 feet thick) occur beneath these critical structures. The static and dynamic analyses include the effects of all soft zones and soft materials that were identified beneath and adjacent to the MFFF and Emergency Generator Buildings. These analyses demonstrate that the identified soft zones will not have any adverse effects on the performance of these structures.

The site geological conditions encountered at the MFFF site are consistent with subsurface conditions at the adjacent F-Area; therefore, the geotechnical engineering information developed for the deeper soils and bedrock profile at SRS F-Area are applicable for the MFFF site. The subsurface conditions beneath the critical structures at the MFFF site were analyzed for the PC-3+ and 1886 Charleston earthquakes, and it was determined that there is no potential for liquefaction of the soils underlying the site. There are, however, isolated pockets at depth where the factor of safety against liquefaction approaches 1. For factors of safety against liquefaction of 1.1 to 2.0, it is assumed that it is possible for excess pore pressures to build up in the soil, which, upon dissipation, may result in soil settlement. Such settlement due to dissipation of excess pore pressures that built up due to an earthquake is referred to as post-earthquake settlement. The post-earthquake settlements will not have any adverse effects on the performance of the critical structures at the MFFF site.

2. INTRODUCTION

The MFFF site is located adjacent to the F-Area, in the Separations Area of the Department of Energy's (DOE) Savannah River Site (SRS) in South Carolina. The MFFF site geotechnical programs were performed on a land area set aside for the MFFF. DOE assigned this site for the MFFF after an evaluation of five sites in the vicinity of the F-Area. This Geotechnical Report presents the results of the detailed geotechnical investigations performed at the MFFF site location in 2000 and 2002.

A detailed field exploration program of the MFFF site was completed in 2000 to define subsurface conditions at the MFFF site. This program included drilling and sampling a total of thirteen (13) exploration borings and performing sixty-three (63) cone penetration test (CPT) soundings. In 2002, a total of seven (7) exploration borings and sixty-two (62) cone penetration test (CPT) holes were performed during a supplemental geotechnical investigation that was performed within the MFFF site. In addition, laboratory testing was performed to determine the classification and engineering properties of representative soil samples obtained from the borings and CPTs. Previous site geotechnical programs, performed by others adjacent to and on this site, were also used to evaluate site subsurface geologic and groundwater conditions. Exploration boring logs and soil classification test results are presented in this report.

The results of the geotechnical programs were used to establish a database of geotechnical information to compare with results of previous investigations performed at SRS, especially those performed within the F-Area. This analysis confirms that subsurface conditions at the MFFF site are consistent with other geotechnical investigations performed in the F-Area, located adjacent to the MFFF site.

The geotechnical exploration and testing programs were performed under the engineering oversight of the Lead Geotechnical Engineer and geotechnical staff of Duke Cogema Stone & Webster (DCS).

2.1 PURPOSE AND SCOPE

The purpose of the geotechnical exploration and testing programs was to obtain geotechnical information to characterize subsurface conditions at the MFFF site and to compare these results with subsurface conditions reported in and around the adjacent F-Area. Specific objectives include:

- Define geologic stratigraphy and compare the continuity, thickness, and relative elevation of the strata to stratigraphic units defined across the F-Area and at the SRS;
- Define the index properties of each stratigraphic layer and make a comparison to geotechnical properties determined for the F-Area stratigraphy;
- Evaluate the subsurface conditions to define geotechnical conditions and suitability for support of the proposed MFFF structures;
- Define any subsurface conditions that may be detrimental to the proposed MFFF structures; and
- Develop geotechnical design criteria for the MFFF.

3. GEOLOGY

3.1 REGIONAL GEOLOGY

The following discussion on the regional and MFFF site geology is based on detailed discussions presented in Section 1.4.3 of WSRC (2000a). The area of interest evaluated includes a radius of about 200 miles from the SRS and MFFF site. The information also provides the basis for understanding the regional and SRS geology applicable to subsurface conditions encountered at the MFFF site.

Many SRS investigations and an extensive literature review reach the conclusion that there are no known capable or active faults within the 320 km (200 mile) radius of the site that influence the seismicity of the region, with the exception of the blind, poorly constrained faults associated with the Charleston seismic zone (WSRS 2000a).

3.1.1 Atlantic Coastal Plain Stratigraphy

The SRS is located on the sediments of the Upper Atlantic Coastal Plain in South Carolina. The Coastal Plain is comprised of stratified sand, clay, limestone, and gravel layers that dip gently seaward. The age of these deposits ranges from Late Cretaceous to Recent. The sedimentary sequence thickens from essentially zero at the Fall Line to more than 1,219 meters (4,000 feet) at the coast. Regional dip is to the southeast, although beds dip and thicken locally in other directions because of locally variable depositional regimes and differential subsidence of basement features such as the Cape Fear Arch and the South Georgia Embayment. A map depicting these regional features and the study area discussed in the following sections is presented in Figure 3-1.

The stratigraphic section in the SRS region, which delineates the coastal plain lithology (see Figure 3-2), is divided into several formations and groups, based principally on age and lithology. The Coastal Plain sedimentary sequence at the SRS consists of about 213 meters (700 feet) of Late Cretaceous quartz sand, pebbly sand, and kaolinitic clay, overlain by about 18 meters (60 feet) of Paleocene clayey and silty quartz sand, glauconitic sand, and silt. The Paleocene beds are in turn overlain by about 107 meters (350 feet) of Eocene quartz sand, glauconitic quartz sand, clay, and limestone, grading into calcareous sand, silt, and clay. The calcareous strata are common in the upper part of the Eocene section in down-dip parts of the study area. In places, especially at higher elevations, deposits of pebbly, clayey sand, conglomerate, and clay of Miocene or Oligocene age cap the sequence. Lateral and vertical facies changes are characteristic of most of the Coastal Plain sequence, and the lithologic descriptions below are, therefore, generalized.

The following sections describe regional stratigraphy and lithologies of the Coastal Plain sediments, with emphasis on variations near the SRS. The data presented are based upon direct observations of surface outcrops, geologic core obtained during drilling of boreholes, microfossil age dating, and borehole geophysical logs. Several key boring locations within the SRS

boundaries and in the adjacent regions (see Figure 3-3) are referenced throughout the following discussions.

3.1.1.1 Upper Cretaceous Sediments

At the MFFF site, as well as the F-Area, about 264 meters (865 feet) of Upper Cretaceous sediments, deposited in fluvial to prodeltaic environments, overlie Paleozoic crystalline bedrock at about El -585 feet, (WSRC, 1996b). This sequence includes the basal Cape Fear Formation and the overlying Lumbee Group, which is divided into three formations (see Figure 3-2). The sediments in this sequence consist predominantly of poorly consolidated, clay-rich, fine- to medium-grained, micaceous sand, sandy clay, and gravel. Thin clay layers are common. In parts of the section, clay lenses and beds up to 21 meters (70 feet) thick are present.

3.1.1.2 Tertiary Sediments

Tertiary sediments, ranging in age from Early Paleocene to Miocene, deposited in fluvial to marine shelf environments, overlie the Upper Cretaceous sediments. The Tertiary sequence of sand, silt, and clay generally grades into highly permeable platform carbonates in the southern part of the study area, and these continue southward to the coast. The Tertiary sequence is divided into three groups: the Black Mingo Group, Orangeburg Group, and Barnwell Group, which are further subdivided into formations and members (see Figure 3-2). The ubiquitous Upland Unit overlies these groups.

3.1.1.2.1 Black Mingo Group

The Black Mingo Group underlies the SRS and the MFFF site and consists of quartz sand, silty clay, and clay that suggest upper and lower delta plain environments of deposition, generally under marine influences. In the southern part of the study area, massive clay beds, often more than 50 feet (15 meters) thick, predominate.

Basal Black Mingo sediments were deposited on the regional "Cretaceous-Tertiary" unconformity of Aadland, which defines the base of Sequence Stratigraphic Unit I. There is no apparent structural control of this unconformity. Above the unconformity, the clay and clayey sand beds of the Black Mingo Group thin and often pinch out along the traces of the Pen Branch and Crackerneck Faults. This suggests that coarser-grained materials were deposited preferentially along the fault traces, perhaps due to shoaling of the depositional surface. This, in turn, suggests movement (reactivation) along the faults. This reactivation would have occurred during Black Mingo deposition; that is, in Paleocene and lower Eocene time.

3.1.1.2.2 Orangeburg Group

The Orangeburg Group underlies the SRS and the MFFF site and consists of the lower middle Eocene Congaree Formation (Tallahatta equivalent) and the upper middle Eocene Warley Hill Formation and Santee Limestone (see Figure 3-2). Over most of the study area, these post-

Paleocene units, comprised of alternating layers of sand, limestone, marl, and clay, are more marine in character than the underlying Cretaceous and Paleocene units.

The group crops out at lower elevations in many places within and near the SRS. The sediments thicken from about 26 meters (85 feet) at Well P-30 near the northwestern SRS boundary to 61 meters (200 feet) at Well C-10 in the south (see Figure 3-3). Dip of the upper surface is 2 m/km (12 ft/mile) to the southeast.

In the central part of the study area, the group includes, in ascending order, the Congaree, Warley Hill, and Tinker/Santee Formations (see Figure 3-2). The units consist of alternating layers of sand, limestone, marl, and clay that are indicative of deposition in shoreline to shallow shelf environments. From the base upward, the Orangeburg Group passes from clean shoreline sand, characteristic of the Congaree Formation, to shelf marl, clay, sand, and limestone, which are typical of the Warley Hill and Santee Limestone. Near the center of the study area, the Santee sediments consist of up to 30% carbonate. The sequence is transgressive, with the middle Eocene Sea reaching its most northerly position during Tinker/Santee deposition.

Toward the south, near Wells P-21A, ALL-324, and C-10 (see Figure 3-3), the carbonate content of all three formations increases dramatically. The shoreline sand of the Congaree undergoes a facies change to interbedded glauconitic sand and shale, grading to glauconitic, argillaceous, fossiliferous, sandy limestone. Down dip, the fine-grained, glauconitic sand and clay of the Warley Hill become increasingly calcareous and grade imperceptibly into carbonate-rich facies comparable to both the overlying and underlying units. Carbonate content in the glauconitic marl, calcareous sand, and sandy limestone of the Santee increases towards the south. Carbonate sediments constitute the vast majority of the Santee in the region from Well P-21A southward.

3.1.1.2.2.1 Congaree Formation

The early middle Eocene Congaree Formation has been traced from the Congaree Valley in east central South Carolina into the study area. It has been paleontologically correlated with the early and middle Eocene Tallahatta Formation in neighboring southeastern Georgia.

The Congaree is about 9 meters (30 feet) thick near the center of the SRS study area, and it consists of yellow, orange, tan, gray, green, and greenish gray, well-sorted, fine to coarse quartz sand, with granule and small pebble zones common. Thin clay laminae occur throughout the section. The quartz grains tend to be better rounded than those in the rest of the stratigraphic column. The sand is glauconitic in places, suggesting deposition in shoreline or shallow shelf environments. To the south, near Well ALL-324 (see Figure 3-3), the Congaree Formation consists of interbedded glauconitic sand and shale, grading to glauconitic, argillaceous, fossiliferous sandy limestone, suggestive of shallow to deeper shelf environments of deposition. Farther south, beyond Well C-10, the Congaree grades into platform carbonate facies of the lower Santee Limestone.

The Congaree Formation was encountered in all of the exploration borings at approximately El 135 across the MFFF site. It is comprised of very dense sand, and it was a consistent geologic marker bed across the MFFF site.

3.1.1.2.2.2 Warley Hill Formation

Unconformably overlying the Congaree Formation are 3 meters (10 feet) to 6 meters (20 feet) of fine-grained, often glauconitic sand and green clay beds that have been referred to, respectively, as the Warley Hill and Caw Members of the Santee Limestone. The green sand and clay beds are referred to informally as the "green clay" in previous SRS reports. Both the glauconitic sand and the clay at the top of the Congaree are assigned to the Warley Hill Formation. In the up-dip parts of the study area, the Warley Hill apparently is missing or very thin, and the overlying Tinker/Santee Formation rests unconformably on the Congaree Formation.

In the SRS study area, the thickness of the Warley Hill Formation (GC) is generally less than 6 meters (20 feet). It is present at the MFFF site, where it generally is less than 2.1 meters (7 feet) thick, averaging approximately 1.2 meters (4 feet) in thickness. The Warley Hill sediments indicate shallow to deeper clastic shelf environments of deposition in the study area, representing deeper water than the underlying Congaree Formation. This suggests a continuation of a transgressive pulse during upper middle Eocene time. To the south, beyond Well P-21A, the green silty sand and clay of the Warley Hill undergo a facies change to the clayey micritic limestone and limey clay, typical of the overlying Santee Limestone. The Warley Hill blends imperceptibly into a thick, clayey, micritic limestone, which divides the Floridan Aquifer System south of the study area.

3.1.1.2.2.3 Tinker/Santee Formation

The Tinker/Santee Formation is about 21 meters (70 feet) thick near the center of SRS, and it averages approximately 10 meters (33 feet) thick at the MFFF site. Sediments of the Tinker/Santee indicate deposition in shallow marine environments. Often found within the Tinker/Santee sediments, particularly in the upper third of the interval, are weak zones interspersed in stronger carbonate-rich matrix materials. The weak zones, which vary in apparent thickness and lateral extent, were noted where rod drops or lost circulation occurred during drilling and low blow counts occurred during SPT drives. These weak zones have variously been termed in the SRS reference documents as "soft zones," the "critical layer," "underconsolidated zones," "bad ground," and "voids." Soft zones, typical to this formation, were also encountered at the MFFF site.

3.1.1.2.3 Barnwell Group

Upper Eocene sediments of the Barnwell Group (see Figure 3-2) represent the Upper Coastal Plain of western South Carolina and eastern Georgia. Sediments of the Barnwell Group are present at the MFFF site, overlying the Tinker/Santee Formation, and they consist mostly of shallow marine quartz sand containing sporadic clay layers. The group is about 21 meters (70

feet) thick near the northwestern boundary of the SRS, 52 meters (170 feet) thick near its southeastern boundary, and it averages approximately 30 meters (100 feet) thick at the MFFF site. The regionally significant Santee Unconformity, which separates the Clinchfield Formation from the overlying Dry Branch Formation (Figure 3-2), is a pronounced erosional surface, observable throughout the SRS region.

3.1.1.2.3.1 Clinchfield Formation

The basal, late Eocene, Clinchfield Formation consists of light-colored quartz sand and glauconitic, biomoldic limestone, calcareous sand, and clay. Sand beds of the formation constitute the Riggins Mill Member of the Clinchfield Formation, and they are composed of medium to coarse, poorly to well sorted, loose, and slightly indurated, tan clay, and green quartz. The sand is difficult to identify unless it occurs between the overlying carbonate layers of the Griffins Landing Member and the underlying carbonate layers of the Santee Limestone. The Clinchfield Formation is about 8 meters (25 feet) thick in the southeastern part of the SRS and pinches out or becomes unrecognizable at the MFFF site, near the center of the SRS.

3.1.1.2.3.2 Dry Branch Formation

The late Eocene Dry Branch Formation is divided into the Irwinton Sand Member, the Twiggs Clay Member, and the Griffins Landing Member. The unit is about 18 meters (60 feet) thick near the center of the study area, and it averages approximately 9 meters (30 feet) thick at the MFFF site. The Dry Branch sediments overlying the Tinker/Santee Formation interval in the central portion of SRS were deposited in shoreline/lagoonal/tidal marsh environments. The shoreline retreated from its position in northern SRS during Tinker/Santee (Utley) time to the central part of SRS in Dry Branch time. Progradation of the shoreline environments to the south resulted in the sands and muddy sands of the Dry Branch being deposited over the shelf carbonates and clastics of the Tinker/Santee (Utley) sequence.

3.1.1.2.3.3 Tobacco Road Formation

The Late Eocene Tobacco Road Formation consists of moderately to poorly sorted, red, brown, tan, purple, and orange, fine to coarse, clayey quartz sand. Pebble layers are common, as are clay laminae and beds. Ophiomorpha burrows are abundant in parts of the formation. These sediments have the characteristics of lower delta plain to shallow marine deposits.

The top of the Tobacco Road is characterized by the change from a comparatively well sorted sand to the more poorly sorted sand, pebbly sand and clay of the "Upland Unit." Contact between the units constitutes the "Upland" unconformity. The unconformity is very irregular due to fluvial incision that accompanied deposition of the overlying "Upland Unit" and later erosion.

The Tobacco Road Formation averages approximately 20 meters (66 feet) thick at the MFFF site and is overlain by the "Upland Unit."

3.1.1.2.3.4 "Upland Unit"/Hawthorn/Chandler Bridge Formations

Deposits of poorly sorted silty, clayey sand, pebbly sand, and conglomerate of the "Upland Unit" cap many of the hills at higher elevations over much of the SRS region. This unit is the upper soil unit at the MFFF site, where it varies in thickness from approximately 0.3 to 5.8 meters (1 to 19 feet). Weathered feldspar is abundant in places. The color is variable, and facies changes are abrupt. The "Upland Unit" is generally considered to be of Miocene age, and the environment of deposition appears to be fluvial. The thickness of the Upland Unit changes abruptly, owing to channeling of the underlying Tobacco Road Formation during "Upland" deposition and subsequent erosion of the "Upland Unit" itself. This erosion formed the "Upland" unconformity. The unit is up to 18 meters (60 feet) thick at SRS.

3.2 SOFT ZONES

Much of SRS, including the F-Area and MFFF site, contains intermittent and isolated, weak soil zones interspersed in stronger, carbonate-rich matrix materials within the Tinker/Santee Formation. These weak soils, which vary in thickness and lateral extent, were noted in previous subsurface investigations at the SRS where rod drops or lost circulation occurred during drilling and low blow counts occurred during SPT sampling. They also have been identified as zones with low penetration resistance during CPT pushes. These weak soil zones within the Tinker/Santee sediments have been termed at the SRS as "soft zones," "the critical layer," "underconsolidated zones," "bad ground," and "voids." The preferred term used to describe these zones within the Tinker/Santee Formation is "soft zones."

Weak soil zones were also encountered in other formations at the F-Area and MFFF site; however, these sediments do not have the same origin or physical behavior as the Tinker/Santee "soft zones." In the following discussions, "soft zones" is used refer to the "soft zones" of the lower Dry Branch (DB4/5) and the Tinker/Santee Formation (ST1 and ST2), and "soft materials" is used to distinguish the weak soils encountered within other geologic formations at the MFFF site.

Extensive studies and analyses of the soft zones at the SRS have been conducted since 1952. Eighteen of the studies, including outside peer consultant reviews, are summarized in WSRC (1999b). WSRC (1999b) also presents current conclusions on the origin, development, and stability of the soft zones, along with an assessment of the engineering properties of the soft zones. WSRC (2000a) presents a detailed assessment of the soft zones found at the SRS. These studies have been used to develop the approach for performing field exploration programs, laboratory testing, and analyses of soft zones encountered at the MFFF site. The results of the previous investigations for the F-Area and the adjacent APSF site led to the decision to relocate the MFFF and BEG Buildings after initial MFFF site investigations identified the presence of major soft zone areas in the eastern portion of the site.

Isopach maps reveal that carbonate thickness and concentration is directly related to the isopach thickness of the Tinker/Santee interval. Where the Tinker/Santee interval is thick, carbonate is

more concentrated – where the interval is thin, carbonate thickness and concentration are reduced. It is further observed that where carbonate is concentrated in the Santee-Utley section, the overlying “Upland Unit” and Tobacco Road/Dry Branch section are generally at higher elevations, and where the carbonate content is reduced or absent, the overlying “Upland Unit” and Tobacco Road/Dry Branch section are generally at lower elevations than elsewhere. This indicates that the removal (dissolution) of carbonate and the thinning of the Tinker/Santee interval occurred in post-Tobacco Road time (WSRC 2000a).

The origin of the carbonates in the Tinker/Santee interval is fairly clear. The carbonate content ranges from zero to approximately 90 percent. The presence of glauconite, along with normal marine fauna including foraminifers, mollusks, bryozoans, and echinoderms, indicates that the limestones and limy sandstones were deposited in clear, open, marine water of normal salinity on the inner to middle shelf. The abundance of carbonate mud (micrite) in the limestones suggests deposition in quiet water below the normal marine wave base. The presence of abraded and well-worn skeletal grains indicates that bottom transport by currents or storm-generated waves alternated with the quiet-water conditions in which the sediments accumulated (WSRC 2000a).

Several hypotheses exist concerning the origin of the soft zones: one being that these zones consisted of varying amounts of carbonate material that has undergone dissolution over geologic time leaving sediments that are now subjected to low vertical effective stresses due to arching of more competent soils above the soft zone intervals (WSRC 2000a). The original thoughts were that the soft zones were the result of the dissolution of the shell debris concentrated in bioherms (oyster banks). This premise has since been proven to be false. Significant study of the deposition of the Tinker/Santee sediments precludes the formation of bioherms.

A second hypothesis is based on recent studies that indicate that soft zones occur where silica replacement/cementation of the carbonate occurred. The silicification (by amorphous opaline silica) of the enclosing carbonate sediment would follow and spread along bedding planes, along microfractures of varied orientations, and along corridors of locally enhanced permeability. The resulting “soft zone” could be in the form of irregular isolated pods, extended thin ribbons, or stacked thin ribbons separated by intervening unsilicified parent sediment.

Careful observations of the grouting programs conducted by the Corps of Engineers in the early 1950s, and more recently for the restart of the K Reactor, corroborate these recent findings. They observed that the grout was not having the desired effect on the subsurface soft zones as was previously thought. The results showed that the grout traveled in thin sheets along preferential pathways. Soft zones that existed prior to grouting still existed after grouting was completed. Soft zones encountered in one CPT could be absent in the neighboring CPT only a few feet away. Only where silicification has spread far enough away from the bedding planes or fractures along which the silica replacement has taken place, where all the intervening sediment is replaced, would the soft zones be large enough and coherent enough to pose a question for the siting of new facilities. In all likelihood, this would be a most uncommon event (WSRC 2000a).

Two primary episodes of freshwater flushing of the Tinker/Santee section in two or more stages of carbonate dissolution are hypothesized based on the multiple episodes of erosion/dissolution of the section. The first occurred at the time of the Santee unconformity; the second at the time of deposition of the "Upland Unit" following the Upland unconformity. During the deposition of the Dry Branch and Tobacco Roads section in the interim period between the two primary episodes of fresh water flushing of the Tinker/Santee section, dissolution of carbonate and precipitation and replacement of carbonate by silica continued, albeit at a slower rate (WSRC, 1999b).

At the F-Area and MFFF site, the Tinker/Santee section is in the saturated zone, well below the water table. Here, the sediments are in a stable chemical environment and the carbonate dissolution is minimal. The further dissolution and removal of the Tinker/Santee carbonate in the next 100 years is a non-issue (WSRC, 1999b).

3.3 FAULTING

Faulting at the SRS is discussed in detail in Section 1.4.3.2 of WSRC (2000a). The locations of faults that involve Coastal Plain sediments that are considered regionally significant based on their extent and amounts of offset near the SRS are shown on Figure 3-4. Based on previous studies at SRS and elsewhere, there are no known capable or active faults within the 320 km (200 mile) radius of the site that influence the seismicity of the region, with the exception of the blind, poorly constrained faults associated with the Charleston seismic zone (WSRS 2000a). The Pen Branch fault is a significant bedrock feature at the SRS, and it has been the subject of a number of investigations to establish its potential seismic risk. These investigations have not indicated any Quaternary movement. WSRC (2000a) determined that the Pen Branch fault is not capable per 10 CFR 100, Appendix A.

3.4 SEISMOLOGY

Significant studies of the local and regional seismology of the SRS have been conducted to support operation of the DOE facilities there. The MFFF project used these studies as a starting point in establishing appropriate design inputs for the MFFF site. Section 1.4.4 of WSRC (2000a) presents a detailed discussion for the seismology at SRS, criteria that have been developed for the DOE facilities at the SRS, and their application to develop design criteria for the MFFF. Pertinent sections of WSRC (2000a) are included in this report.

3.4.1 Earthquake History of the General Site Region

This section includes a broad description of the historical seismic record (non-instrumental and instrumental) of southeastern U.S. and the SRS. Aspects that are of particular importance to the SRS include the following:

- The Charleston, SC, area is the most significant seismogenic zone affecting the SRS.
- Seismicity associated with the SRS and surrounding region is more closely related to South Carolina Piedmont-type activity. This activity is characterized by occasional,

small, shallow events associated with strain release near small-scale faults, intrusive bodies, and the edges of metamorphic belts.

3.4.1.1 Regional Earthquake History

The earthquake history of southeastern U.S. (of which the SRS is a part) spans a period of nearly three centuries, and it is dominated by the catastrophic Charleston earthquake of August 31, 1886. The historical database for the region is composed essentially of two data sets, which extend back to as early as 1698. The first set is comprised of pre-network, mostly qualitative data (1698-1974), and the second set covers the relatively recent period of instrumentally recorded seismicity (1974-present). Today seismic monitoring results from all southeastern seismic networks are cataloged annually in the Southeast U.S. Seismic Network bulletins. Significant earthquakes within 320 km (200 miles) of the SRS (Modified Mercalli Intensity (MMI) > IV or magnitude > 3) are presented in WSRC (2000a).

The Charleston, SC, area is the most significant source of seismicity affecting the SRS, in terms of both the maximum historical site intensity and the number of earthquakes felt at the SRS. The greatest intensity felt at the SRS has been estimated at MMI VI-VII, and it was produced by the earthquake (moment magnitude, $M_w = 7.3$) that struck Charleston, SC, on August 31, 1886. An earthquake that struck Union County, SC, located about 160 km (100 miles) north-northeast of the SRS, on January 1, 1913, is the largest event located closest to the SRS outside of the Charleston area. It had an intensity that was greater than or equal to MMI VII. This earthquake was felt in the Aiken-SRS area with an intensity of MMI II-III. Several other earthquakes, including some aftershocks of the 1886 Charleston event, were felt in the Aiken-SRS area with intensities estimated to be equal to or less than MMI IV. The locations of historical seismic events are presented in WSRC (2000a).

Several large earthquakes outside the region were probably felt at SRS, including the earthquake sequence of 1811 and 1812 that struck New Madrid, Missouri (about 535 miles west-northwest of SRS) and the earthquake that struck Giles County, Virginia (about 280 miles north of SRS), on May 31, 1897.

3.4.1.2 Seismic Activity Within 50 Mile Radius of the SRS

The SRS is located within the Coastal Plain physiographic province of South Carolina. However, seismic activity associated with SRS and the surrounding region displays a marked lack of clustering in zones, which is more characteristic of the occasional energy strain release occurring through a broad area of central Piedmont province of the state. Epicenter locations for events near (within 50 miles from center of site) the SRS are presented in WSRC (2000a).

3.4.2 Paleoseismic Data

Estimating seismic recurrence intervals of moderate to large earthquakes within the southeastern U.S. is difficult due to the relatively short (300 years) historical record and an absence of surface faulting, offset features, or prehistoric ruptures. Geologic field study methods developed to

extend the seismic record assess both the temporal and spatial distribution of past moderate and large earthquakes. This assessment is carried out through identification and dating of secondary deformation features resulting from strong ground shaking. In the southeast, this extension of the seismic record has been accomplished through field searches for earthquake-induced liquefaction flowage features called "sand blows" associated with prehistoric earthquake-induced paleoliquefaction features.

These features are attributed to prehistoric earthquake-induced liquefaction as defined by the transformation of sediments from solid to liquid state caused by increased pore water pressure (WSRC, 2000a). The increased pore pressure is caused during or immediately after an earthquake. "Sand blows" are features formed where earthquake shaking causes liquefaction at depth, followed by the venting of the liquefied sand and water to the surface.

The following summarizes paleoliquefaction studies in the southeastern United States. Aspects that are of particular importance to SRS include the following (WSRC, 2000a):

- No conclusive evidence of large prehistoric earthquakes originating outside of coastal South Carolina has been found.
- Young fluvial terraces at, or slightly above, the level of the modern floodplain and Carolina bays are the most likely depositional environments for potentially liquefiable deposits in the SRS region.

3.4.2.1 Paleoliquefaction Studies in the Eastern United States

Widespread occurrences of earthquake-induced sand blows have been documented throughout the meizoseismal area of the 1886 Charleston, SC, earthquake (WSRC 2000a). Excavation and detailed analyses of these liquefaction flow features provided the first insight into the pre-history of the Charleston earthquake. Other pre-1886 liquefaction flow features (mostly sand blows) were discovered and investigated near the town of Hollywood, about 25 km (15 miles) west of Charleston. Searches for sand blows were continued throughout the Charleston area and expanded to the remaining coastal South Carolina areas. Eventually, areas of study were broadened to include Delaware, Virginia, North Carolina, and Georgia. The objective was to identify other epicentral regions, if they existed, and to estimate the sizes of pre-1886 earthquakes assuming the areal extent of sand blows caused by an earthquake is a function of earthquake intensity in areas of similar geologic and groundwater settings.

Figure 3-5 shows the study region of current paleoliquefaction areas of interest (WSRC, 2000a). To date, no conclusive evidence of large prehistoric earthquakes originating outside of coastal South Carolina have been found (WSRC, 2000a).

In coastal South Carolina investigations, identification of paleoliquefaction features generally adheres to specific local geologic criteria. Some specific relations between liquefaction susceptibility and subsequent formation of liquefaction features (sand blows) are summarized below (WSRC, 2000a):

- A water table very near the ground surface greatly increases susceptibility to liquefaction (depth < 1 m (< 3 feet)).
- Virtually all seismically induced liquefaction sites are located in beach-ridge, back barrier, or fluvial depositional environments. Of these, beach-ridge deposits were found to be the most favorable for the generation and preservation of seismically induced liquefaction features.
- Due primarily to the effects of chemical weathering, materials older than about 250 ka were less susceptible to liquefaction than were younger deposits. This indicates that the probabilities of sand blows forming in deposits of late Pleistocene and early Holocene age are extremely low.
- The liquefied materials are generally fine-grained, well-sorted (i.e., uniformly graded), clean beach sand. The principal properties of sand that control liquefaction susceptibility during shaking are degree of compaction (measured as relative density by geotechnical engineers), sand-grain size and sorting, and cementation of the sand at grain-to-grain contacts. Fine grained, well-sorted sand of modern beaches are much more susceptible to liquefaction than compacted well-graded sand used in engineered construction.
- Features large enough to be interpreted as possibly having an earthquake origin in the low country were found only in sand deposits having total thickness greater than 2 to 3 meters (7 to 10 feet).
- The depth of the probable source beds at liquefaction sites is generally less than 6 to 7 meters (20 to 23 feet), and the groundwater table is characteristically less than 3 meters (10 feet) beneath present ground surface.

Utilizing the above methods, at least four pre-1886 liquefaction episodes occurred at approximately 580 ± 104 (CH-2); $1,311 \pm 114$ (CH-3); $3,250 \pm 180$ (CH-4); and $5,124 \pm 700$ (CH-5) years before the present (WSRC, 2000a). CH refers to Charleston source with CH-1 designated as the 1886 earthquake. An even older episode (CH-6) was found to be cut by a CH-5 feature.

Changes in hydrologic conditions (groundwater levels) play an important role in determining an area's susceptibility to liquefaction. On the basis of published sea-level curves, groundwater levels in the southeastern U.S. have been assumed at or near present levels for only the past 2,000 years. Consequently, the paleoliquefaction record is probably most complete for this period (WSRC, 2000a). However, beyond the 2,000-5,000 year range, knowledge of groundwater conditions is considerably less reliable, making gaps in the paleoseismic record much more probable.

3.4.2.2 Paleoliquefaction Assessment of the SRS Region

A paleoliquefaction assessment of the SRS was prepared by WSRC in 1996. This investigation indicated that several hydrologic, sedimentological, and logistical conditions must be met for seismically induced liquefaction (SIL) to occur and be identified. These included: (1) the presence of Quaternary-age deposits; (2) the presence of a shallow groundwater table; (3)

proximity to potential seismogenic features; (4) geologic sections of several different types of unconsolidated deposits; and (5) quality and extent of exposure.

Based on these considerations, the floodplains of the Savannah River and its tributaries were identified as the areas on the SRS with the highest potential for generating and recording Holocene SIL features. The terraces of the Savannah River and tributaries were also considered potential areas for recording Quaternary SIL features, though these features would likely be older than those in the floodplains. The upland areas on the SRS have a low potential for recording Quaternary SIL because they are pre-Quaternary in age, partially indurated, and generally high above the water table. Paleoliquefaction investigations in the SRS uplands, therefore, only targeted those sites postulated by previous workers as containing evidence of SIL.

Conclusions from this paleoliquefaction assessment fell into two categories: (1) field studies of floodplain deposits along the Savannah River, and (2) evaluation of previously reported paleoliquefaction and neotectonic features located in pre-Quaternary sediments. A brief summary of findings in these two areas follows.

Investigation of banks along 110 km (68 miles) of the Savannah River adjacent to the SRS revealed a large number of excellent exposures of floodplain deposits. Most of the exposed deposits were clay and silt and had a low liquefaction potential. Locally, however, clean sand deposits with a high liquefaction potential were present. Given the extensive amount of exposure and the local presence of liquefiable materials, SIL features likely would be present in these deposits if strong earthquakes had occurred after they were deposited. However, the presence of buried historical objects and radiocarbon dates from these materials illustrated that most or all of the exposed floodplain deposits were historical in age. As no strong ground motions have occurred in historical times in the SRS area, SIL features could not exist in these deposits. Furthermore, the fact that they date to historical times precludes them from providing any information of earlier earthquake history.

The absence of SIL features in the bank exposures does not preclude the possibility that SIL features exist deeper in the section or on the older, higher terraces. In fact, the local presence of liquefiable materials in the Modern floodplain deposits suggests that, if strong prehistoric earthquakes had occurred, SIL features are probably present at depth in the floodplain deposits or on the older/higher terraces. These key areas were not investigated, and exposure is limited.

The upland areas of the SRS were considered to have a low potential for recording Quaternary SIL because the deposits are old (pre-Quaternary), generally high above the water table (> 10 meters (> 30 feet)), and are indurated. However, previous investigators described several features in the Tertiary section as clastic dikes and attributed them to SIL and/or neotectonic activity. The sites were evaluated to determine if they have the diagnostic characteristics that have recently been documented for true SIL.

Four types of post-depositional features were identified during the investigations at SRS: (1) irregularly shaped cutans; (2) structurally controlled cutans; (3) joints; and (4) faults. Cutans are

a modification of the texture, structure, or fabric of the host material by pedogenic (soil) processes, either by a concentration of particular soil constituents or in situ modification of the matrix. These features were interpreted through the process of elimination procedure of multiple working hypotheses. None were thought to be the result of SIL (WSRC, 2000a).

3.4.3 Development of the SRS Design Basis Earthquake

The basic approach that has been used to develop the Design Basis Earthquake (DBE) spectra at the SRS is described in detail in Section 1.4.4.3 of WSRC (2000a). The following section presents a brief discussion of the DBE for the SRS.

DOE-STD-1023-95 provides criteria for determining ground motion parameters for the design earthquake for the SRS and for determining the acceptable design response spectral shape. It specifies a broadened, mean-based, Uniform Hazard Spectrum (UHS), representing a specified annual probability of exceedance for a systems, structures, and components (SSC) performance categories (e.g., PC-1 through PC-4) and a historical earthquake deterministic spectrum that ensures the design earthquake developed from the UHS at least captures the known seismicity of the site. For the SRS, the deterministic spectrum is represented by a repeat of the 1886 Charleston earthquake. The development of the SRS design basis spectra used a statistical methodology to verify that a mean-based response was achieved at the soil free-field surface.

The current PC-3 and PC-4 SRS site-wide spectra are based on the WSRC analysis developed in 1997 (WSRC, 1997), and they incorporate variability in soil properties and soil column thicknesses applicable for the SRS. Following the development of PC-3 and PC-4 design basis spectra, the Defense Nuclear Facilities Safety Board (DNFSB) had several interactions with the DOE and WSRC on seismic design spectra. As a result, additional conservatisms were applied to the PC-3 spectral shape at low and intermediate frequencies (Gutierrez 1999). The shape change was incorporated in SRS Engineering Standard 01060. The shape change, illustrated in Figure 3-6, increased the response for low (0.1-0.5 Hz) and intermediate frequencies (1.6-13 Hz) of the design basis spectrum.

PC-3 spectra are applicable to DOE essential facilities, as described in DOE-STD-1020 (DOE 1996), and the PC-4 spectra are reserved for more critical facilities, such as nuclear reactors. The current design basis spectra for the PC-3 and PC-4 design events are shown in Figures 3-6 (curve based on Gutierrez, 1999) and 3-7, respectively. These design spectra were intended for simple response analysis of SSCs; they are not appropriate for geotechnical assessments.

3.4.4 Selection of MFFF Site Design Earthquake Motion

DCS, 2000dThe MFFF geotechnical data are consistent with the SRS site-specific data used to develop the PC-3 and PC-4 design spectra for the SRS. On this basis, the application of the PC-3 and PC-4 design spectra is confirmed to be appropriate for the MFFF site in accordance with WSRC (1997c). Analysis of the MFFF geotechnical data in WSRC (2001a) further confirmed that the site-wide criteria are also applicable to the MFFF site and that those criteria can be used

to establish the design earthquake (DE) for the MFFF site. Therefore, the PC-3 earthquake is applicable to the MFFF site, and it can be used to establish the DE for the MFFF site.

The calculation titled "Selection of Extreme Natural Phenomena for MOX Design" (DCS, 2000e) documents the basis for the MFFF DE, and itDCS (2000z demonstrates that designing the MFFF SSCs for the Reg. Guide 1.60 spectrum anchored to 0.20g horizontal acceleration is adequate to ensure that high consequence facility events are highly unlikely to occur. On this basis, the Reg. Guide 1.60 spectrum anchored to 0.20g horizontal acceleration was conservatively selected as the horizontal design spectrum at the soil surface for the MFFF site. Figure 3-8 presents the Reg. Guide 1.60 spectrum anchored to 0.20g, along with the PC-3 and PC-4 surface response spectra. As shown, the Reg. Guide 1.60 spectrum anchored to 0.20g lies between the PC-3 and PC-4 soil surface spectra.

The Reg. Guide 1.60 spectrum, anchored to 0.20g, is the same spectrum that was used for design of the Vogtle Nuclear Power Station, which is located directly across the Savannah River from the SRS. This response spectrum is intended for simple response analyses of SSCs; it is not appropriate for evaluation of the response of the soils beneath the site to earthquake loadings. For those analyses, which include the site response analyses that are performed to develop strain-compatible soil properties for use in the soil-structure interaction analyses and analyses of liquefaction potential and post-earthquake settlements, bedrock motions based on the SRS PC-3 bedrock spectrum will be used, scaled so that when amplified through the MFFF soil profile, the resulting surface motion will have a horizontal peak ground acceleration of (PGA) 0.20g. Section 6.2.3 of this report provides further discussion of the control motion used in the MFFF geotechnical analyses.

The horizontal peak ground acceleration (PGA) at the surface of the MFFF site for the DE was established at 0.20g (DCS, 2000d). The one-dimensional free-field site response analyses for a 0.20g surface response at the MFFF site are presented in Section 6.2 of this report. The results of liquefaction and post-earthquake settlement analyses are presented in Section 8.1 and 8.2, respectively, of this report.

4. GEOTECHNICAL EXPLORATION AND TESTING PROGRAMS

4.1 APPROACH

Geotechnical exploration and testing programs were conducted for the MFFF facilities in 2000 and 2002. Both programs included drilling and sampling borings and performing cone penetration test (CPT) soundings at the site. In addition, laboratory testing was performed on samples of the soils obtained during the exploration programs. Soft soils were found in some of the initial borings and CPTs completed in 2000 at the location of the MFFF facilities initially proposed in 2000. As a consequence of this, the MFFF was relocated approximately 400 feet to the west-northwest. Subsurface information from previous SRS explorations indicated that the revised site location was less likely to be underlain by large zones of soft soils. The latter portion of the 2000 explorations and all of the 2002 explorations were made at the revised MFFF site location shown in Figure 4-1.

The original exploration program consisted of thirteen (13) exploration borings and was initially planned to include thirty-seven (37) CPT soundings. However, after thick soft zones were encountered in the eastern portion of the MFFF site at the original building locations, twenty-six (26) additional CPTs were performed, for a total of sixty-three (63) soundings. Five dilatometer test (DMT) holes were performed at representative locations near CPT soundings and exploration borings to evaluate in situ stress conditions and to collect in situ data for correlation with the CPTs, exploration borings, and laboratory test results.

Fewer soft layers were indicated in the additional CPTs and borings completed in 2000 to the north and west of the initially planned site. Therefore, the MFFF site was relocated to the north and west of the original location, to the location shown on Figure 4-1, to reduce potential problems associated with soft soil layers.

The soils that were excavated from the APSF site were spoiled on top of the MFFF site. Because of the steep slopes along the sides of the APSF spoils pile, the drill rig and the CPT rig could not access all locations required to properly characterize the subsurface profile. Therefore, following construction of an access road along the perimeter of the APSF spoils pile, a supplemental geotechnical investigation was performed in 2002. This program consisted of seven (7) exploration borings and sixty-two (62) CPT soundings, which were performed within the final MFFF proposed site to obtain subsurface information in areas that could not be accessed by the rigs during the 2000 investigation and at other locations to better define the extents of soft zones encountered in the borings and the CPTs.

A total of fourteen (14) borings and 96 CPTs were performed at the MFFF site at the locations shown on Figure 4-1. The CPTs were pushed to cone refusal, which occurred at some locations before penetrating to the desired depth, the Congaree formation. Where a second attempt was performed at a nearby location, an "A" was added to the CPT identifier to distinguish it from the original CPT. For example, SCPT-87 hit refusal before penetrating the ST2 layer; thus, a second

attempt was made ~3 ft away from SCPT-87 and this SCPT was identified as SCPT-87A. These two CPTs are considered to have been performed at the same location.

The primary purpose of the exploration borings was to obtain SPT results for correlation with CPT results and to collect representative soil samples for laboratory testing. Several of the borings were drilled to a sufficient depth to establish the contact between the upper soil units and the Congaree Formation. The Congaree Formation is an established geologic marker bed in the F-Area and at the SRS.

Each CPT provided a continuous vertical log of the soil stratigraphy and provided data for use in evaluating site subsurface conditions and properties. CPTs have been used extensively and successfully at the SRS and the F-Area in recent years to define subsurface conditions for engineering and groundwater evaluations. The extensive use of the CPT at SRS provides an extensive database for correlation with the MFFF site program.

Tip resistance, pore water pressure, and sleeve resistance were measured in all CPTs. Downhole measurements of compression (P) and shear (S) wave velocities at depth intervals of 5 feet were performed in forty-four (44) of the CPT's. These CPTs were designated as seismic CPTs or SCPTs. Electrical resistivity measurements were performed for the full depth of penetration in seventeen (17) of the CPTs. Pore water pressure dissipation tests were performed at selected locations to determine the depth to groundwater.

Boring SPT penetration resistance (N) values, tip stresses and other data obtained from the CPTs, and laboratory tests from SPT samples and samples obtained from the tubes pushed in the CPTs, were correlated in DCS (2003q) and DCS (2003r). In general, the data from the borings and CPTs are consistent. The logs and other information from the borings and the CPTs, as well as the laboratory test results, were analyzed to develop data for several of the calculations, including DCS (2003d, 2003f, 2003c, and 2003d).

Soft zone and soft materials found in the borings and CPTs from the 2000 investigation were investigated in 2002 with more closely spaced CPT soundings than generally are used for standard geotechnical programs so that the extent any soft soils in the vicinity of critical structures could be more fully identified. For example, soft zone soils were found at elevations between approximately 175 and 185 feet in CPT-61. This CPT was located approximately 70 ft south of the southwestern corner of the MFFF Building, as shown in Figure 5-1. SCPT-66, CPT-67, CPT-103, and CPT-118 were performed between CPT-61 and the southwestern corner of the MFFF Building during the 2002 Supplemental Geotechnical Investigation. Except for CPT-103, no soft soils were found in any of these 2002 CPTs, nor were soft zones encountered in CPT-58 and CPT-62, which were completed in the area during the 2000 investigation. CPT-103 is located approximately 40 feet north of CPT-61 and approximately 30 feet south of the southern wall of the MFFF Building, as shown on Figures 4-1 and 5-1. CPT-58 and CPT-118 are located approximately 10 feet north of the southern wall of the MFFF Building. Therefore, the extent of the soft soils in the vicinity of CPT-61 are constrained based on the information from the six (6) additional CPTs performed in the surrounding area.

A thin-walled sampler was utilized in some of the CPT soundings to obtain soil samples in identified softer layers at depth. All of the exploration borings, CPTs, and DMTs were advanced and grouted in compliance with established SRS procedures to prevent cross flow or contamination from the upper aquifer system to the Congaree aquifer system beneath the site.

The laboratory testing program was developed to establish a database of index properties and the results of static and dynamic testing of the soils obtained from the various soil strata at the MFFF site. The testing program was designed to assist in the classification of subsurface engineering units for correlation with test data available from the F-Area and other relevant SRS sites and for use in establishing the engineering properties of the soils at the MFFF site.

Samples of cuttings from exploration borings and all soil samples were tested by SRS Health Physics personnel to verify whether radiological contamination was present at the site. For this extensive exploration and sampling program across the MFFF site, no radiological contamination was identified in any of the soil samples tested. No soil samples were removed from the SRS until cleared by SRS Health Physics personnel.

4.2 METHODOLOGY

The geotechnical exploration and testing programs were conducted in accordance with MOX Project Procedure PP 9-19, Geotechnical Exploration and Testing (DCS, 2000e). All field exploration programs were conducted under the engineering oversight of DCS Field Engineers, as outlined in DCS (2000e). The DCS Field Engineer performed engineering oversight and field documentation of all test boring and sampling activities, including preparation of the Log of Borings, selection of soil sampling type and location, and sample handling, packaging, storage, and shipment. The DCS Field Engineer also performed engineering oversight and field documentation of field activities associated with conducting the CPT soundings and DMT testing, including coordination with SRS Health Physics personnel for radiological testing of cuttings from exploration borings and samples collected for laboratory testing.

Miller Drilling Company, Inc. (Miller) performed the exploration borings and soil sampling in accordance with Specification for Geotechnical Test Borings and Sampling, DCS01-WRS-DS-SPE-G-00002, Rev. A (DCS, 2000b) and Rev. B (DCS, 2001h). All quality-related technical field activities for soil exploration and sampling were performed by the DCS Field Engineer in accordance with DCS (2000e). The drop-hammer weight for SPT testing was certified under the DCS Quality Assurance Program.

The CPT program was performed by Applied Research Associates, Inc. (ARA) in accordance with Specification for Cone Penetration Testing of Soil, DCS01-WRS-DS-SPE-G-00001, Rev. A (DCS, 2000a) and Rev. B (DCS, 2001g). ARA implemented their Quality Assurance Program requirements for all work performed per this specification. The DCS Field Engineer provided engineering oversight of the CPT program in accordance with DCS (2000e).

The soils testing programs were performed by MACTEC (formerly know as LawGibb Group, Inc., and Law Engineering and Environmental Services, Inc.) in accordance with Specification

for Laboratory Testing of Soils, DCS01-WRS-DS-SPE-G-00003-A (DCS, 2000c). Selection of samples for laboratory testing and definition of the soils testing program was prepared by DCS geotechnical engineers, under the supervision of the DCS Lead Geotechnical Engineer, in accordance with DCS (2000e).

4.3 SUBSURFACE INVESTIGATIONS

4.3.1 General

The geotechnical exploration programs for the MFFF site consisted primarily of cone penetration testing (CPT) and soil exploration borings. The initial CPT program began on May 31, 2000, approximately two weeks before the soil borings, so that preliminary analysis of the CPT data could be used to revise boring locations, as needed. The initial soil boring exploration program was completed on July 22, 2000 and the CPT program was completed on July 24, 2000. The 2002 Supplemental Geotechnical Investigation was performed in June and July of 2002. In addition, the results of geotechnical programs performed previously by others (Raymond, 1973; Geomatrix, 1998; WSRC, 1999a) adjacent to and on the MFFF site were used to evaluate subsurface soil and groundwater conditions. The locations of soil borings and CPT holes advanced by DCS, as well as those by others that were used to help characterize the MFFF subsurface soils, are shown on Figure 4-1. In addition to CPT and soil borings, dilatometer testing and seismic downhole testing were performed at the site. The following sections describe work performed as part of the MFFF geotechnical exploration programs.

4.3.2 Exploration Boring Program

Soil exploration borings were drilled at the MFFF site to depths ranging from approximately 115 feet to 181 feet below the present site grade. All of the borings were advanced using a CME-75 truck-mounted drill rig and the mud-rotary drilling method. Six-inch diameter PVC casings were installed in borings BH-2, BH-5, and BH-10 to facilitate downhole geophysical testing, as discussed in Section 4.3.5. The main purpose of the borings was to correlate the results of the CPT soundings, obtain soil samples for laboratory testing, and identify the Warley Hill Formation ("green clay" GC) and the top of the Congaree Formation (CG). A complete description of the boring program and the Logs of Borings are presented in Attachment 1.

4.3.3 Cone Penetration Tests (CPT)

During the 2000 investigation, sixty-three (63) CPT soundings were advanced to depths ranging from 85 feet to 166 feet below present site grade. All soundings were conducted with piezocones (P-CPT). Fifteen (15) soundings were conducted with a combined piezocone and seismic cone (S-CPT), and 20 soundings were conducted with a combined piezocone and resistivity cone (R-CPT). The target depth of the CPT soundings was the top of the Congaree Formation. However, this depth was not achieved in all of the soundings due to reaching the push capacity of the truck (60,000 pounds) before reaching the target depth.

The main purpose of the CPT soundings was to obtain a continuous profile of the subsurface conditions at several locations across the MFFF site. In this regard, the CPT is a particularly useful method for identifying soft zones. A thin-walled sampler was also used in conjunction with the CPT rig to obtain samples of potential soft zone materials for laboratory classification testing.

The initial CPT program consisted of 37 soundings, but additional soundings were performed as a result of the need to further delineate identified soft zones and to investigate the relocated sites for the MFFF and Emergency Generator Buildings.

During the 2002 Supplemental Geotechnical Investigation, cone penetrometer test soundings were performed at sixty (60) different locations, with second attempts made at the locations of SCPT-78 and SCPT-87. These were advanced to depths ranging from 105 to 165 feet below present grade. All CPTs measured tip stress, sleeve stress, and penetration pore pressure. At thirty locations (30), seismic wave measurements were recorded at five-foot intervals. At eight (8) locations, the cone penetrometer was advanced through hollow-stem augers in an attempt to penetrate the stiffer soils overlying the Congaree Formation. At these locations, compression waves were not acquired because they would have represented the P-waves of the steel casing rather than the P-waves of the soils. Shear waves were generated and acquired from the bottom of the casing to CPT refusal. Pore pressure dissipation tests were conducted in the majority of the soundings, as directed by the DCS Field Engineer. In addition to CPT soundings, twelve (12) soil samples were collected using ARA's thin-walled CPT soil sampler. All sounding locations were grouted upon completion as the cone was extracted from the hole.

The details of the CPT program conducted at the MFFF site, along with test results, are presented in ARA (2000 and 2003).

4.3.4 Dilatometer Tests

Dilatometer testing (DMT) was attempted in some of the CPT soundings made during the investigation performed in 2000 to provide additional in situ test data to correlate with the CPT, SPT, and laboratory test results.

High push pressures, generally greater than 500 psi, were required to advance the dilatometer probe into the predominately sandy soils. The high push pressures caused disturbance around the probe and resulted in calculated moduli values considerably lower than indicated by the adjacent CPT and SPT test results. The DMT test results were not considered representative of subsurface conditions indicated by the other CPTs and borings and were not used in further analysis. The data from the DMT holes is presented in ARA (2000).

4.3.5 Seismic Downhole Testing

Seismic downhole testing was performed in three of the soil borings (BH-2, BH-5, and BH-10) drilled at the original MFFF site. The primary purpose of this testing was to obtain shear wave and compression velocity data using alternative methods to the CPT and to obtain data at greater

depths. The seismic downhole testing was conducted from September 26 through September 28, 2000, after all of the CPT and drilling activities had finished in order to have a relatively "quiet" site for recording the seismic data.

The boreholes in which the testing was conducted were each located adjacent to an S-CPT sounding in order to obtain correlations between the downhole survey and S-CPT data. The boreholes were cased with 6-inch-diameter PVC plastic pipe, and the annular space between the outside of the casing and the borehole wall was grouted with lean cement grout.

Based on the results of the seismic downhole testing (discussed in Section 6.2.1), it appears that a solid coupling of grout between the casings and boreholes was not achieved in the lower sections of BH-5 and throughout BH-2. A solid coupling is important between the casing and soil to transmit the seismic waves from the ground to the geophones placed inside the casing. Loose soil along the casing can result in significant attenuation of seismic energy being measured. This lack of coupling between the soil and casing resulted in a reduced quality of data being obtained in BH-5 and BH-2.

A detailed description of the seismic downhole testing conducted at the MFFF site, along with test results, are presented in Bay Geophysical (2001). As indicated in that report, the S-wave interval velocity data measured in BH-10 compared favorably with those measured in CPT-34, which was located in close proximity to BH-10. The S-wave interval velocities were consistent with S-wave interval velocities found in similar soils. The P-wave interval velocities measured in BH-10 were higher than competent soils typical of the SRS area. Note, however, that due to the relocation of the MFFF Buildings to the location shown in Figure 4-1, the borings used for the downhole testing are no longer located in the vicinity of the planned MFFF structures.

4.4 LABORATORY TESTING PROGRAM

Laboratory testing was conducted on soil samples collected during the geotechnical field investigations. All testing was performed in accordance with the procedure outlined in DCS specification DCS01-WRS-DS-SPE-G-00003-A (DCS, 2000c). The purpose of the testing was to determine the index and engineering properties of the site soils pertinent to the geotechnical analyses and design for the MFFF facilities. The results of the testing program were also correlated with published laboratory test data from the APSF site, the F-Area Northeast Expansion area, and the F-Area to help identify the major soil units in the shallow (<200 feet) stratigraphy.

The testing conducted and the procedures followed included:

- Visual classification (ASTM D2487 and ASTM D2488)
- Moisture content (ASTM D2216)
- Wet and dry density (DCS01-WRS-DS-SPE-G-00003-A)
- Specific gravity (ASTM D854)
- Particle size analysis (ASTM D422 and ASTM D1140)
- Plasticity (ASTM D4318)

- Consolidation characteristics (ASTM D2435)
- Shear strength parameters (ASTM D4767)
- Dynamic behavior (shear modulus reduction and damping) (ASTM D3999 and ASTM D4015)

Samples for laboratory testing were selected based on a review of the soil boring logs and CPT results in order to obtain information most representative of the soils encountered. Revisions to the testing program were made as necessary, based on observations made in the laboratory. The results of the laboratory testing are discussed in Section 6 of this report. A description of the laboratory testing program and test results are presented in LawGibb (2001) and MACTEC (2003).

The laboratory Quality Assurance Manager was responsible for ensuring that the QA procedures outlined in DCS specification DCS01-WRS-DS-SPE-G-00003-A were followed. DCS QA personnel conducted an audit of the testing laboratory prior to the beginning of sample testing to ensure that the testing facilities and procedures conformed to the DCS QA requirements. Throughout the time period over which the testing was conducted, the DCS lead and/or field geotechnical engineers provided guidance, as necessary, and visited the laboratory to review the testing procedures and the results of the testing program.

5. SUBSURFACE CONDITIONS

5.1 ENGINEERING STRATIGRAPHIC UNITS

5.1.1 Subsurface Stratigraphy

The basis for the stratigraphic subdivisions used at the SRS site, as described in the following sections, was developed by WSRC (1996b, 1999a). The correlation of that alphanumeric system, which identifies strata at the site as "engineering units", with site geologic units, is summarized in Table 5-1. A detailed discussion of the geologic units is presented in Section 3.1.

Estimated elevations of the top of each of the various engineering units interpreted from the MFFF site CPT logs are summarized in Table 5-2 (DCS, 2003p). Engineering units shown on the boring logs in Attachment 1 (DCS, 2003n) are based on the units established for the CPTs. Six (6) geotechnical sections, located as shown in Figure 5-1, were developed to illustrate the subsurface stratigraphy to depths of approximately 130 to 165 feet below existing grades. These sections are provided in Figures 5-2 through 5-7.

In general, the subsurface stratigraphy of the MFFF site is consistent with the conditions found at the APSF site, located immediately south of the MFFF site, and the F-Area Northeast Expansion Area, located about 150 yards southeast. In addition, the average material properties for each of the stratigraphic layers discussed below correlate quite well with those found at the APSF and F-Area Northeast Expansion sites. A summary of the material properties for the MFFF subsurface soils, with comparisons to published averages for F-Area, APSF, and F-Area Northeast Expansion soils, is presented in Table 6-2. This table shows that layer thickness and engineering unit index properties for the subsurface units at the MFFF site are reasonably consistent with those found at the F-Area sites.

5.1.1.1 TR1

The TR1 layer is sometimes referred to as the "Upland Unit." In general, TR1 soils consist of red, purple, and brown poorly sorted sands, clayey sands, and silty sands in a medium dense to dense state. The base of the unit is characterized by an irregular erosional surface. This unit ranges from zero to about 70 feet thick at the SRS.

The TR1 layer is typically found at El 270 or higher at the MFFF site, and it often contains some fine gravel and is less fine-grained than the underlying TR1A. The TR1 layer is characterized by moderate CPT tip resistances and relatively high friction ratios. TR1 ranges in thickness from approximately 1 to 19 feet at the MFFF site. The top of TR1 ranges between approximately elevations 272 to 286 feet.

5.1.1.2 TR1A, TR2A, TR2B, and TR3/4

The TR1A, TR2A, TR2B, and TR3/4 layers designate the Tobacco Road Formation. Sediments of the Tobacco Road Formation were deposited in low energy, shallow, marine, transitional

environments, such as tidal flats. As a result, these sediments exhibit a relatively distinct laminated structure consisting of red, brown, and purple, medium dense to dense, poorly sorted sands and clayey sands. The boundary between TR1A and TR2A is often identified by an increase in CPT tip resistance and notably lower sleeve friction values, resulting in substantially lower friction ratios. Although TR2A and TR2B have very similar material properties, TR2B is typically identified by an increase in CPT tip resistance.

The TR1A unit ranges in thickness from about 1 to 17 feet, and has an average top elevation of approximately 270 feet at the MFFF site. TR2A varies from approximately 12 to 35 feet in thickness at the MFFF site and has an average top elevation of 263 feet. The thickness of TR2B ranges from approximately 18 to 34 feet. The average elevation of the top of TR2B is 237 feet.

The TR3/4 layer consists primarily of stiff clay and sandy clay, interbedded with loose to medium dense clayey sands and sandy silts. The fine-grained fraction (minus No. 200 sieve) of the TR3/4 soils is moderately to highly plastic. The upper boundary of the TR3/4 layer is defined by a significant decrease in CPT tip resistance and an increase in friction ratio and pore pressure, relative to the TR2B layer. The TR3/4 layer appears to be continuous across the MFFF site, ranging in thickness from about 3 to 17 feet, and has an average top elevation of approximately 212 feet.

5.1.1.3 DB1/3 and DB4/5

The DB1/3 and DB4/5 units are used to designate the Dry Branch Formation. The DB1/3 layer corresponds to the Irwinton Sand member, and it consists mainly of silty sands and poorly graded sands, with widely interspersed thin sandy clay and clayey sand layers. The sands are generally medium dense, with widely interspersed pockets of loose and dense to very dense material. The fines within this layer are notably more plastic than those reported in the DB1/3 layer at the APSF and F-Area Northeast Expansion sites, but they are closer to the average values reported for F-Area (WSRC, 1996b and 1999a). DB1/3 is characterized by variable, but generally high, CPT tip resistances, low friction ratios, and near hydrostatic pore pressures. The DB1/3 layer at the site ranges in thickness from about 12 to 32 feet, and it has an average top of layer elevation of approximately 204 feet.

The DB4/5 layer consists mainly of loose to medium dense, medium to highly plastic, clayey and silty sands. In general, this layer is more clayey and silty than the underlying ST1 layer. The DB4/5 layer typically exhibits moderate to low CPT tip resistances and moderate friction ratios. The DB4/5 layer has been extensively characterized within the APSF site because of the presence of several "soft zones" (defined at SRS as zones having CPT tip resistance of 15 tsf or less or an SPT N-value of 5 blows/ft or less). Some soft zones were also identified in the DB4/5 layer at the MFFF site, as discussed in Section 5.2 below. At the MFFF site, the DB4/5 layer ranges in thickness from about 4 to 16 feet, and it has an average top of layer elevation of approximately 183 feet.

5.1.1.4 ST1 and ST2

The ST1 and ST2 units are used to designate the Santee/Tinker Formation, which is generally regarded as the most complex geologic unit in the shallow subsurface of F-Area (WSRC, 1999a). Soils in this formation are characterized by highly variable material properties. The Santee/Tinker Formation is generally distinguished from the overlying Dry Branch Formation by CPT tip resistances and friction ratios exhibiting a pronounced saw tooth profile, with large variations over small vertical intervals. This pattern is consistent with lenses of clayey and silty sands, interfingering with more resistant, silica-cemented sediments and less resistant, calcareous sediments.

The ST1 and ST2 layers consist mainly of silty sands and poorly sorted sands. In general, the ST1 layer is dense to very dense, while the underlying ST2 layer is loose to medium dense. The ST1 layer is characterized by markedly higher CPT tip resistances and sleeve friction than either the DB4/5 or ST2 layers. At the MFFF site, the ST1 layer ranges in thickness from about 17 to 26 feet, with an average top elevation of about 174 feet. The ST2 layer ranges in thickness from about 6 to 16 feet, and it has an average top elevation of approximately 153 feet.

5.1.1.5 GC

The term "green clay" is an informal stratigraphic name used at the SRS for the medium dense to dense green, brown and gray, clayey sands, silty sands, sandy silts, and stiff to very stiff sandy clays that mark the Warley Hill Formation, which underlies the Santee/Tinker Formation at the site. The GC layer is locally continuous across F-Area, and it typically is used at the SRS to define the lower boundary of the shallow stratigraphy. The GC layer found in the CPTs and borings performed at the MFFF site ranges in thickness from about 1 to 7 feet, and it has an average top elevation of approximately 141 feet. The borings and CPTs indicate that the GC layer is continuous across the MFFF site.

The GC unit also contains some isolated soft soils that are less than 2 feet in thickness, as discussed in Section 5.2.

5.1.1.6 Congaree to Bedrock

The Congaree Formation at the MFFF site is identified as very dense sand. Once the Congaree Formation was reached, boring refusal ($N > 100$ blows/foot) and CPT refusal (tip resistance > 400 tsf) was quickly achieved.

The Congaree Formation is considered to be continuous across the MFFF site, and it has an average top elevation of approximately 137 feet. It is underlain by Paleozoic crystalline bedrock at an elevation of approximately -585 feet (WSRC, 1996b).

5.2 SOFT ZONES AND SOFT MATERIALS

Soft zones at the MFFF site are defined using the same criteria applied to the APSF site and F-Area Northeast Expansion (WSRC, 1996b, 1999a, and 1999b), which are described as follows:

- Soils found within the lower Dry Branch or Tinker/Santee geologic units that exhibit a corrected CPT cone tip resistance equal to or less than 15 tons per square foot (tsf) or a Standard Penetration Test (SPT) N-value equal to or less than 5 blows/ft over a continuous interval equal to or greater than 2 feet in thickness. In accordance with site practice, the Lower Dry Branch geologic unit is engineering unit DB4/5 and the Tinker/Santee geologic units are engineering units ST1 and ST2.
- If two or more soil layers within the DB4/5, ST1, or ST2 engineering units with CPT cone tip resistances equal to or less than 15 tsf or SPT N-values equal to or less than 5 blows/ft are separated by less than 1 foot of firmer soil, they are considered a soft zone if the total aggregate thickness of the soft soils is equal to or greater than 2 feet. The total thickness of such soft zones is the sum of the soft layers, and it does not include the thickness of any intermediate firmer soils.

“Soft Materials” are materials within engineering units other than DB4/5, ST1, and ST2 that otherwise conform to the same criteria specified above for “soft zones.”

The soft zones and soft materials were found in the CPTs and borings at the MFFF site, as illustrated in Figure 5-1 and Table 5-3 (DCS, 2003f). They are also shown on the geotechnical sections included as Figures 5-2 through 5-7. The lateral extent of the soft layers shown on the sections was estimated based on whether a soft layer was found in adjacent CPTs in the same engineering unit and at nearly the same elevation. If so, the soft layer was estimated to extend to the adjacent CPT or boring. If not, the soft layer was estimated to extend to approximately midway between the CPT and adjacent CPTs and/or borings.

Table 5-3 shows that SCPT-81 encountered the thickest soft zone found during the MFFF geotechnical investigations, and this soft zone was 11.8 feet thick. This SCPT was located outside of the footprint of the MFFF Building, approximately 65 ft west of the western edge of building. CPT-99, Boring BH-14, and CPT-82 were completed to the north, east, and south of SCPT-81, respectively, in order to evaluate the extent of the soft zone encountered in SCPT-81, and they demonstrated that the soft zone found in SCPT-81 is not continuous across this portion of the site. Therefore, the 11.8-ft thick soft zone encountered in SCPT-81 is an isolated soft zone, and it does not extend under the footprint of the MFFF Building..

5.3 GROUNDWATER CONDITIONS

Section 1.4.2 of WSRC (2000a) provides a detailed discussion for the groundwater hydrology at SRS and the F-Area. This section presents a summary of groundwater hydrology for the MFFF site.

5.3.1 Groundwater Aquifers

Groundwater at the MFFF site flows vertically and laterally. In the unconfined Upper Three Runs Aquifer, lateral flow is generally to the northwest, across the MFFF site, toward discharge points near Upper Three Runs Creek (Figure 5-8); vertical flow is downward, toward the GC

layer, which acts as a confining unit for the underlying Gordon Aquifer. Groundwater in the Gordon Aquifer also flows generally northwestward until it discharges along Upper Three Runs Creek. Elevation heads are approximately 60 feet higher in the Upper Three Runs Aquifer than in the Gordon Aquifer. This condition creates the potential for downward flow across the GC layer and into the Gordon Aquifer. However, laboratory and field data demonstrate that the GC layer is a significant barrier to downward vertical flow in this area (Aadland, et al., 1995).

The deeper Crouch Branch Aquifer is the principal water-producing aquifer at SRS. Groundwater in the Crouch Branch Aquifer flows southwestward, toward the Savannah River floodplain. In F-Area and at the MFFF site, there is a well defined "head reversal" across the Crouch Branch Confining Unit. In this area, elevation heads are approximately 30 feet higher in the Crouch Branch Aquifer than in the overlying Gordon Aquifer. This condition effectively prevents downward flow from the Gordon Aquifer, and naturally protects the Crouch Branch Aquifer from contaminants present in shallow groundwater.

Groundwater surface elevations estimated from CPT pore pressure dissipation tests made in the CPTs are summarized in Table 5-4 (DCS, 2003p). The data indicate the groundwater surface elevation ranges between approximately 175 and 207 feet. The site groundwater levels are consistent with groundwater contours presented for the Upper Three Runs aquifer in WSRC (2000a and 2000b). At the time of the field exploration programs, SRS had been experiencing drought conditions. Long-term groundwater monitoring in the F-Area indicates that the groundwater level can fluctuate as much a 10 feet seasonally (WSRC, 1999a).

The design groundwater level at the location of the MFFF and BEG Buildings has been conservatively established at El 210, which is approximately 60 feet below planned final grade for the site.

5.3.2 Groundwater Quality

Groundwater quality in F-Area and MFFF site is not significantly different from that for SRS as a whole. It is abundant, usually soft, slightly acidic, and low in dissolved solids. High dissolved iron concentrations occur in some aquifers.

WSRC (2000b) provides a comprehensive discussion of groundwater contamination plumes in the F-Area, and it covers the MFFF site. Also, WSRC (1995a) defines the soil and groundwater contamination from past disposal practice into the Old F-Area Seepage Basin, which is located just northwest of the MFFF site area. The contaminated soil zone within the Old F-Area Seepage Basin was remediated in 2000.

As noted in WSRC (1995a), the contamination plume from the Old F-Area Seepage Basin migrates to the north, away from the MFFF Building area, and it is located at depth within the groundwater aquifer. Part of this plume passes under the northwestern corner of the MFFF site within the boundary area located northwest of the transmission corridor.

WSRC (2000b) characterized groundwater conditions in and around the F-Area and delineated contamination plumes migrating from the Mixed Waste Management Facility, located southeast of F-Area. This report indicates that there are no known soil or groundwater contamination plumes originating from the Mixed Waste Management Facility that will pass beneath the MFFF building areas. The absence of subsurface site radiological contamination was confirmed with the recent comprehensive geotechnical investigations conducted during 2000 and 2002 at the MFFF site. Radiological testing was performed on drill cuttings and samples obtained from the exploration activities. No radioactive contamination was encountered during this program in the Upper Three Runs or Gordon Aquifers, which are the upper aquifers at the MFFF site.

Although no radiological contamination was found during the 2000 and 2002 field investigations, subsequent depth-discrete groundwater sampling at the MFFF site and to the immediate southwest proved the existence of contaminated groundwater in the Upper Three Runs Aquifer, about 80 to 130 feet beneath the MFFF site (WSRC, 2002a). Shallow groundwater in this area is contaminated with various heavy industrial and nuclear contaminants, including tritium, nitrates, trichloroethylene, and alpha and beta emitters. Groundwater contamination is present beneath the entire MFFF site, but is most pronounced beneath the far western edge of the site, in the flow path of a plume(s) originating at the Old F-Area Seepage Basin and from other F-Area facilities.

Any existing or future groundwater contaminant plumes beneath the MFFF Building site would be located at least 60 feet or deeper in the subsurface, within the Upper Three Runs and/or Gordon Aquifers. The anticipated construction, site preparation, and development for the MFFF facilities will be confined to elevations well above this zone. The construction and operation activities for the MFFF, as planned, will not have any adverse effects on the existing aquifer systems beneath the MFFF site area.

6. ENGINEERING PROPERTIES

6.1 STATIC PROPERTIES

6.1.1 General

The engineering properties for static analyses were developed using the results of field and laboratory tests. The details of the geotechnical exploration programs are discussed in Section 4.3. Field in situ test measurements consisted of SPT N-values and CPT data, which included measurement of seismic wave velocities, tip resistance, sleeve friction, pore pressures, and soil resistivity. Dilatometer testing was performed at selected locations adjacent to CPT test holes during the subsurface investigation that was performed in 2000. It was difficult to push the DMT probes into and through the very dense soil layers in the subsurface profile. It appears the difficult pushing caused the probes to “wobble” somewhat, so that the sides of the probes were not in full contact with the surrounding soils. Therefore, data from the DMTs did not appear to be consistent and representative of conditions indicated by the adjacent CPTs and, consequently, the results of the dilatometer testing were not considered representative of in situ soil conditions. Therefore, the DMT results have not been used to develop engineering properties. Downhole seismic testing also was performed to obtain shear and compressional wave velocities; however, only one (BH-10) of the three test locations provided good data and, as explained in Section 4.3.5, after relocating the MFFF to the location shown in Figure 4-1, BH-10 is no longer within the area proposed for the MFFF structures.

Laboratory tests were performed on representative samples of the soils obtained for the various engineering units to establish physical and static engineering properties for the soils. Laboratory testing consisted of testing for moisture content, unit weight, particle size analysis, plasticity, consolidation characteristics, and shear strength. The details of the laboratory testing program are discussed in Section 4.4.

The field and laboratory test results were combined to create a database for each engineering unit. The results of testing for the MFFF site were compared to results published for the F-Area Northeast Expansion (WSRC, 1999a), Significance of Soft Zone Sediments at the Savannah River Site (WSRC, 1999b), APSF Additional Geotechnical Investigation Program Plan (WSRC, 1998), Final Geotechnical Report Actinide Packaging Storage Facility (APSF) (Geomatrix 1998), and F-Area Geotechnical Characterization Report (WSRC, 1996b).

6.1.2 CPT and SPT Field Test Results

The results of the CPT and SPT testing from the field exploration programs are summarized by engineering unit in Table 6-1. The results are presented as an average of properties for each engineering unit. The averages of SPT N-values include the N-values obtained within soft layers.

The CPT tip resistance values were corrected using the net area concept, as discussed in ARA (2000 and 2003). The corrected tip resistance is referred to as q_{cor} (same as q_t in ARA, 2000 and 2003).

The results are presented in Table 6-1 DCS, 2001c for each engineering unit and are compared with average values available in the F-Area and Northeast Expansion reports. Data comparisons were also made where data was available for the APSF area. The average SPT and CPT test values for the MFFF site compare well with those obtained from the other nearby F-Area studies. The N-values and q_{cor} for the MFFF site trend slightly lower to approximately the same as the values defined for the same engineering unit in the F-Area, except for ST1, where the MFFF values are higher than those in the F-Area. The shear wave velocities determined for each engineering unit are approximately the same as those determined in the other studies. With the high number of exploration holes used for the MFFF site, the N-values, q_{cor} , and shear wave velocities for the MFFF site are considered representative for each engineering unit and are recommended for use in engineering analysis. No unusual site conditions were encountered at the MFFF site, and the subsurface conditions are similar to those anticipated, based on results from the geotechnical studies of adjacent sites.

6.1.3 Classification and Physical Property Test Results

Classification and physical property testing consisted of Atterberg limits, water content, grain size analysis, hydrometer analysis, and density determinations. The averages determined for each engineering unit are presented on Table 6-2 (DCS, 2001c and 2003k).

The liquid limit (LL) and plasticity index (PI) averages for the fines content of soil samples obtained from the MFFF site are slightly higher than the results listed in the APSF and Northeast Expansion reports. The water content, dry density, and percent sand content averages are approximately the same as reported in the other geotechnical reports. As shown by the averages, the percent sand content is generally greater than 60 percent. The sandy nature of the subsurface soil units is also confirmed by the CPT results, which indicate a low friction ratio (f_s) and a low pore pressure during testing, as indicated in Table 6-1. Even though the percentage of fines is low in the samples, the fines content in each engineering unit generally classifies as a CL or CH.

The classification and physical test result averages presented for each engineering unit are considered representative of the subsurface engineering units for the MFFF site. The values are considered appropriate to use for engineering analysis and evaluation of each engineering unit.

6.1.4 Strength Test Results

Triaxial shear tests were performed on soil samples obtained from nine representative locations at the site, which represent five engineering units. All of the samples tested were clayey sand, and the results presented are only considered representative of the clayey sands that would be encountered in these respective engineering units. The samples obtained for testing were also representative of the softer and lower density materials encountered in the engineering unit.

Representative undisturbed samples of the cleaner, denser sand could not be effectively obtained during the exploration program, because of the difficulty inherent in trying to obtain such samples.

The results of these tests are presented in Table 6-3 (DCS, 2001c), and they should only be used to evaluate the softer, lower density, and more clayey zones within the engineering units. The test results for the MFFF site compare favorably with test results reported in the F-Area and APSF reports for the TR3/4 and DB4/5 engineering units. The shear strength results presented for the TR3/4 and DB4/5 units are considered appropriate for these two softer units. Other strength values presented in Table 6-3 are not considered representative of the average strength of the engineering unit. The N-values and q_{cor} results presented in Table 6-1 are considered more appropriate to estimate the in situ strength of the sandy subsurface materials, and they have been used in the geotechnical analyses.

6.1.5 Consolidation Test Results

Consolidation tests were performed to obtain representative consolidation properties for each of the engineering units. Sampling was generally limited to the more clayey and softer materials within the engineering unit. The average results for the consolidation tests performed in each engineering unit are presented in Table 6-4 (DCS, 2001c).

The average values of C_c , C_r , and P_c for MFFF are presented as two values. The first value in each of these columns generally represents the values reported by the laboratory (LawGibb, 2001). The LawGibb Group interpreted these values in accordance with conventional methods used in soil mechanics practice. The values that are enclosed within parentheses in Table 6-4 represent DCS's re-interpretation of the consolidation test results based on practical field experience and conditions existing at the MFFF site.

There is little difference between the C_c values, which is to be expected, because the method used in interpreting the C_c values is exactly the same. The single value of C_c that changed, the one for TR3/4, went from 0.41 to 0.34 because of a typographical error and the inclusion of two additional test reports that were omitted in the earlier determination of the average C_c for this engineering unit.

The differences shown between the two sets of C_r values are the results of differences in the method of interpretation. C_r values were originally determined using the average of the values determined from the rebound-reload cycle and the final rebound cycle. The values in parentheses were determined based solely on the rebound-reload cycle, as recommended by Leonards (1976) for estimating consolidation settlements of shallow foundations on overconsolidated clay. The differences between these C_r values are insignificant for the sandier engineering unit soils near the surface of the profile and are slightly more significant for the more clayey engineering units at depth.

The results from the MFFF site show close correlation with results from the F-Area and APSF results for void ratio, C_c , and C_r . The variation seen in the average test results between the areas

is to be expected. Disturbance of the sandy soils during sampling and sample preparation for testing is reflected in the shape of the consolidation curves. The maximum past pressure values (preconsolidation pressures, P_c) are somewhat underestimated due to the sandy nature of the site soils and observed disturbance effects in the consolidation test curves. Recent re-interpretation of the P_c values, recognizing the geological history of the site and the trends apparent in the virgin compression portion of the better-quality test results, yields better agreement between the P_c values from the MFFF tests and those from other areas at the SRS.

The settlement analyses that were performed, which are described in Section 7 of this report, are based on the first value of C_c and C_r presented in Table 6-4. However, recognizing that these soils are overconsolidated, the P_c values used in those analyses were set large enough to ensure that the recompression indices would be used to estimate settlements. As discussed in Section 7, an additional "what-if" analysis was performed assuming that these soils were normally consolidated, and it illustrated that settlements on the order of 30 inches would be estimated if these soils were actually normally consolidated. Settlement data measured for comparably loaded foundations in other areas of the SRS over nearly 20 years indicates that settlements of this magnitude are inappropriate for these soils (WSRC, 2002b).

6.1.6 Soft Zone Engineering Properties

Engineering properties of the soft zones at SRS have been studied extensively over several years and are summarized in WSRC (1999b). A sufficient number of CPT, SCPT and exploration borings were performed to confirm the lateral and vertical extents of the soft soil layers identified in the vicinity of the MFFF and BEG Buildings. All soft soil layers were determined to be isolated and limited in vertical and lateral extent. A constant CPT cone tip resistance (q_t) indicates there are no voids in any of soft soil layers. Soil samples were obtained from the identified soft soil layers for laboratory testing. The CPT, SCPT, exploration boring, and laboratory test results are considered adequate to classify and define engineering properties of the soft soil layers identified beneath the MFFF and BEG Building locations. The in situ test results and laboratory test results indicate that the soft soils are consistent with soft zones described in WSRC (1999b).

The analysis of the soft soil layers beneath the MFFF and BEG Building locations indicates that the measured index and mechanical properties are consistent for each engineering unit (DCS, 2003f and 2003j). The assessment of engineering properties demonstrates that these soft soil layers have a soil structure that is intact and does not exhibit any characteristics indicative of the presence of voids or collapsible soils. The in situ condition and engineering properties also indicate that these soft soil layers are at least normally consolidated and are supporting the full overburden pressures.

Soil classification and engineering properties are similar for each engineering unit; therefore, a single set of geotechnical properties can be used for all of the soft soil layers identified beneath the MFFF and BEG Building locations. These properties are presented on Table 6-17, Soft Soil Layer Classification and Engineering Properties, BMF and BEG Building Location. On Table 6-

Shear wave velocities for deeper soils were based on data from the APSF site, located approximately 800 feet south of the MFFF Building area, and other areas within the SRS (Geomatrix, 1997b). The bedrock within F-Area is reported to be crystalline in nature and very strong, with an estimated shear wave velocity of 11,000 ft/sec (WSRC, 1996b). The generalized geologic profile for the MFFF site is presented on Table 6-5 and shown on Figure 6-1. The generalized low-strain shear wave velocity profiles for the MFFF site are shown on Figure 6-2 (DCS, 2003a). The upper 130 feet of the generalized geological profile (above the Congaree) was developed using MFFF site-specific data, and the lower profile (below the GC) was based on Geomatrix (1997b). The upper 130 feet of the 18 individual low-strain shear wave velocity profiles developed for site response analyses are presented on Figures 8-112 through 8-129.

The compacted select structural fill was assumed to have a shear wave velocity of 1,300 fps for design purposes. This results in a dynamic shear modulus, G_{max} , of 7,600 ksf; dynamic Poisson's ratio, μ_{dyn} , of 0.35; and dynamic elastic modulus, E_{max} , of 20,500 ksf.

6.2.1.1 Seismic CPT Data

Of the 125 CPT soundings performed at the MFFF site, 44 were seismic CPTs. Of the 44 SCPTs performed at the MFFF site, 32 were performed within the Perimeter Intrusion Detection and Surveillance (PIDAS) fence line of the relocated MFFF site. The locations of the SCPTs are shown on Figure 4-1. Table 6-6 lists the 18 SCPTs selected from representative locations among the 44 SCPTs within the PIDAS, which were used in ProShake analyses on individual soil columns.

The results of the shear wave velocity tests from the SCPTs are presented in reports by ARA (2000 and 2003). After identifying the various engineering units on each of the 32 SCPT traces, the shear wave velocity for each layer was taken as the mean of all SCPT velocities for that layer. Since the SCPTs extend only as deep as the "Green Clay" (GC) layer, this methodology was adopted to determine the generalized shear wave velocity profile from the ground surface to the GC layer. The statistical summary of shear wave velocity data computed from the SCPT sounding data is presented in Table 6-7. The interval velocities for each SCPT compared to the generalized profile (down to the GC layer) are shown on Figures 6-3A and 6-3B (DCS, 2003a).

6.2.1.2 Seismic Downhole Survey Data

Seismic downhole surveys were conducted at the MFFF site in three boreholes during the geotechnical investigation that was performed in 2000, as discussed in Section 4. The results of the surveys are presented in the final report of the geophysical testing prepared by Bay Geophysical (2001). As discussed previously, the downhole survey data are considered questionable apparently because of poor coupling between the soil and borehole casings. While relatively good agreement was achieved with the adjacent SCPT soundings in the upper 50 to 60 feet of BH-5 (SCPT-19) and BH-10 (SCPT-34), there was a significant divergence between the data at greater depths. In BH-2, there was no discernible correlation of data with SCPT-11. Because of the lack of data correlation with adjacent SCPTs and the poor quality of the grouting

of the PVC casing, the downhole survey data were used only in the MFFF analyses when it was considered representative of adjacent SCPT data.

6.2.1.3 Maximum Shear Modulus

The maximum shear modulus (G_{\max}) of the soil is used to calculate strain-compatible shear wave velocities, as discussed in Section 6.2.3.4. The maximum shear modulus represents the stiffness of the soil at very small strain levels and is computed as:

$$G_{\max} = \rho V_s^2$$

where: ρ = mass density of the soil (slug or $\text{pcf}/(\text{ft}/\text{sec}^2)$) and V_s = shear wave velocity measured in the field (ft/sec).

6.2.1.4 Shear Modulus and Damping Variations with Strain

As strains increase in a soil mass, the soil behavior becomes progressively more nonlinear, with a reduction in shear modulus and an increase in material damping. The reduction in shear modulus is typically normalized with respect to G_{\max} and expressed as a normalized (G/G_{\max}) modulus reduction versus strain relationship. Both modulus reduction and damping ratio variations with strain are dependent upon material type. In the site response analyses, the nonlinear dynamic soil behavior is accounted for through iteration of soil properties using an equivalent linear approach. The peak shear strain developed in the center of each soil layer is computed for each iteration. An effective strain representative of the average strain level of each layer during the earthquake is computed based on the assumption that it is equal to 65 percent of the peak strain value. The dynamic shear modulus and damping ratio to be used for each layer in the next iteration are evaluated based on their compatibility with the effective shear strain. The variations of normalized strain-compatible shear moduli (with respect to their low-strain value) with effective shear strain are defined by shear modulus reduction curves. The variations of damping ratio with effective shear strain are defined by damping curves.

Based on the results of an extensive study of SRS soils, WSRC (1996a) developed a set of recommended modulus reduction and damping curves for the major SRS soil units. Tables 6-8 and 6-9 present the recommended values, which also are shown graphically in Figures 6-4 and 6-5.

Cyclic triaxial and resonant column testing were conducted on a limited number of soil samples from the MFFF site to evaluate the applicability of the WSRC-recommended modulus reduction and damping curves to the site soils. The modulus reduction and damping ratio relationships resulting from these tests are shown in Figures 6-6 through 6-9, along with the WSRC-recommended curves for the same soil units (DCS, 2001b). From the figures, it is apparent that the modulus reduction values for the MFFF site soils compare quite well with the SRS-recommended values. However, the MFFF damping ratios are considerably higher than those recommended by SRS. Based on evidence presented by Stokoe, et. al. (WSRC, 1996a) from an

analysis of numerous dynamic laboratory test results, the overestimation of damping is likely due to the effects of excitation frequency at small strains that occur when using the resonant column test (DCS, 2001b). Based on the good agreement between the laboratory and SRS modulus reduction values, the SRS-recommended modulus reduction and damping values were used in the free-field site response analyses conducted for the MFFF site, as discussed in Section 6.2.3.

6.2.2 Dynamic Poisson's Ratio

Dynamic Poisson's ratio values of the near-surface soil strata were computed (DCS, 2003b) using wave velocity data measured in the seismic CPTs that were performed during MFFF geotechnical investigations in 2000 and 2002 (ARA, 2000 and 2003). Twenty-two of the seismic CPTs performed at the MFFF site included measurements of shear and compression wave velocity data at the same depth. These seismic CPTs are identified in Table 6-10, and their locations are shown in Figure 4-1. The velocity of the compression wave (V_p) in water is much higher than V_p in the soils; therefore, V_p measurements of saturated soils below the groundwater table would generally manifest the V_p of the water. Therefore, the V_p of water is frequently used to identify the location of water table in a soil profile. However, the reports by ARA (2000 and 2003) do not include compression wave values below the groundwater table.

Equation [1], below, was used to calculate the values of Poisson's ratio, μ , for each depth within each CPT data file where both shear and compression wave velocities were measured. Equation [1] was obtained by simple manipulation from Equation [2] below, which is from Eq. [3.82] in Das (1993).

$$\mu = \frac{1}{2} \cdot \frac{\left[\left(\frac{V_p}{V_s} \right)^2 - 2 \right]}{\left[\left(\frac{V_p}{V_s} \right)^2 - 1 \right]} \quad \text{Eq. [1]}$$

Where V_s = Shear wave velocity
 V_p = Compression wave velocity
 μ = dynamic Poisson's ratio

$$\frac{V_p}{V_s} = \sqrt{\frac{2(1-\mu)}{1-2\mu}} \quad \text{Eq. [2]}$$

Poisson's ratios computed using Eq. [1] at all available pairs of wave velocity measurements from the 22 seismic CPT data files are presented in Attachment B and summarized in Table 3 of Calculation G-00015-B (DCS, 2003b). These Poisson's ratios are considered as raw data that need to be filtered to eliminate data that are erroneous and out of the typical ranges observed for soils in geotechnical engineering.

To establish a typical range of Poisson's ratio values for the MFFF soils, the predominant soil type, density, and moisture content, etc, were evaluated and are summarized in Table 3 of the calculation. Typical ranges for Poisson's ratio for soils are provided in Table 2-7 of Bowles (1996). Based on the soil type/condition-dependant value ranges and the dominant soil types at MFFF site, a lower end value of 0.20 and an upper end value of 0.40 were selected for the MFFF soils that are above groundwater table. These boundary values bracket the recommended values for all sands, gravelly sand, silts, and unsaturated sandy clays, which are typical types of soil encountered at MFFF site.

Table 4 of Calculation G-00015-B (DCS, 2003b) presents the Poisson's ratios included in Table 3 of the calculation after filtering based on the established range identified above. Table 6-11 included herein summarizes the data, after filtering, for each engineering unit, presenting the average, minimum, maximum, and standard deviation of the filtered values for the engineering units above the groundwater table. The recommended values of Poisson's ratio for dynamic analyses of the MFFF site are presented in Table 6-12.

6.2.3 One-Dimensional Free-Field Site Response Analyses

6.2.3.1 General

One-dimensional free-field site response analyses were performed for the MFFF site to estimate the response characteristics of the soil column and the dynamic soil properties representative for the small to moderate cyclic strains generated during the design-level earthquake. Three sets of site response analyses were performed as described below:

- In the first, an generalized soil column and associated material properties were developed as described in Section 6.2.3.3. This set of data was analyzed using a modified PC-3 time history, as described in Section 6.2.3.2 (DCS, 2003a). The strain-compatible dynamic properties discussed in Section 6.2.3.5 were developed from this set of analyses. In addition, the resultant cyclic stress ratios from the best-estimate case in the analyses were used in the evaluation for potential of liquefaction and post-earthquake settlements.
- The second set consisted of site response analyses on the generalized soil column using the 1886 Charleston earthquake control motion (DCS, 2003e). The results were used to evaluate the liquefaction potential associated with a large, distant event.
- The third set of analyses consisted of performing site response analyses on 18 individual soil columns and associated material properties, which were developed at

selected locations within the MFFF site, as described in Section 6.2.1. Both the modified PC-3 motion and 1886 Charleston earthquake control motion were used as input to the individual soil columns in the site response analyses (DCS, 2003h). The purpose of this set of analyses was to evaluate the variability of the individual SCPTs to the composite site response using the generalized soil column and material properties.

The strain-compatible dynamic soil properties computed from the first analysis were input into the dynamic soil-structure interaction analyses of the critical MFFF structures. The cyclic stress ratios computed from the first and second sets of analyses and those from the third set analyses using the 1886 Charleston control motion were input into the liquefaction analyses performed for the MFFF site, as described in Section 8.

The site-response analyses were performed using the computer program ProShake, Version 1.1, which is a product of EduPro Civil Systems, Inc. In this program the geo-material mass is represented by a 1-D soil column, and the soil nonlinear and inelastic properties are simulated by equivalent linear properties through iteration. Validation of this program was documented in a separate calculation (DCS, 2001d).

6.2.3.2 Control Ground Motion

6.2.3.2.1 Modified PC-3 Motion

The bedrock motion used as the design basis motion in the site response analyses is based on the SRS PC-3 uniform hazard rock design response spectrum. The spectrum-compatible acceleration time history for this design spectrum was developed by WSRC (1998), and it has a peak ground acceleration (PGA) at rock outcrop of 0.11g and a probability of exceedance of 5×10^{-4} (WSRC, 2000).

As indicated in Section 3.4.4, convolution analyses of the MFFF subsurface profile were performed, and it was determined that when the PC-3 bedrock motion was scaled by a factor of 1.25, a horizontal PGA of 0.20g was obtained at the surface of the site. Therefore, for use as the design basis motion in the site response analyses, the PC-3 rock motion was increased by a factor of 1.25, yielding a peak ground acceleration at rock outcrop of 0.14g with an estimated probability of exceedance of 3.2×10^{-4} (WSRC, 2000c). To distinguish this design basis motion from the PC-3 motion, it is referred to herein as the PC-3+ control motion. The response spectrum for the PC-3+ rock motion is shown on Figure 6-10 (DCS, 2003a). The strain-compatible soil properties, the cyclic stress ratio profile, and the post-earthquake settlements were calculated using the PC-3 acceleration time history increased by a factor of 1.25.

6.2.3.2.2 1886 Charleston Motion

Additional response analyses of the MFFF site were performed using the 1886 Charleston earthquake (50th percentile), attenuated to rock at the APSF site. These analyses were conducted to evaluate the liquefaction potential of the MFFF site based on a large, distant event. Note that

the northern boundary of the APSF site is located approximately 300 ft south of the MFFF site. The spectrum-compatible acceleration time history for this motion was also developed by WSRC (1998) and has a rock outcrop PGA of about 0.05g. The response spectrum at rock for the 1886 Charleston motion also is shown on Figure 6-10 (DCS 2003h).

6.2.3.3 Generalized Soil Column and Soil Properties

The stratigraphy within the MFFF site is reasonably uniform and nearly horizontal, as indicated by the cross sections through the site presented in Figures 5-2 through 5-10. The generalized horizontally layered soil profile developed for the site response analyses is based on the results of 95 CPTs located within or near the MFFF and BEG Buildings. The CPT data are discussed further in Section 6.2.1.1. The shallow generalized subsurface profile based on CPT results extends to the base the GC layer at about El 137.

As discussed in Section 5, the shallow (above El 137) subsurface conditions at the MFFF site were established to be similar and consistent with the shallow subsurface geologic conditions reported in other F-Area geotechnical studies (DCS, 2003a). Shallow subsurface properties were determined from the results of borings and CPTs performed at the site. Average shear wave velocities were determined based on the results of the 32 SCPT soundings in the vicinity of the MFFF structures. The subsurface profile and material properties below El 137 assumed for the APSF site response analyses (Geomatrix 1997) are considered appropriate for use at the MFFF site. The APSF deep soil profile was based on the confirmatory drilling study performed in the central portion of the SRS (Geomatrix, 1997 and WSRC, 1996a). The deep soil profile, assumed to be representative of the MFFF site is presented on Figure 6-1 (DCS, 2003a). This generalized soil profile developed for MFFF site compares well with the SRS generic site column that was used for development of the PC-3 and PC-4 SRS site-wide design basis spectra (WSRC, 1997).

Low-strain shear wave velocities developed from the MFFF geotechnical investigations were assigned to the soils down to the Green Clay layer (GC). The individual profiles of shear wave velocity at the 32 seismic CPTs recommended by ARA (2000 and 2003) are presented in Figures 6-3A and 6-3B. The arithmetic means of the measured shear wave velocities for each engineering unit are summarized in Table 6-7 and were used as representative "best-estimate" shear wave velocities in the analyses. Shear wave velocities assigned to the deeper materials are the same as those used in the APSF site response analyses (Geomatrix, 1997). The low-strain shear wave velocity profile used for the site response analyses is shown in Table 6-13 and Figure 6-2. Also shown in Table 6-13 are the total unit weight for each soil unit assumed for the analyses (DCS, 2003a).

According to the recommendations of ASCE 4-98 (ASCE, 2000) for safety-related nuclear structures, the strain-compatible dynamic soil properties used in SSI analyses should include lower-bound and upper-bound values in addition to the best estimate values. In accordance with ASCE 4-98 recommendations, the upper- and lower-bound dynamic shear moduli are assumed to be equal to 1/1.5 and 1.5 times the best-estimate values, respectively. Also, the upper- and

lower-bound moduli established should cover the variations in soil properties discovered during field investigations.

The upper- and lower-bound low-strain shear wave velocity profiles were calculated by calculating maximum shear modulus values from the best-estimate shear wave velocities, then applying the 1.5 and 1/1.5 factors to the "best-estimate" shear moduli to obtain upper- and lower-bound values. The resultant strain-compatible shear moduli from ProShake runs for SSI analyses were then compared against the variations identified in each engineering unit by the field investigations and the ASCE 4-98 requirements, as discussed in Section 6.2.3.6 (DCS, 2003a).

DCS, 2003hFigure 6-11 presents a comparison of the best estimate shear wave velocities obtained from the 2002 Supplemental Geotechnical Investigation with those obtained from the original subsurface investigation, which was performed in 2000. The best-estimate shear wave velocities measured during the 2002 investigation plus the four seismic CPTs from the 2000 investigation that were located in the vicinity of the MFFF structures (i.e., within the PIDAS fence) are plotted using the solid line, and the best-estimate shear wave velocities measured during the 2000 investigation are plotted using the dashed line in this figure. This plot confirms that the shear wave velocity profile in the vicinity of the MFFF structures is consistent with the shear wave velocity profile used in the geotechnical calculations that formed the bases for the dynamic soil properties developed from the data from the 2000 investigations.

The shear modulus reduction and damping ratio versus shear strain relationships used in the analyses are discussed in Section 6.2.1.4 and are presented in Tables 6-8 and 6-9 and in Figures 6-6 to 6-9 (DCS, 2001b).

6.2.3.4 Soil Column and Material Properties for Individual SCPTs

The soil column for each of the selected 18 SCPTs down to the GC layer was defined based on the layer picks for each CPT. The interval shear wave velocities were prepared based on measured data points from each SCPT sounding. In intervals where no velocity data was collected, the average velocity (based on the results of the 32 SCPTs within the MFFF site) for that engineering unit was used. The total unit weights used in the analyses are the average unit weights used in the analysis of the generalized soil column, and are shown in Table 6-13 (DCS 2001d).

6.2.3.5 Response Analyses

The site response analyses were performed using the computer program ProShake, which is a Windows version of the DOS program SHAKE91 (Idriss and Sun, 1992) with some added graphic features. The control motions described in Section 6.2.3.2 are defined in the analyses as rock outcrop motions, input at the base of the soil column. The 33 Hz cut-off frequency used in the analyses is the same as the maximum frequency adopted in the dynamic soil-structure interaction analyses for the MFFF Building. All ProShake runs converged within the specified error allowance of two percent.

6.2.3.5.1 PC-3+ Control Motion

The site response analyses were performed for best-estimate, lower-bound, and upper-bound dynamic soil properties (shear wave velocities and shear moduli). The surface response spectrum of the PC-3 control motion increased by a factor of 1.25 (PC-3+) for the generalized soil column and best-estimate dynamic soil properties is shown on Figure 6-12. Also shown on this figure are the response spectra for the 18 individual SCPT soil columns and the NRC Reg. Guide 1.60 surface spectrum anchored to 0.20g. Figure 6-13 presents the average response spectrum from the 18 SCPTs compared to the spectrum for the generalized soil column and best estimate soil properties. The results indicate that the response of the generalized soil column is very close to the average of the 18 SCPTs (DCS 2003o).

As shown in the figures, the Reg. Guide 1.60 spectrum envelopes the spectra generated by the PC-3+ in the frequency range that is typically of structural interest. As can be seen by these results, the PC-3+ bedrock time history produces a surface PGA of 0.20g and a surface spectrum that correlates well to the Reg. Guide 1.60 surface spectrum. The MFFF PC-3+ bedrock time history, therefore, satisfies the requirement for a bedrock time history that can be used for dynamic analysis at the MFFF site, as specified in Section 3.4.4 (DCS, 2003h).

6.2.3.5.2 1886 Charleston Control Motion

The responses of the generalized soil column (with best-estimate soil properties) to the 1886 Charleston bedrock motion attenuated to the SRS were also computed (DCS, 2003e). The surface response spectra for the generalized soil column with the best-estimate properties, along with those for the 18 individual SCPT soil columns and the Reg. Guide 1.60 surface spectrum, is shown in Figure 6-14. Again, the response of the generalized soil column is very close to the average, and a good representative, of the 18 individual SCPTs (DCS 2003o). Therefore, it is considered that the 1-D analysis using a generalized soil column for the MFFF site response analysis is appropriate and adequate.

6.2.3.6 Strain-Compatible Dynamic Soil Properties

Profiles of the best estimate, upper-, and lower-bound strain-compatible shear-wave velocities, shear moduli, and damping ratios for the PC-3+ ground motion are shown in Figures 6-15 through 6-17, as well as in Table 6-14. These values were computed using the generalized soil column and material properties, and they are recommended as appropriate for use in the dynamic soil-structure interaction (SSI) analyses of the MFFF critical structures (DCS, 2003e).

According to ASCE 4-98 (ASCE, 2000), the range of dynamic soil properties for the SSI analysis shall meet the uncertainty requirements, which include a minimum uncertainty factor, C_v , of 0.5 for the shear moduli. Also, the recommended range of soil dynamic properties in the SSI analysis shall cover the variation in soil properties discovered during the field investigations. The upper- and lower-bound shear moduli should then be set equal to the best-estimate multiplied by $(1 + C_v)$ and divided by $(1 + C_v)$, respectively. Values greater than 0.5 shall be used for C_v if field data indicates. Figure 6-18 shows the profiles of best-estimate, upper-, and

lower-bound strain-compatible shear moduli recommended for SSI analyses based on ProShake runs described as the “first set” analyses in Section 6.2.3.1. The upper- and lower-bound profiles enveloped the ASCE 4-98 (ASCE, 2000) required range of variations (profiles labeled as “1.5 × best-estimate” and “best-estimate / 1.5”), therefore, are adequate.

6.2.3.7 Cyclic Stress Ratio Profiles

6.2.3.7.1 PC-3-Based Control Motion

As part of the input for the liquefaction analysis of the MFFF site (Section 8.1), a best estimate profile of cyclic stress ratio (CSR) was computed using ProShake for the PC-3+ based control motion, and it is shown in Figure 6-19 and Table 6-15. This profile was developed using the generalized soil column and material properties discussed in Section 6.2.3.3. Also shown in Figure 6-19 are the CSR profiles computed for each of the 18 individual SCPTs. Table 6-15 also presents the effective shear strain, peak shear strain, peak shear stress, and peak ground acceleration profiles for the generalized soil profile with the PC-3+ based control motion.

6.2.3.7.2 1886 Charleston Control Motion

DCS, 2003aDCS, 2003eThe CSR profile computed for the generalized soil column (with best-estimate soil properties) was also computed utilizing the 1886 Charleston control motion, and it is shown in Figure 6-20. Also shown in Figure 6-20 are the CSR profiles computed for each of the 18 individual SCPTs. It can be seen that the CSR profile for the generalized soil column compares well with the profiles for the individual SCPTs (DCS 2003o). The CSR profile, together with the effective shear strain, peak shear strain, peak shear stress, and peak ground acceleration profiles for the generalized soil profile are summarized in Table 6-16.

7. ENGINEERING EVALUATION

7.1 FOUNDATION DESIGN CRITERIA

The MFFF and BEG Buildings are QL-1a (IROFS, Items Relied on for Safety) structures. The locations of the structures are shown on Figure 4-1.

Preliminary foundation design loads (TBV) have been provided for the MFFF and BEG Buildings and are discussed below.

7.2 FOUNDATION PREPARATION

The MFFF Building and the adjacent BEG Building will each be monolithic, reinforced concrete structures. As shown in Figure 4-1, the north-south dimension of the MFFF Building will be approximately 300 feet, and the east-west dimension will be between approximately 408 and 460 feet (DCS, 2003d). The main floor elevation over most of the structure (BMP – Main Processing area) will be 273 feet MSL. Floors in basements in the BSR (Shipping and Receiving) area, located at the northwestern portion of the structure, and in the BAP (Aqueous Polishing) area, located at the southwestern portion of the structure, as shown in Figures 5-2, 5-4, and 5-5, will be 14 feet (elevation 259 feet) and 17.5 feet (elevation 255.5 feet), respectively, below the main floor elevation (DCS, 2003d).

An approximately 9-foot thick security wall system will form the outer wall of the MFFF structure. All BMP, BSR, and BAP floors will be 4-feet thick and will form a continuous mat foundation to support the structure. Ten (10) feet of the natural soils beneath the BMP floor and 5 feet of the natural soils beneath the BAP and BSR basement floors will be excavated and replaced with select structural fill.

Average gross static bearing pressures beneath the lower floors of the MFFF structure have been estimated to be approximately 6.11 ksf in the BMP area, 6.80 ksf in the BSR area, and 7.93 ksf in the BAP area. The pressures are based on the weight of the structure and other long-term loads within the structure. Bearing pressures beneath the outer security wall system should be approximately 8.64 ksf for the walls adjacent to the main building floors and approximately 11.22 ksf for the walls adjacent to the BAP and BSR basement floors (Li, 2002b).

The BEG is approximately 42 feet by 141 feet in plan dimension and will have a 3-foot thick floor. The foundation pressure beneath the BEG, estimated assuming a rigid foundation and mat, is 2,000 psf. The BEG will be supported by 5 feet of engineered select structural fill.

A review of the subsurface conditions at the MFFF and BEG building locations indicates that there is considerable variability in soil strength in the soils near planned foundation grade. Based on the subsurface conditions that exist below planned foundation grades for the MFFF and BEG Buildings, it has been determined that these variable upper soils will be removed and replaced with a high strength structural fill. The structural fill will provide a firm, uniform, foundation

bearing material for the high static and dynamic loads applicable for these structures, and it will also provide for smoothing out effects of potential differential settlement.

At the present time it is anticipated that 10 feet of select structural fill will be placed beneath the main foundation level for the MFFF Building. Approximately five (5) ft of select structural fill will be placed below the BEG Building and sublevel area of the MFFF Building. The near-surface TR1 and TR1A engineering unit soils that will be found at the proposed structure bottom grades can be somewhat variable in density and stiffness. The primary purpose of the select structural fill is to provide a high density, well-compacted layer immediately beneath the structures to provide a uniform bearing material and to help distribute concentrated static and earthquake edge pressures into the underlying subgrade. Typical fill placement for these structures is shown on Figures 5-2 through 5-7. Engineering requirements for the select structural fill are presented in Section 6.1.7.

The select structural fill will extend at least 10 feet out from the edge of the mat foundations. The fill will then slope downward to the bottom of the excavation, or upward to the bottom of the select structural fill beneath the other, higher, parts of the buildings on a 1:1 (horizontal:vertical) slope. The engineered structural fill will be compacted to a density of at least 95 percent of the maximum modified Proctor dry density as determined by ASTM D-1557. Excavated site materials can be utilized as backfill adjacent to the engineered structural fill and adjacent to the foundations. The site soils will be placed either as common backfill or as structural fill. Common fill will be placed to at least 90 percent maximum dry density and structural fill will be placed and compacted to a density of at least 95 percent of the maximum dry density as determined by ASTM-1557.

The subsurface soils will be excavated to the planned final subgrade for the engineered structural fill placement and proofrolled. Prior to placement of the engineered structural fill, any soft areas will be moisture conditioned and recompacted to structural fill density requirements or excavated and replaced with engineered select structural fill.

7.3 BEARING CAPACITY

The overall bearing capacity of the MFFF and BEG Buildings, as well as factors of safety against bearing capacity failures, were evaluated for the MFFF and BEG Buildings (DCS, 2003g). Building widths of 42 and 300 feet, as discussed in Section 7.2, were assumed for the analysis of the BEG and the MFFF structures, respectively. As indicated in Tables 6-2 and 6-3, the moist unit weight of the soils ranges from approximately 108 pcf to approximately 125 pcf, and angles of internal friction (ϕ) range from approximately 26° to 35° (DCS, 2003d). Average drained cohesive strengths (c') of samples tested in the laboratory ranged from 0 to approximately 900 psf.

For the bearing capacity analysis, the soils beneath the MFFF site were assumed to be sands with an angle of internal friction (ϕ) of 26°, drained soil cohesion (c') of zero, and a moist soil unit weight (γ) of 108 pcf. These are very conservative soil parameters with respect to the

determination of bearing capacity. "Soft zones" and "soft materials" have not been incorporated into the analysis due to the limited thickness and lateral extents of those layers at the site.

The groundwater surface was assumed to be within 4 feet of the ground surface (Elevation 269 feet), which is 59 feet above the site design groundwater elevation of 210 feet. That is also a conservative assumption because it reduces the soil unit weight to the buoyant weight for all of the soils beneath the foundation, including the 59 feet of unsaturated soils between the bottom of the foundation and the design groundwater elevation.

An ultimate bearing capacity of approximately 71,180 psf and a factor of safety against bearing capacity failure of 11.7 was determined by the analysis for the MFFF structure (DCS, 2003g). That factor of safety is based on the average foundation pressure of 6,110 psf beneath the BMP portion of the MFFF structure. If the average foundation pressure across the entire MFFF structure is very conservatively assumed to be 11,220 psf, which is the pressure beneath the 9-foot wide security walls along the BAP basements, then the factor of safety against a bearing capacity failure is 6.3.

The ultimate bearing capacity indicated for the BEG structure is approximately 13,525 psf. The factor of safety against bearing capacity failure of the BEG structure for the average foundation pressure of 2000 psf is 6.3.

The ultimate bearing capacities calculated for the MFFF and BEG Buildings are based on conservative soil strength parameters and a very conservative groundwater surface elevation, which was assumed to be at the bottom of the foundations (rather than at the design elevation at a depth of 59 feet below the ground surface). The minimum bearing capacity factor of safety of approximately 6 calculated for the MFFF and BEG Buildings using the conservative soil parameters and groundwater levels are much larger than factors of safety of 1.7 to 2.5 customarily considered acceptable for mat foundation designs (Bowles, 1996).

7.4 SETTLEMENT

7.4.1 General

Two methods of settlement analysis were used to provide a detailed evaluation of estimated settlements for the MFFF and BEG Buildings. The FLAC computer program (Itasca, 2000b) was used to evaluate the potential effect of variations in structure properties (E and I), soft zone and soft material parameters (C_c , ϕ , overconsolidation ratio), and engineering unit parameters (preconsolidation pressures, compression indices, ϕ) on model results and to provide a detailed settlement analysis and deformation profile for the MFFF and BEG Buildings. A conventional settlement analysis was performed for comparison to FLAC model results. Both settlement analyses assume that the existing soil fill covering the MFFF site will be removed prior to construction of the MFFF and BEG Buildings and that rebound of the underlying soils will have occurred from unloading. No consideration for this fill loading has been assumed in the settlement analyses, since any settlement from the fill was considered primarily as

recompression. Both analyses also assume the removal of 5 to 10 feet of subsurface soils directly beneath the MFFF and BEG structures and replacement of those soils with engineered select structural fill, as discussed in Section 7.2.

7.4.2 Conventional Settlement Analysis

The settlement at the edge and center of a 415-foot wide, flexible foundation, uniformly loaded to 6.11 ksf was estimated (DCS, 2002) using the classical consolidation equation (Bowles, 1996, page 83):

$$S = (H) [C / (1+e_o)] \log [(P_o + \Delta P) / P_o]$$

- where:
- S = settlement (inches)
 - H = thickness of soil layer (inches)
 - C = compression index
 - e_o = void ratio
 - P_o = overburden pressure (psf)
 - ΔP = change in pressure (psf)

Boussinesq stress distributions were used to determine the change in pressures (ΔP) with depth at the edge and center of the foundation. Recompression indices (C_r) were selected for the analysis as they result in estimated settlements that more closely correlate with measured structure settlements at the SRS site, as discussed below in Section 7.4.3.3. Other appropriate soil parameters shown in Tables 6-2 to 6-4 (DCS, 2002) were assumed. Subsurface conditions indicated by CPT-54, which is located approximately 35 feet east of the west wall of the MFFF building, were used to represent soil conditions at the edge of the foundation. Subsurface conditions indicated by CPT-55, which is located approximately 240 feet east of the west MFFF building wall, were used to represent the center of the foundation. A groundwater surface elevation of 210 feet MSL was used. Soft zone and soft material layers were not included in the estimates. The foundation was assumed to be underlain by 10 feet of structural fill. Estimated settlements were approximately 1.7 inches at the edge of the foundation and approximately 3.0 inches at the center of the foundation.

7.4.3 FLAC Settlement Analysis

7.4.3.1 FLAC Model

The FLAC computer program (Itasca, 2000a) solves small- to large-strain applications in geomechanics using a finite-difference approach. The FLAC program is a “shell” that allows users to select from several different constitutive soil models. The constitutive soil model utilized depends on the ease of use, the application, and the primary aspect of soil behavior being modeled.

The Mohr-Coulomb model uses failure criterion that forms the basis for many limit equilibrium problems in geomechanics (e.g., bearing capacity, limiting lateral earth pressures, and slope stability). The Mohr-Coulomb relationship was developed to describe the limit state (i.e., incipient failure) in soil as a function of the difference between the maximum and minimum principal stresses.

The Mohr-Coulomb criterion defines the limiting state of stress at failure based on the principal stress difference in the material being modeled. Soil deformations, or strains, associated with changes in the principal stresses are not accounted for with the Mohr-Coulomb model. The soil behaves essentially as a rigid, perfectly plastic material. The elastic response of soils during loading can be modeled in FLAC by use of the elastic constants of bulk modulus, shear modulus, and Poisson's ratio. Soil strains prior to failure are modeled using the elastic constants. Soil strains mobilized after the failure condition has been reached are modeled using the flow rule for plastic deformations in shear and the energy-based formulation scheme. The flow rule for perfectly plastic deformations is that shearing can continue indefinitely without changes in volume or effective stress (Wood, 1990).

The Mohr-Coulomb model of FLAC has been used to develop estimates of initial in situ stresses beneath the F-Area Actinide Packaging and Storage Facility (APSF) site for use as input into calculations to estimate stress redistribution and two-dimensional deformations, both adjacent to soft zones in the soil profile and at the ground surface (Bechtel, 1998). Consolidation settlements of the soft zone soils in those analyses were computed outside of the FLAC model (i.e., uncoupled analysis where the settlements were computed using spreadsheets or hand calculations). The computed settlements did not account for stress redistribution around the soft zone during consolidation. The consolidation settlements were incorporated in the FLAC model by forcing the top boundary of the soft soil layers to move down by an amount equal to the computed one-dimensional settlement. FLAC was then used to compute the settlement profile at the ground surface due to the consolidation at depth. The use of the Mohr-Coulomb model for that approach was acceptable because the consolidation settlements were input manually into the FLAC model.

Consolidation (settlement) results from soil volume changes due to stress changes in the soil from imposed structural loads. The Mohr-Coulomb model and elastic constants do not model the soil consolidation process.

Critical state models are a class of constitutive soil model that includes volumetric strains in the failure criterion by replicating the stress-strain behavior of the soil. The Cam-Clay model available in the FLAC program is a critical state soil model that is appropriate for engineering applications involving consolidation. Volumetric and stress changes that occur during soil consolidation are specifically modeled in the Cam-Clay model. The Cam-Clay model also includes algorithms to model the response of soils to small, elastic strains due to imposed shear stresses not addressed by consolidation theory methods alone. Model inputs for the various soil layers include compression indices and preconsolidation pressures to define stress-strain

relationships during consolidation, as well as parameters such as shear modulus, bulk modulus, Poisson's ratio, and specific volume for modeling elastic responses. Modulus of elasticity (E) and moment of inertia (I) values for the structure can also be included for coupled soil-structure interaction modeling.

The FLAC Cam-Clay model was used for the evaluations of the MFFF area structure settlement (DCS, 2003d). The Mohr-Coulomb model was used for some analyses to evaluate the potential effects of compression of soft material and soft zone soils following techniques used for settlement analysis at other SRS facilities (Bechtel, 1998), and for comparison to the results obtained from analysis made using the Cam-Clay model. The FLAC modeling is discussed in detail in "Estimates of Static Settlement of MFFF Structures Using FLAC Model" (DCS, 2003d), and are summarized in the following sections.

7.4.3.2 Model Configuration

A two-dimensional FLAC model was developed for each of the six geotechnical sections (Sections A through F) shown in Figures 5-2 through 5-7. The top of the model was set at elevation 269 feet, which is 4 feet lower than the main floor elevation of the MFFF structure and at the bottom of the 4-foot thick floor of the BMP area. The elevations of the bottom of the floors in the BSR and BAP basement areas were set 14 and 17.5 feet below the top of the model elevation of 269 feet, as indicated in Section 7.2.

The MFFF and BEG Buildings were modeled as stiff, monolithic reinforced concrete structures, as previously discussed in Section 7.1. Overall moments of inertia (I) of 3,140,102 feet⁴ and 14,100 feet⁴ were used for the MFFF and BEG structure floors, respectively. Those moments of inertia are based on typical sections through the structures. An equivalent moment of inertia of 50 feet⁴/foot of width was used for the BSR and BAP basement walls. A modulus of elasticity (E) of 5.8 x 10⁵ ksf (based on a concrete compressive strength of 5,000 psi) was used. The effect of variations of the stiffness (EI) of the structures on the predicted results was evaluated, as discussed below.

The average static bearing pressures beneath the lower floors of the MFFF structure (i.e., approximately 6.11 ksf in the BMP area, 6.80 ksf in the BSR area, and 7.93 ksf in the BAP area, as previously discussed in Section 7.2) were used in the FLAC models. Bearing pressures beneath the outer security walls were set at approximately 8.64 ksf beneath the walls adjacent to the main building floors and at approximately 11.22 ksf beneath the walls adjacent to the BAP and BSR basement floors. A static bearing pressure of 2 ksf was used for the BEG structure.

The engineering unit soils, soft zones, and soft materials were incorporated into the models at the depths and elevations shown in the sections. Some small adjustments to the elevations and thickness of the materials were made to accommodate the 5-foot by 5-foot finite-difference grid size used for materials within the zone that extended at least one half-structure width to each side of the structure and 200 feet below the structures. A 5-foot thick layer of select structural fill

was used beneath the BAP and BSR basements and the BEG Building. A 10-foot thick layer of select structural fill was used beneath the BMP area floors.

Soil properties assumed for the engineered select structural fill, engineering unit soils, and soft zone and soft materials in the FLAC Cam-Clay models are those shown in Table 7-1. Parameters used in the FLAC Mohr-Coulomb model are shown in Table 7-2. Recompression indices (C_r) were used for the engineering unit soils. The effects of potential variations of soil parameters on the model results were systematically evaluated.

7.4.3.3 Engineering Unit Preconsolidation Pressures and Compression Indices

The soils underlying the MFFF site that would contribute to the settlement of the MFFF Building are those within the Tobacco Road, Dry Branch, and Santee/Tinker Formations, which were deposited approximately 36 to 52 million years ago during the Eocene Period (WSRC, 1996a). Soils designated as engineering units TR1, TR1A, TR2A, TR2B, and TR3/4 are Tobacco Road Formation soils, those designated as engineering units DB1/3 and DB4/5 are Dry Branch Formation soils, and those designated as engineering units ST1 and ST2 are Santee/Tinker Formation soils (WSRC, 1996b). Soils immediately beneath the Santee/Tinker Formation are associated with the Warley Hill (engineering unit GC) and Congaree (engineering unit GC) Formations, and are much less compressible than the overlying formations.

Clinchfield Formation soils that were also deposited over the Santee/Tinker Formation eroded from the MFFF area prior to deposition of the overlying Dry Branch and Tobacco Road Formations (WSRC, 1996a). The eroded surface at the top of the Santee/Tinker Formation is called the Santee Unconformity. At least part of the "Upland Unit"/Hawthorn/Chandler Bridge Formations overlying the Tobacco Road Formation also have eroded, creating a surface called the Upland Unconformity (WSRC, 1996a). The depth of the eroded soils, and, therefore, the overburden pressures from those soils prior to their erosion, is not well established. However, the weight of the eroded Clinchfield Formation soils and any soils eroded from the Upland Unit should have resulted in "preconsolidation pressures" in the remaining soils that are larger than current overburden pressures.

The effects of preconsolidation pressures (P_c) and compression indices (C_c and C_r) on MFFF structure settlements predicted by the FLAC model were evaluated by varying the preconsolidation pressures for the engineering unit soils in the FLAC Cam-Clay model. Normal compression indices (C_c) are used in the model for normally consolidated soils and for total ground pressures (the sum of the effective overburden pressure and pressure from structure-imposed loads) that exceed the soil preconsolidation pressure (P_c). Recompression indices (C_r) are used for settlement analysis for total ground pressures that are less than the preconsolidation pressure.

Geotechnical Section E was used for the evaluations as the initial foundation pressure from the MFFF structure along the entire section, except for beneath the exterior security walls, is a uniform 6.11 ksf. The pressure beneath the 9 foot exterior security wall is 8.64 ksf. The

stiffness (EI) of the MFFF structure was included in all the evaluations. Other than the preconsolidation pressures, soil parameters used for the engineering unit soils and soft soil layers were those indicated in Table 7-1. Soft soil layers were assumed to be normally consolidated in all the parametric evaluations.

The results of the parametric evaluations of the effects of the engineering unit preconsolidation pressure are summarized in Figures 7-1, 7-2 and 7-3. Curve 1 on each of the figures assumes there are no soft soil layers and a preconsolidation pressure sufficiently large that it is not exceeded by the sum of the preconstruction soil pressures plus the pressure increase due to structure loads. This approach ensures that the results in consolidation settlement of the engineering unit soils being determined entirely from recompression indices (C_r). Total settlements of from 2.7 to 2.9 inches were indicated by the model for those conditions.

The model was also run assuming the same conditions as discussed above for Curve 1 but with the soft soil layers included. As indicated by Curve 2, Figure 7-1, 2.9 to 3.5 inches of settlement were indicated with the soft soil layers included.

Preconsolidation pressures of engineering unit soils estimated from laboratory consolidation tests on samples of those soils were incorporated into a FLAC model run. The average preconsolidation pressure estimated from the test data for soils of each of the engineering units, summarized in Table 7-1, was assumed unless that pressure was less than the overburden pressure from the weight of the overlying soils. For those cases, preconsolidation pressures used for the units were the current overburden pressure (normally consolidated soils). Between 7.2 and 8.2 inches of settlement were predicted by the model, as shown by Curve 3, Figure 7-1.

Curve 4 of Figure 7-1 illustrates the effect of assuming all of the subsurface soils are normally consolidated (preconsolidation pressures equal to current overburden pressures). From 26.6 to 27.7 inches of settlement were predicted by that model.

Ground pressures predicted by FLAC for each of the conditions discussed above are shown on Figure 7-2. Changes in pressure due to the building loads are shown in Figure 7-3 for a vertical section located near the center of the area underlain by soft soils. The initially applied pressures from the building have been redistributed by the underlying soils and the stiff structure, resulting in less pressure in the area underlain by the soft soil layers, and more pressure in areas beneath outside walls of the building. The smallest redistribution occurred for the model that included preconsolidated engineering unit soils and no soft soil layers (Curve 1, Figures 7-2 and 7-3). For that case, consolidation properties used for all the subsoils are reasonably uniform. The largest redistributions from the area underlain by the soft soil layers are predicted for cases for which all or part of the engineering unit soils are assumed to be preconsolidated (Curves 2 and 3, respectively). The less compressible, preconsolidated engineering unit soils effectively redistribute pressures from the more compressible, soft soil layer areas. Changes in pressure in the area of the soft soil layers for the case using normally consolidated soils (Curve 4) are greater than were obtained for the case with no soft soil layers and preconsolidated engineering units (Curve 1), and less than were obtained for cases that used preconsolidated engineering unit soils

(Curves 2 and 3). The engineering unit soils are more compressible, and the differences between the consolidation properties of the engineering unit and soft soils are less for that case.

The differences in pressure distributions for each of the cases contribute to differences in the predicted settlements (Figure 7-1). However, the large differences in the predicted settlements are primarily due to differences in the compression indices (C_c or C_r) indicated by the different preconsolidation pressure assumptions.

Settlements of several of the structures at the SRS have been measured during and after their construction (WSRC, 2001b, 2002b). Foundation movements of tanks and associated structures in the H-Area have been reported to vary from approximately a quarter inch of upward movement to approximately 2 ¼ inches of settlement, with most of the movements occurring within about 3 to 5 years after completion of construction (WSRC, 2001b). Detailed information concerning subsurface conditions, structure and foundation dimensions, and foundation pressures were not included in the summary of the measurements.

Maximum measured settlements and approximate foundation pressures at most of the S-Area structures are less than 0.9 inches and 2.5 ksf, respectively, as summarized in Table 7-3 (WSRC, 2002b). Measured settlements at Building 221-S (Vitrification Building) range from approximately 1.4 inches at monument 13 at the southern end of the foundation mat to approximately 3.0 inches at monument 26 at the northern end.

A typical geologic section (Figure 3 of WSRC, 2002b) indicates the S-Area site is underlain by at least 160 feet of medium dense to dense, clean to clayey sands (SP, SP-SC, SC) and that the groundwater surface is approximately 80 to 90 feet below the ground surface. Standard Penetration Test (SPT) N values indicated on the logs shown on the typical section indicate the sands to the depth of 160 feet are similar to the soils in the Tobacco Road, Dry Branch, and Santee/Tinker Formations (Engineering Units TR1A, TR2A, TR2B, TR3/4, DB1/3, DB4/5, ST1, and ST2). Those subsurface conditions are similar to those at the MFFF site (DCS, 2003p), except that no soft soil layers were indicated for the S-Area and the depth of soils of interest with respect to settlements at the MFFF site is approximately 130 feet.

Building 221-S is approximately 362 feet (north-south) by 117 feet (east-west) in plan dimensions and is founded with an 8 foot thick concrete mat (WSRC, 2002b). The bottom elevation of the mat is 270 feet beneath the most of the structure, and is at elevation 256 feet beneath the north end of the structure. The average building load is reported to range between approximately 5 and 5.5 ksf. Construction of the building began in May 1984. Excavations for the foundations (from preconstruction site elevations between 274 and 278 feet) took place between the first and third week of May 1984. Foundation mat concrete placement began in August 1984 and continued until December 1984. The structure was essentially completed in January 1988. After January 1988 (page 2, WSRC, 2002b), "Continuing work included installation of the mechanical equipment and other interior components. These components contribute very small loads to the building foundation."

Settlement measurements at Building 221-S began in May of 1984, and continued through April 2002 (WSRC, 2002b), a period of 18 years. As indicated in Figures 7-4 and 7-5, settlement (primary consolidation) of the structure began concurrent with completion of the foundation mat in December 1984. At monument 13, approximately 70 percent of the total settlement that had been measured at the structure through April 2002 occurred by January 1988, the completion of construction. Primary consolidation continued approximately 4 months after the January 1988 completion of the structure at monument 13, by which time approximately 86 percent of the total measured settlement had occurred. At monument 26, approximately 67 percent of the total settlement that had been measured at the structure through April 2002 had occurred by the end of construction in January 1988, and primary compression continued until approximately May 1989 by which time approximately 83 percent of the total settlement had occurred. Secondary compression then continued for approximately 3 years at monument 13 (until 1991) at the south end of the foundation (Figure 7-4), and for approximately 9 years (until 1998) at the monument 26 at the north end of the foundation mat (Figure 7-5). Movements measured since 1991 at monument 13 and since 1998 at monument 26 have been very small (0 to 0.04 inches, respectively).

The foundation mat supporting Building 221-S is not as wide as the mat that will support the MFFF Building (117 feet for Building 221-S, 300 feet for the MFFF Building), however, both structures are sufficiently wide to impose stresses throughout the compressible soils underlying the structures. The average foundation pressures from the MFFF Building (6.11 ksf) are only about 10 to 20 percent larger than those of Building 221-S (5 to 5.5 ksf). Subsurface conditions beneath both of the structures are similar. Therefore, predicted settlements for the MFFF Building should be similar to those measured at Building 221-S.

The MFFF Building settlements of approximately 27 inches (Curve 4, Figure 7-1) that were predicted for normally consolidated engineering unit soils are unreasonable. Predicted settlements of the order of 7 to 8 inches (Curve 3, Chart F-1), obtained assuming at preconsolidation pressures estimated from laboratory test results, are over twice those measured at Building 221-S and are also large considering the similarities of the structures and subsurface conditions at the two sites. Measured settlements of existing structures of similar size and founded on similar soils are generally a more reliable indicator of potential settlements at proposed structures than are analysis based on laboratory tests due to difficulties in obtaining high quality, undisturbed samples of subsoils for laboratory tests. The settlements predicted by the FLAC model that included no soft soil layers and assumed preconsolidation pressures larger than the sum of the existing overburden stresses and stresses imposed by the MFFF structure (Curve 1, Figure 7-1) are somewhat larger than the maximum settlements at Building 221-S (2.6 inches of primary consolidation settlement and 0.4 inches of secondary consolidation settlement). However, the MFFF structure width and expected foundation pressures are also somewhat larger than those at Building 221-S. Therefore, the predicted settlements of the MFFF structures and those measured at Building 221-S are consistent. The models with

preconsolidation pressures larger than the sum of the existing overburden stresses and stresses imposed by the MFFF structure were used for the subsequent FLAC Cam-Clay analyses.

7.4.3.4 Parametric Evaluations

The effect of variations in structure stiffness (EI), soft zone and soft material compression indices (C_c), soft zone and soft material friction angles (ϕ), and engineering unit soil friction angles on Cam-Clay model results were evaluated. Model runs were made with the stiffness of the MFFF structure set at a value approximately 95 times larger than would be indicated by the E and I indicated in Section 7.4.3.2. Soft zone and soft material compression indices of 0.25, 0.50, and 1.0, and friction angles of 10° and 28° were evaluated, in addition to those shown in Table 7-1. Engineering unit friction angles were varied from 26° to 35° . The results of those parametric evaluations indicated the potential variations did not have large effects on model results.

Section B (Figure 5-3) was modeled using FLAC assuming the foundation pressures indicated for the structure in Section 7.2 (6.11 ksf in BMP area, 6.80 ksf in BSR area, and 8.64 ksf below exterior walls) were applied directly to the foundation soils at elevation 269 feet via a flexible mat (no structure stiffness, $EI = 0$). Soil parameters shown in Table 7-1 were used, and soft zone and soft material layers were not included. A maximum settlement of approximately 3.4 inches was indicated from the FLAC model near the midpoint of Section B, and approximately 1.9 and 2.0 inches were indicated at the edges of the section, all locations underlain by 10 feet of engineered select structural fill. Those estimated settlements are consistent with those obtained from the calculation (DCS, 2002) discussed in Section 7.4.2, considering the somewhat larger applied pressures used for the FLAC analysis and the accuracy of the estimating techniques of either of the calculation methods.

The parametric settlement analyses discussed above, and in Section 7.4.3.5, used normally consolidated soft soil layers. Previous studies (WSCR, 1999b) have suggested that soft zone soils may be underconsolidated, with an overconsolidation ratio (OCR) of 0.7. The potential effects of underconsolidated soft zone soils on settlements calculated using the Cam-Clay model were evaluated by assuming the OCR of each of those layers was 0.7 (DCS, 2003d). The preconsolidation pressure of the soils in each of the soft zones was changed from the overburden pressure to 70 percent of the overburden pressure. Other structure and soil parameters used for the model remained as previously discussed.

Approximately 2.7 to 3.8 inches of MFFF Building settlement and approximately 1.4 to 2.0 inches of BEG Building settlement were indicated along the various geotechnical sections (DCS, 2003d). Those settlements range from no additional settlement to approximately 0.3 inches of additional settlement in excess of the settlements predicted using normally consolidated soft zone soils (Section 7.4.3.5). Final ground pressures beneath the buildings predicted using underconsolidated soft zone soils are similar to those obtained using normally consolidated soft zone soils (DCS, 2003d). Those small increases in settlement are well within the accuracy of the model parameters and techniques.

7.4.3.5 Estimated Settlements and Pressures

The FLAC Cam-Clay model was used to predict MFFF and BEG Building settlements and bearing pressures due to static loads along each of the six geotechnical sections (A through F) using the soil parameters indicated in Table 7-1 and structural moments of inertia discussed in Section 7.4.3.2. Normally consolidated soft zone and soft material layers were included in the analysis. The results of the FLAC analysis along each of the sections were used to develop contours of estimated settlement and pressures beneath the MFFF and BEG Buildings, which are presented in Figures 7-6 and 7-7.

Settlement measurements indicate that secondary consolidation of existing Building 221-S are approximately 15 to 17 percent of the primary consolidation settlements (Figures 7-4 and 7-5). Based on the similarities between the MFFF structure and Building 221-S, as previously discussed, and the estimated 2.7 to 3.5 inches of primary consolidation settlement of the MFFF structure (Figure 7-6), approximately ½ inch of secondary consolidation settlement should be added to the settlements shown in Figure 7-1. That results in total (primary plus secondary consolidation) estimated settlements of the MFFF structure are from approximately 3.2 to 4.0 inches.

The magnitudes and patterns of settlements and ground pressures indicated by FLAC are typical of those for stiff structures founded on subsurface soils such as those at the MFFF site. Large differential settlements were not predicted, and the largest settlements occurred over areas underlain by the thicker layers of more compressible materials (soft zone and soft material layers beneath Sections A and E). The initially applied pressures from the structures to the soils were redistributed through the stiff structures, resulting in less pressure under interior floors and more pressure under exterior walls and the interior BSR and BAP basement area walls. Such pressure patterns are typical of those for stiff structures (Bowles, 1996).

The maximum primary consolidation settlement of approximately 3.5 inches predicted by the FLAC model for cases considering the effect of structure stiffness and soft zone and soft material layers represents approximately 0.2 percent of the approximately 200 feet of compressible soils included in the models. That percentage of settlement is relatively small, and it suggests that the total predicted settlements and the minor differences in the predicted settlements are within the accuracy of the models.

The FLAC model results also illustrate the redistribution of initially applied pressures and the effect of the soft zone and soft material layers. The largest redistribution of initially applied pressures at the ground surface occurs in areas underlain by soft soil layers. The smallest changes in pressure at depth occur in the soft soil layers. Changes in pressure that would normally be indicated at those depths are redistributed from the weaker and more compressible soft zone and soft material soils to the adjacent stronger and less compressible engineering unit soils.

The redistribution of pressures directly affects structure settlement. The soft zone and soft material layers contribute to more settlement at the ground surface than would be anticipated if

those layers were not present. However, the stiff structure effectively redistributes the pressures so that differential settlements at the ground surface along the structure are not large.

The estimated settlements and pressures are functions of the building properties, soil properties, and applied building loads that were used in the FLAC models. Different combinations of properties or loads would result in different patterns and magnitudes of predicted settlements and ground pressures. No redistribution of applied loads, more differential settlement, and less representative settlement magnitudes and patterns would be predicted if the stiffness (EI) of the building was not included in the models.

Direct data, other than the settlement measurements of existing structures discussed in Section 7.4.3.3, are not available for evaluation of time rate of MFFF area building settlements. That data for Building 221-S indicates that most of the structure loads and approximately 70 percent of the total measured settlement of the structure occurred by the completion of construction. Primary consolidation of the structure continued for approximately 5 to 18 months after completion of the structure. Approximately 83 to 86 percent of the total measured settlement occurred during that period. Secondary compression then continued for approximately 3 to 9 years.

The rate of settlement of Building 221-S is consistent with structures founded on granular soils. That is, most of the settlement occurs shortly after all the foundation loads are applied. The Building 221-S building settlement data (WSRC, 2002b), and data from other structures at the SRS (WSRC, 2001b), indicates that assuming that approximately 90 percent (primary consolidation) of the predicted MFFF structure settlement shown on Figure 7-6 will occur within approximately 6 months after the foundation loads are applied, is reasonable. The remaining 10 percent of the predicted settlements (secondary compression) shown on Figure 7-6 should occur within approximately 5 to 10 years thereafter. That time-rate of settlement is illustrated in Figure 7-8.

Coefficients of subgrade reaction (soil spring constants) were estimated for use in structural modeling (ANSYS) of the MFFF and BEG Buildings to approximate the stress-strain response of the foundation soils to static structure loads. The estimates were made by dividing the estimated pressures shown in Figure 7-7 by the estimated settlements shown in Figure 7-6 to establish control points at the locations where the estimated pressure and settlement contours crossed. The estimated coefficients of subgrade reaction shown in Figure 7-9 were interpolated from the control points.

The coefficients of subgrade reaction are not a true soil property, as they approximate nonelastic consolidation of the entire soil mass beneath the structures at specific structure pressures. As such, the estimated coefficients represent elastic springs, and the magnitude of settlement indicated at a particular location within the structural model will be proportional to the pressure applied to the spring at that location. The coefficients of subgrade reaction are "best estimate" values based on the combinations of applied static pressures, structure properties, and subsoil properties used in the FLAC models. They can be used in the structural model to approximate

the estimated building settlements from the FLAC model. However, differences in the magnitude and pattern of settlements predicted by the FLAC model and the structural model should be expected, as the distribution of forces, loads, and moments of inertia incorporated in the structural model should be more detailed than can be incorporated into the FLAC model. The estimated coefficients of subgrade reaction from the FLAC model may need to be adjusted in the structural model to obtain a better correlation between the pattern and magnitude of settlements indicated by the two models.

7.4.3.6 Mohr-Coulomb Collapse Model

Previous analyses (Bechtel, 1998) have evaluated potential settlements due to soft zone soils by assuming "soil arches" that support the full overburden pressure have formed in the engineering unit soils over the soft zone soils. That allows the soft soils to remain underconsolidated. The analyses also assume the soil arches will be weakened sufficiently during an earthquake event to subject the underlying, underconsolidated soft zone soils to the full overburden pressure. The settlement of the soft zone soils is calculated using the classic consolidation equation. Settlement at the ground surface due to the soft zone soil settlement is computed using the FLAC Mohr-Coulomb model.

The Mohr-Coulomb collapse model method has been used to evaluate potential ground surface settlements at the MFFF site (DCS, 2003d). The settlement of the soft soils in the each of the soft material and soft zone layers along each of the geotechnical sections (Figures 5-2 through 5-7) were calculated using a compression ratio of 0.24 and an OCR of 0.7, consistent with the previous analysis (Bechtel, 1998 and WSCR, 1999b). Substituting those values into the consolidation equation results in the settlement of the soft soil layers (S) being 3.7 percent of the thickness (H) of the particular layer. The thickness of each of the soft soil layers used in the calculation was the thickness indicated by the borings and CPTs (Table 5-3).

The settlement at the ground surface due to the soft soil layers were computed by incrementally "pulling down" the top of each soft layer in the FLAC Mohr-Coulomb model of each of the geotechnical sections by the calculated amount of the settlement of the soft soils (DCS, 2003d). Soil parameters used for the engineering unit soils in the Mohr-Coulomb model are those summarized in Table 7-2. The models did not include the effects of the building stiffness or loads, only the "collapse" of the soil arches and resulting compression of the soft soil layers.

Computed ground surface settlements along geotechnical section E, shown in Figure 7-10 show that up to approximately 2.6 inches of ground surface settlement (Curve 2, Figure 7-10) were indicated by the Mohr-Coulomb collapse model.

The previous analysis of ground surface settlements at the SRS (Bechtel, 1998) used 15 percent of the shear modulus (G) and a bulk modulus (K) calculated directly from shear wave velocities (V_s) shown in Table 7-2. The effect of reducing engineering unit shear and bulk moduli to 15 percent of the values shown in Tables 7-2 is illustrated in by Curve 4 of Figure 7-10. Up to approximately 0.7 inches of additional ground surface settlement was predicted by the model.

The Mohr-Coulomb model is a rigid, perfectly plastic model, as discussed in Section 7.4.3.1. Soil deformations (strains) prior to failure are modeled using elastic constants. Those model conditions are not consistent with soil consolidation (settlement). During consolidation, individual soil particles within a soil mass move (shear) relative to each other in response to changes in stress within the mass. The movement of the soil particles causes the volume of the soil mass to change. Stresses within the soil mass change concurrently with changes in the soil volume. The process continues until the soil mass comes to equilibrium with the changes in stress that initiated the consolidation.

The Cam-Clay model replicates the processes of soil consolidation, and was used to model the effects of underconsolidated soft zone soils on ground surface settlements (DCS, 2003d). Geotechnical section E was used as the largest settlements were computed along that section using the Mohr-Coulomb model. Soil parameters used for the soft zone soils, and for the soft material and engineering unit soils, were those used for the Cam-Clay models (Table 7-1). The compression ratio of the soft zone soils is 0.25 using the void ratio (e_0) and compression index (C_c) indicated in Table 7-1. The soft zone soil layers were assumed to be underconsolidated, with an OCR of 0.7. Therefore, the same soft zone soil properties used for the Mohr-Coulomb collapse model are used in the Cam-Clay model.

The MFFF Building was not included in the Mohr-Coulomb collapse model or in the Cam-Clay model. Therefore, the Cam-Clay model only predicted changes in the subsurface soils as equilibrium was established between the underconsolidated soft zone soils and the surrounding engineering unit soils. The model can be interpreted as simulating the effects of the weakening of "soil arches" in engineering unit soils over underconsolidated soft zone soils, the conditions assumed for the Mohr-Coulomb collapse model, or the progressive effects of the compression of the assumed underconsolidated soft zone soils over any assumed time period during or since their development.

Results of the Cam-Clay model are shown as Curve 5 in Figure 7-10. Effective stresses in the subsurface soils at a vertical section located near the center of the area underlain by the soft zone soils (the area of the maximum ground surface settlement of approximately 2.6 inches predicted by the Mohr-Coulomb collapse model) are shown in Figure 7-11. Initial effective stresses in all soils except those of the soft zone layer at a depth of approximately 100 feet below the top of the model are the overburden pressures (Curve 1, Figure 7-11). Initial effective stresses in the soft zone layer are 70 percent of the overburden pressure. Final effective stresses at the interfaces between the engineering unit and soft zone soils at the top and bottom of the soft zone layer must be the same for the model to reach equilibrium. The model indicates the effective pressures in the engineering unit soils above and below the soft zone decreased and remained essentially the same in the soft zone soils, to achieve equilibrium (Curves 2 and 3, Figure 7-11). The changes in engineering unit soil stresses extend approximately 40 feet above to approximately 65 feet below the soft zone layer (Curve 3, Figure 7-11). The equalization of stresses was achieved by small volume increases in the engineering unit soils above and below the soft zone, and small decreases in volume of the soft zone and soft material soils (Figure 7-12). Those small volume

changes are equivalent to a maximum of 0.03 inches of incremental expansion of any of the 5 foot thick model elements associated with the engineering unit soils, 0.24 inches of incremental compression of the 5 foot thick element associated with the soft zone layer at a depth of 100 feet, and 0.02 inches of incremental compression of the 5 foot thick soft material layer at a depth of 75 feet (Figure 7-12). The net result of the sum of the small volume changes at depth is a maximum of 0.19 inches of ground surface settlement (Curve 5, Figure 7-10).

Final effective stresses at the interfaces between the engineering unit and soft zone soils at the top and bottom of initially underconsolidated soft zone layers must be the same for a settlement model to reach equilibrium, as indicated in the previous paragraph. The compression of the soft zone soils input into the Mohr-Coulomb collapse model is calculated based on the assumption that stresses in underconsolidated soft zone soils increase to the overburden stress. The model forces (pulls) the top of each soft zone layer to move down, in small increments, by an amount equal to the calculated compression of the layer. The effects of changes in engineering unit soil stresses and volumes on the potential compression of the soft zone soils is not considered in the soft zone compression calculation or in the Mohr-Coulomb model. Therefore, ground surface settlements of up to approximately 2.6 inches predicted by the Mohr-Coulomb collapse model are unrealistically large and, at best, should only be considered as representing the upper limit of potential earthquake induced ground settlements. However, contours of ground surface settlements computed from the Mohr-Coulomb collapse model results were estimated using the results from all the geotechnical sections (DCS, 2003d). Those contours are also shown in Figure 7-13.

The Cam-Clay model more accurately models the assumptions of underconsolidated soft zone soils and their compression due to weakening of overlying "soil arches" during an earthquake event. Ground surface settlements of up to approximately 0.2 inches indicated by the model (Curve 5, Figure 7-10) are consistent with the results of other models that incorporate MFFF area buildings and assume normally consolidated soft soils (Section 7.4.3.5) and underconsolidated soft soil layers (Section 7.4.3.4).

MFFF Building settlements predicted by the FLAC Cam-Clay model assuming underconsolidated soft zone soils are less than approximately 0.3 inches larger than settlements predicted using normally consolidated soft zone soils. Ground pressures beneath the building predicted using underconsolidated soft zone soils are also similar to those obtained using normally consolidated soft zone soils. Those settlements and pressures, which include the building loads and incorporate the redistribution of stresses and settlements due to the building stiffnesses, are not much different from settlements and pressures based on normally consolidated soft zone soils.

8. STABILITY OF SUBSURFACE MATERIALS

8.1 LIQUEFACTION

8.1.1 Methodology

8.1.1.1 Overall Approach

The liquefaction potential of the MFFF site within the proximity of the MFFF and BEG Buildings was evaluated using the Cyclic Stress Approach, as described in the Proceedings of the NCEER Workshop on Evaluation of Liquefaction Resistance of Soils (NCEER, 1997). This approach is well suited for utilizing both SPT N-values and CPT tip resistances for estimating the cyclic resistance of soils. This method characterizes earthquake loading by the amplitude of an equivalent number of cycles of uniform shear stress ratio (CSR), and it characterizes soil liquefaction resistance by the amplitude of the uniform cyclic shear resistance ratio (CRR) required to develop liquefaction in the same number of cycles. The liquefaction potential is then evaluated by comparing the earthquake load with the liquefaction resistance throughout the soil profile ($FS_L = CRR/CSR$).

If the CSR is close to, or greater than the CRR, liquefaction is possible. For the MFFF analysis, full liquefaction is considered to have been triggered when the factor of safety against liquefaction ($FS_L = CRR/CSR$) is less than 1.1 (USNRC, 2001). For factors of safety of 1.1 to 2.0, it is possible for excess pore pressures to build up in the soil, thus causing a temporary reduction in strength and stiffness, which may result in soil settlement as the excess pore pressure dissipates.

It should be noted that the Cyclic Stress Ratio Approach was developed based on field observations and experiments on relatively clean sands with little cohesion. It has been recognized that an increase in soil cohesion tends to decrease the potential of liquefaction. However, this effect has not been quantitatively incorporated into the method used in this calculation of the factor of safety against liquefaction, which is conservative. Therefore, the use of the Cyclic Stress Ratio Approach for analyzing the liquefaction potential of the MFFF soils, which, typically, are not clean sands and which possess various degrees of cohesion, is considered to provide a lower-bound factor of safety against liquefaction.

It is entirely possible that a cyclic stress ratio analysis would predict that a soil deposit is liquefiable when such an occurrence would be highly unlikely or impossible due to the cohesive nature of the soil. In the MFFF analysis, the liquefaction potential of cohesive soils was evaluated using the following criteria:

- cohesive soils having a fines content (smaller than No. 200 material) greater than 30 percent and fines that either classify as clays, or have a Plasticity Index greater than 30 percent are not generally considered liquefiable; and

- soils with a clay content greater than 15 percent and a liquid limit greater than 35 percent, occurring at a natural water content lower than 90 percent of the Liquid Limit, are considered non-liquefiable. (Wang, 1979)

8.1.1.2 Earthquake Load

The earthquake load, or seismic demand, placed on a layer of soil is expressed in terms of a cyclic stress ratio (CSR), defined as:

$$CSR = \frac{\tau_{ave}}{\sigma'_{vo}} = 0.65 \left(\frac{a_{max}}{g} \right) \left(\frac{\sigma_{vo}}{\sigma'_{vo}} \right) r_d \quad (8-1)$$

where:

- τ_{ave} = average cyclic shear stress
- a_{max} = maximum horizontal acceleration at ground surface
- g = acceleration due to gravity
- σ_{vo} and σ'_{vo} = total and effective vertical overburden stresses
- r_d = stress reduction factor (dependent on depth).

The CSR profile from the design earthquake was estimated directly using the ProShake computer program as part of the free-field site response analysis for the MFFF Structure Vicinity (DCS, 2003a). The second part of Equation 8-1, used for the simplified method, was not used in this analysis. At any depth, if the CSR is close to or greater than the CRR, liquefaction is possible in liquefiable soils. For the MFFF analysis, full liquefaction is assumed to be possible when the factor of safety against liquefaction, $FS_L = \left(\frac{CRR}{CSR} \right)$, is less than 1.1. For factors of safety of 1.1

to 2.0, it is assumed that it is possible for excess pore pressures to build up in the soil; thus, causing a temporary reduction in strength and stiffness, which may result in soil settlement, referred to as post-earthquake settlement, upon dissipation of these excess pore pressures.

A groundwater depth of 60 feet (El 210 feet) was used to compute all of the CSR profiles (DCS, 2003a). This groundwater depth is the MFFF site design groundwater level and is considered conservative. The groundwater level across the MFFF site presently averages over 70 feet deep. Section 5.3.1 discusses the groundwater conditions at the MFFF site in detail.

8.1.1.3 Determination of Soil Capacity (Cyclic Resistance Ratio)

The resistance of the soil to liquefaction (i.e., its strength) is expressed in terms of the “cyclic resistance ratio” (CRR), where:

$$\text{CRR} = \frac{\tau_{\text{cyc}}}{\sigma'_{\text{vo}}} \quad (8-2)$$

The CRR profile was estimated using SPT and CPT data, as discussed in the following sections. The empirical correlation between CRR and boring or CPT data in the NCEER method was developed based on a magnitude 7.5 earthquake. For earthquakes of other magnitudes, CRR must be scaled by an appropriate Magnitude Scaling Factor (MSF). For the moment magnitude 6.0 assigned to the PC-3-based motion, a magnitude scaling factor (MSF) of 2.0 was used to compute the normalized CRRs, based on the recommendations of the NCEER workshop. For the 7.3 M_w 1886 Charleston earthquake-based motion, the magnitude scaling factor used in the analyses was 1.1. The PC-3+ motion was developed from a hazard that incorporates many earthquake magnitudes and distance pairs. Based on the recommendations of WRSC (2000), liquefaction and post-earthquake settlement analyses were conducted using several magnitudes and the results were weighted based on the contributions from the available hazards; EPRI, LLNL, and USGS. The evaluation showed that the 1886 Charleston (50th percentile) motion provide an upper bound to the liquefaction and post-earthquake settlement at the MFFF site (DCS, 2003j).

8.1.1.4 Cone Penetration Tests

The results of the CPT soundings located within the boundary of the PIDAS fence surrounding the MFFF, as shown in Figure 4-1, were used to evaluate the liquefaction potential of the soils underlying the MFFF and BEG Buildings. Of the 125 CPTs performed during the 2000 and 2002 subsurface investigations, 95 were located within or very close to the proposed structure footprints of the MFFF and BEG Buildings. The remaining CPTs were drilled during the original MFFF geotechnical investigation performed in 2000, prior to relocating the MFFF to its present location. After relocating the MFFF to its current location, as shown in Figure 4-1, these CPTs were located sufficiently east of the PIDAS fence shown in this figure that it was considered inappropriate to include them in the MFFF liquefaction analyses. The CRR was estimated directly from CPT data utilizing the methodology outlined by Robertson and Wride (1997) in the NCEER workshop.

A key parameter in the CPT liquefaction analysis is the correction of tip resistance for fines content. A relatively good correlation between the CPT-estimated fines contents and laboratory data at the MFFF site was obtained using site-specific equations developed for use at SRS (WSRC, 2000). The CRR profile below the groundwater table was computed for each of the 95 CPTs without regard to cohesiveness of the soils (DCS, 2003c and 2003q).

The CPT tip resistance is normalized to correct for overburden stress using the following expression:

$$q_{cIN} = \left(\frac{q_c}{P_{s2}} \right) C_q \quad (8-3)$$

This is a dimensionless quantity, where:

q_c = measured cone tip resistance

$$C_q = \text{correction for overburden stress} = \left(\frac{P_s}{\sigma'_{vo}} \right)^{0.5}$$

P_s = reference pressure of 100 kPa in same units as σ'_{vo} ; $P_s = 100$ kPa if σ'_{vo} is in kPa.

P_{s2} = reference pressure of 100 kPa in same units as q_c ; $P_{s2} = 0.1$ MPa if q_c is in MPa.

A maximum value of $C_q = 2$ should be applied to CPT data at shallow depths. The groundwater table at each CPT was assumed to be at El 210.

To estimate the fines content from the CPT data, the SRS-specific fines content correlation developed by WSRC (2000) was used. The fines contents estimated by this correlation agree reasonably well with the gradation analyses performed on SPT samples obtained from the borings drilled at the MFFF site.

The SRS equation for estimating fines content from CPT data is:

$$\text{Fines Content, FC (\%)} = 0.3 (I_{fc}^{3.5}) + 2 \quad (8-4)$$

$$\text{where } I_{fc} = 1.1 + \left[(1.5 - \log Q_t)^2 + (\log Fr + 1.7)^2 \right]^{0.5} \quad (8-5)$$

$$Q_t = \text{normalized penetration resistance, } Q_t = \left(\frac{q_t - \sigma_{vo}}{\sigma'_{vo}} \right) \quad (8-6)$$

$$Fr = \text{normalized friction ratio, } Fr = \left(\frac{f_s}{q_t - \sigma_{vo}} \right) \times 100 \quad (8-7)$$

q_t = CPT tip stress corrected for unequal area effects

f_s = CPT sleeve friction stress

The equivalent "clean sand" corrected CPT penetration resistance is obtained by:

$$(q_{cIN})_{cs} = \Delta(q_{cIN}) + (q_{cIN}) \quad (8-8)$$

$$\text{where: } \Delta q_{cIN} = \frac{K_{CPT}}{1 - K_{CPT}} q_{cIN} \quad (8-9)$$

presented in Figures 6-19 and 6-20. The FS_L s for the 95 CPTs located within or near the proposed structure footprints of the MFFF and BEG Buildings, computed with CSRs from the generalized soil column, PC-3+ and the Charleston control motions, are presented in Figures 8-1 through 8-95.

For the PC-3+ motion the factors of safety against liquefaction based on the CPTs generally are high, exceeding 1 for all of the CPTs and generally exceeding 1.5. Factors of safety against liquefaction of 1.1 were obtained only for very thin zones in only a few, isolated locations. These included zones that were 3.5 inches thick in CPT-27, 6.5 inches in SCPT-86, 2.5 inches in SCPT-87A, 14.8 inches in SCPT-89A, 3.9 inches in CPT-101, 8 inches in CPT-117, and 0.72 inches in CPT-118. It is important to recognize that the correlation between CRR and q_{cIN} in the NCEER procedures is based on average CPT values for a given soil layer. Applying the correlation to every single measured CPT value in soil deposits may result in factors of safety at one or a few points that are substantially lower than the average of that layer. This or these factors of safety should be considered as not representative of the layer and, consequently, are very conservative.

Even if liquefaction of the soils in such thin, isolated zones could occur, it would not be a concern for the MFFF site. The FS_L ranges between 1.2 and 1.5 at certain depths in several CPTs; however, overall, the total thickness of soils with FS_L greater than 1.5 prevails at the site.

For the Charleston earthquake-based motion, factors of safety against liquefaction were similarly greater than 1 at all locations; therefore, liquefaction will not occur for the Charleston-based motion. However, relatively more areas had factors of safety of less than 2. As discussed in Section 8.2, post-earthquake settlements are assumed to occur for factors of safety against liquefaction of less than 2. Therefore, estimated post-earthquake settlements for the Charleston earthquake will be greater than the estimates for the PC-3+ earthquake. The following discussion details the implications of the lower factors of safety for the Charleston motion.

The factors of safety against liquefaction based on the CPTs for the Charleston motion exceed 1.0 for all of the CPTs, except CPT-65 and CPT-114, where $FS_L = 1.0$ was computed for three very thin soil intervals – a 2.54-inch thick interval and a 0.88-inch thick interval in CPT-65 and a 1.73-inch thick interval at CPT-114. Because the computed factors of safety against liquefaction were rounded to one decimal place, the FS_L for all of the three thin intervals are shown as 1.0. The minimum computed FS_L values was 1.04 for all of these intervals. All three thin intervals are in the ST2 layer, which is the stratum immediately above the Green Clay formation at approximately elevation 153 ft. Therefore, these thin intervals are isolated weak seams at great depth below the foundations of the structures. Post-earthquake settlements within these thin zones would not cause any measurable impact to the structures founded near the surface of the site at approximately El 270; i.e., approximately 120 ft above these thin zones.

Statistical analyses were performed of the factors of safety against liquefaction at the MFFF site based on the CPT data. The average FS_L was computed for each engineering unit below the groundwater table and above the non-liquefiable GC stratum; these included Engineering Units

TR3/4, DB1/3, DB4/5, ST1, and ST2. The averages were obtained as weighted values, considering the variation in engineering unit thickness from CPT to CPT. Equation 8-10 was used to calculate the average FS_L for each engineering unit:

$$FS_{L,avg} = \frac{\sum_{i=1}^{95} \sum_{j=1}^n FS_L \times dt}{\sum_{i=1}^{95} \sum_{j=1}^n dt} \quad (8-10)$$

where $FS_{L,avg}$ = average FS_L for an engineering unit

FS_L = factor of safety computed of each tested interval

dt = thickness of soil interval (typical thickness approximately 1.0 inches)

n = number of soil intervals actually penetrated by each CPT within each unit; n varies between CPTs.

95 = total number of CPTs evaluated. (Note: Did not use SCPT-87. Used SCPT-87A, which was performed adjacent to SCPT-87 and fully penetrated the ST2 layer.)

The resultant averages of the factors of safety against liquefaction by engineering unit are listed in Table 8-1 and are shown in Figure 8-96. It can be seen in Table 8-1 and Figure 8-96 that the average factors of safety against liquefaction for all of the soils underlying the MFFF site exceed 1.3, indicating that these soils will not liquefy due to cyclic shear stresses resulting from the design earthquake (i.e., $FS_L > 1$).

The lowest factor of safety was calculated for the ST2 layer, the deepest engineering unit in the profile above the Green Clay stratum. The average FS_L of the overlying layers is higher. Immediately above the ST2 layer is Engineering Unit ST1, which is much thicker than ST2 and has an average FS_L of 4.35. The presence of this liquefaction-resistant layer and the thick zone of soils above the groundwater table at the site, which are not susceptible to liquefaction, preclude any adverse effects at the surface due to liquefaction of the underlying layer even if it could occur.

According to Ishihara (1985), based on field observations, an overlying liquefaction-resistant stratum has a significant influence on surface damage induced by an underlying liquefiable soil stratum. As shown in Figure 8-97 (from Ishihara, 1985), liquefaction-induced ground damage is a function of seismic ground acceleration, thickness of the liquefaction-resistant surface soil layer, H_1 , and thickness of the liquefiable sand layer, H_2 . For the case of the MFFF site under an assumed 1886 Charleston (50th percentile) control motion, the maximum ground acceleration would be on the order of 0.11g (DCS, 2003f). Conservatively using the boundary curve for "Max. acc. 200 gal" in Figure 8-97, liquefaction-induced ground damage will not occur due to liquefaction of a deeper-lying soil layer if there is an overlying liquefaction-resistant soil layer that is at least 3 meters (10 ft) thick.

In the case of MFFF site, the groundwater table is approximately 60 ft below the design foundation elevation. This 60 ft of unsaturated soils is much thicker than the thickness of a liquefaction-resistant soil layer (i.e., $H_1 = 10$ ft, as shown in Figure 8-97, from Ishihara, 1985) required to preclude damage due to liquefaction of an underlying layer. The other engineering units overlying the ST2 layer also have factors of safety against liquefaction indicative of liquefaction-resistant soil layers, especially the ST1 layer (average $FS_L = 4.35$). Therefore, the thickness of liquefaction-resistant soil layers overlying the layer with the least resistance to liquefaction at the site, the ST2 layer, will preclude any adverse effects from liquefaction of the ST2 layer even if it could occur.

The conclusion that liquefaction will not occur due to shaking caused by the design earthquake is also demonstrated by evaluation of the shear wave velocity characteristics of the MFFF site. According to Seed et al (1983) based on world-wide field observations, values of shear wave velocity can be used as a reliable indicator for liquefaction susceptibility of a site. Seed et al conclude that *“Liquefaction will never occur in any earthquake if the shear wave velocity in the upper 50 feet of soil exceeds about 1,200 fps.”* For the MFFF site, the measured shear wave velocities within the upper 58 feet (from the design elevation of the foundation base at El 270 to the top of Engineering Unit TR3/4 at El 212) are greater than 1,200 fps (DCS, 2003e), as illustrated in Figure 8-96. This demonstrates that the subsurface soils at MFFF site are not susceptible to liquefaction due to shaking caused by the design earthquake.

8.1.2.2 Standard Penetration Tests

The factors of safety against liquefaction based on SPT data from the fourteen borings located within or near the proposed structure footprints of the MFFF and BEG Buildings, computed using CSRs from the generalized soil column and the PC-3+ and Charleston based control motions, are presented in Figures 8-98 through 8-111. For the PC-3+ control motion the factors of safety against liquefaction at all of the borings are generally high, with exceptions at seven, isolated locations in six of the borings. For these seven isolated locations, values of FS_L range from 1.2 and 1.4; elsewhere, all FS_L exceed 1.5. The scale and impact of FS_L being less than 1.5 at these seven locations are discussed as follows (DCS, 2003c):

8.1.2.2.1 BH-7

There was one SPT blowcount resulting in a FS_L of less than 1.5 in Boring BH-7. The sample was at El 179 from the DB4/5 layer, and it had a $(N_1)_{60cs}$ of 6 and a FS_L of 1.4. The material within five feet above and below the sample had blowcounts resulting in factors of safety greater than 1.5.

The measured tip resistance values at SCPT-23 (ARA, 2000), located approximately 35 ft away from BH-7, also show a dip at El 179 ft, but with very limited thickness (approximately 2.5 ft).

8.1.2.2.2 BH-11

Boring BH-11 had one SPT sample that resulted in a FS_L of less than 1.5. At El 205 in this boring, $(N_1)_{60cs} = 6$ for Sample 9A, which had a fines content of 12.1 percent, resulting in $FS_L = 1.4$. This sample was taken from the DB1/3 layer, located about five feet below the conservatively assumed design groundwater level of El 210.

The elevation of the groundwater table was measured in dissipation tests that were performed in many of the CPTs. As shown in Figure 4-1, the location plan of the geotechnical investigations, the CPTs closest to this boring include CPT-59, CPT-67, CPT-68, CPT-83, and CPT-84. The elevation of the groundwater table measured at the other CPTs in the vicinity of BH-11 were as follows: El 199 at CPT-67, El 189 at CPT-68, and El 193 at CPT-84 (Note, a dissipation test was not performed in CPT-59). Based on these results, it is likely that the soils at the depth of this sample will not be saturated should the design earthquake occur, and even if they were, they still would not liquefy based on the calculated FS_L in excess of 1.

8.1.2.2.3 BH-13

There was one sample at El 182, which had an $(N_1)_{60cs}$ of 6 that resulted in a FS_L of 1.4. This sample was from the DB4/5 layer. No laboratory tests were conducted on this sample. The samples within five feet above and below this sample had FS_L values of 5.5 and 5.6, respectively.

8.1.2.2.4 BH-16

There was one sample at El 182 with a $(N_1)_{60cs}$ of 5, resulting in a FS_L of 1.3. This sample was from the DB4/5 layer, and it was an SM material with 19.2 percent of moderately to highly plastic fines. The LL was 56 percent and the PI was 26 percent. The sample two feet above it had a FS_L of 1.9.

8.1.2.2.5 BH-18

There was one sample, Sample 4A at El 178, which had an $(N_1)_{60cs}$ of 4, resulting in a FS_L of 1.2. This sample was from the DB4/5 layer, and it was an SP-SM material with a 9.8 percent of nonplastic fines. The samples within five feet above and below this sample had FS_L values greater than 3.

8.1.2.2.6 BH-20

There were two SPT blowcounts resulting in FS_L of less than 1.5 in Boring BH-20. The first one was at El 165, and it had a $(N_1)_{60cs}$ of 5 and a FS_L of 1.4. This sample was from the ST1 layer, and it was an SM material with 9.7 percent nonplastic fines. The sample five feet below it had blowcounts resulting in a FS_L of 5.1. Blowcounts were not recorded for the sample 5 ft above at El 170 due to an accidental 10-ft drop of the rods. The top eight inches of the sample at El 170 was sandy silt with 32.1 percent passing sieve No. 200 and a PI of 26 percent. This material is unlikely to liquefy.

The second sample was from El 140, and it had a $(N_1)_{60cs}$ of 5 and a FS_L of 1.4. This sample was described as moderately plastic sandy clay with 70.8 percent passing No. 200 sieve and a PI of 20.

Factors of safety against liquefaction from the SPT analyses using the Charleston earthquake-based motion were similarly higher than 1.5 except at a few isolated locations. There were nine such locations consisting of the seven detailed above for the PC-3+ based motion and two additional locations in Boring BH-7 ($FS_L = 1.4$ at El 189) and Boring BH-11 ($FS_L = 1.2$ at El 142). The sample at El 142 in boring BH-11 is described as sandy silt with clay lamina with 65.1 percent passing the No. 200 sieve. The lowest FS_L calculated for all of the SPT measurements at the 168 locations from the design groundwater level (El 210) to the GC unit within the vicinity of the MFFF based on the Charleston earthquake motion was 1.1, which was obtained at two locations; El 178 in Boring BH-18 and El 165 in Boring BH-20. Samples five feet above and below the sample at El 178 in Boring BH-18 had factors of safety against liquefaction of 2.9 and 4.2 respectively. The factor of safety against liquefaction was 4.1 for the sample five feet below the sample at El 165 in Boring BH-20. As noted in the discussion of this location for the PC-3+ earthquake, the sample five feet above El 165 in Boring BH-20 has high plasticity fines and is a non-liquefiable material.

8.1.3 Summary of Liquefaction Analyses for the Generalized Soil Profile

The results of the liquefaction analyses, using either CPT or SPT data, indicate that the soils within the MFFF Structure Vicinity will experience no liquefaction as a result of the design earthquake. This is mainly due to the medium dense to dense state of the overall soil profile and the substantial fines contents of these soils, combined with the generally cohesive nature of the soils, as described in Section 5. In addition, the substantial depth (~60 ft) to the groundwater also contributes to the stability of the subsurface soils with respect to resistance to liquefaction.

8.1.4 Liquefaction Results for the Soil Profiles Based on Individual SCPT

The liquefaction potential for 18 seismic cone penetration test data and adjacent borings performed in 2000 and 2002 was evaluated using cyclic stress ratio (CSR) profiles for each SCPT with the results detailed in the following sections. A similar analysis was performed on 15 seismic cone penetration test data and adjacent borings performed in 2000 as detailed in DCS (2001j). The results of the prior analysis and other liquefaction analyses (DCS, 2003c and 2003q) show that the 1886 Charleston (50th percentile) motion is more critical with respect to factor of safety against liquefaction and post-earthquake settlement. Consequently the evaluation of the liquefaction potential based on individual SCPTs was performed only with the more critical Charleston motion. The measured tip stresses and sleeve stresses were averaged per foot of depth and the NCEER procedures were applied to the resulting stresses (DCS, 2003j). This averaging procedure smoothes out the spikes in the field measurements and minimizes misleading conclusions DCS, 2003j.

8.1.4.1 Soil Columns by SCPT and 1886 Charleston Motion

The FS_L s for the 18 SCPTs, computed with CSRs calculated by individual SCPT and the 1886 Charleston control motion, are presented in Figures 8-112 through 8-129. The factors of safety against liquefaction are generally high; they are equal to or exceed 1.1 for all depths (DCS, 2003j).

8.1.4.2 Soil Columns by SCPT and 1886 Charleston Motion (SPT Data)

The FS_L s based on SPT data from three borings (BH-14, BH-16, & BH-20) located adjacent to SCPTs, computed with CSRs from the individual SCPT profiles and 1886 Charleston control motion, are presented in Figures 8-116, 8-124, and 8-128 (DCS, 2003j). The FS_L based on SPTs are all greater than 1.1, except for one measurement at El. 182 at BH-16 where the $FS_L = 1.1$.

8.1.5 Summary of Liquefaction Results Based on Individual SCPT

The factors of safety against liquefaction using cyclic stress ratios (CSR) calculated from 18 individual SCPT profiles (DCS, 2003j) are of the same order of magnitude as the generalized profile. These factors of safety, which are obtained at depths of over 60 ft for individual sampling points, require an evaluation of the interaction of these sampling points with surrounding materials. In both the generalized soil column and the individual CSR profiles, the lowest factors of safety typically occur in zones of limited extent and are bounded by materials with higher factors of safety against liquefaction.

As discussed in Section 6, in the one-dimensional ground response analysis, the characteristics of the site are best represented by the average properties at the site. The site will most likely respond to an earthquake as simulated by a generalized soil column, rather than to a soil column developed based on individual seismic CPTs. An adequate amount of data were obtained in the latest investigations (2002) for the average values to accurately characterize the site and, therefore, it seems prudent to use the generalized soil column for evaluation of liquefaction and estimation of post-earthquake settlement.

8.2 POST-EARTHQUAKE SETTLEMENT

Post-earthquake settlements due to two assumed scenarios are addressed. One scenario is the dissipation of excess pore pressures, which can build up as a result of cyclic shearing of the soils within the profile during an earthquake. The method recommended by Ishihara & Yoshimine (1990) was used to estimate the magnitude of the settlement at each boring and CPT within the MFFF Structure Vicinity, as detailed in Section 8.2.1. Section 8.2.2 addresses the increment of post-earthquake settlement applicable to the ST1 and ST2 layers for those CPTs that could not penetrate these layers because of stiffer overlying layers at those locations.

Also addressed is the hypothesis proposed in Bechtel (1998) regarding the potential for consolidation settlement of the "soft zone" soils to occur following the design earthquake. The premise is that shearing stresses due to the earthquake cause the destruction of postulated zones

of arched soils above the soft zones, resulting in increases in the vertical stresses applied to the presumably underconsolidated soft zone soils to the full overburden pressures at that depth in the profile. In this scenario, additional settlement is anticipated to follow the earthquake as the soft zone soils consolidate under these increased vertical stresses, ultimately reaching the ground surface. The possibility of this type of post-earthquake settlement is discussed in detail in Section 8.2.3.

Section 8.2.4 presents the results of the post-earthquake settlement analyses and Section 8.2.5 provides a summary of the discussion included herein regarding post-earthquake settlements.

8.2.1 Settlement Due to Dissipation of Excess Pore Pressure Buildup from Seismic Loadings

The post-earthquake settlement at the MFFF site was estimated using the Ishihara & Yoshimine (1990) method. The term “factor of safety for liquefaction (F_L)” defined in the Ishihara & Yoshimine (1990) method is the same as FS_L described above (NCEER, 1997). Ishihara & Yoshimine assume that volumetric strain due to earthquake-induced cyclic shearing will occur in clean sands if the factor of safety for liquefaction (F_L) is less than 2.0. This volumetric strain occurs when excess pore pressures, which can build up as a result of cyclic shearing of the soils within the profile during an earthquake, dissipate. Ishihara & Yoshimine use the term “post-liquefaction settlement” to identify this settlement, even though there has been no liquefaction of these soils (i.e., $FS_L > 1$). In this report, the term “post-earthquake settlement” is used to identify this settlement, to dispel the notion that liquefaction of these soils has actually occurred. As discussed above, FS_L exceeds 1 for all of these soils; therefore, they will not liquefy due to cyclic shearing from the design earthquake.

Figure 8-130 presents the relationship proposed by Ishihara & Yoshimine between factor of safety for liquefaction (F_L), volumetric strain (E_v), soil relative density (as a function of equivalent SPT blowcount or CPT tip resistance), and maximum cyclic shear strain (γ_{max}). The post-earthquake settlement of a soil layer is calculated as the volumetric strain multiplied by the thickness of the corresponding soil layer.

The post-earthquake settlements calculated based on the CPT tip resistance values and SPT blowcounts were computed for those layers judged to be potentially liquefiable. Based on industry-accepted practice, soils considered to be non-liquefiable include those that:

- i. classify as clays based on the USCS;
- ii. have a plasticity index (PI) of greater than 30 percent; or
- iii. have clay content greater than 15 percent, a liquid limit of greater than 35 percent, and occur at a natural water content of less than 90 percent (Wang, 1979).

These criteria were applied to the analysis of the borings, where applicable. The cutoff elevations for calculating post-earthquake settlements are El 210 and El 140. The design groundwater table is at El 210; therefore, the soils above this elevation are not saturated and,

thus, are non-liquefiable. Below El 140, the soils are "Green Clay" or the underlying Congaree formation, comprised of very dense sands and, thus, are non-liquefiable.

In determining the thickness of soil corresponding to an SPT blowcount indicating that it may be liquefiable, the thickness of the potentially liquefiable layer is assumed to extend halfway between the sample in question and the adjacent samples above and below.

The post-earthquake settlements calculated based on the CPT values were computed for all CPT tip resistances with estimated fines contents of 30 percent or less, without considering the cohesion of the soil; this conservatively overestimates the post-earthquake settlement. As discussed in DCS (2003j), soil behavior type data provided by ARA (2000 and 2003) show soils with fines content greater than 30% are clays and, therefore, they should be excluded from the determination of post-earthquake settlement. The data also shows areas with fines content of less than 30% that classify as clay; however, these soils were included in the calculation of post-earthquake settlements. Inclusion of these soils (those with fines contents < 30%) in the calculation of post-earthquake settlement for these areas simplified the numerical process and leads to a conservative overestimation of the post-earthquake settlement applicable to the MFFF site.

8.2.2 Additional Post-Earthquake Settlements for CPT Soundings that Hit Refusal Before Penetrating the ST2 Layer

As noted in Section 8.2.1, the elevation of concern for susceptibility of liquefaction and post-earthquake settlement is between El 210 and El 140, which includes engineering units TR3/4, DB1/3, DB4/5, ST1, and ST2. The CPT records indicate that some CPTs did not penetrate engineering units ST1 and ST2 because the overlying soils were strong enough to prevent penetration by the cone, even at tip stresses as high as 800 tsf. There were forty-four such CPT soundings out of the total of ninety-five (95) CPT soundings in the area. The average strain in the units that were fully penetrated was used to estimate the post-earthquake settlements of the layers below the bottom of the partially penetrating CPTs. The additional post-earthquake settlement of the CPTs that did not fully penetrate the ST1 and ST2 layers was obtained by multiplying the average volumetric strain that occurred in these engineering units by the thickness of the portion of the units not penetrated by the CPTs.

8.2.3 Settlement Due to Consolidation of Soft Zone Soils as a Result of Earthquake-Induced Increase in Overburden Pressures

The MFFF site geotechnical investigations (DCS, 2003f) noted that some isolated zones of soft clayey materials are present within the TR3/4, DB1/3, and GC layers beneath the MFFF site. These pocketed zones are deep (typically 90 to 140 feet below the ground surface), and they are very limited in lateral and vertical extent (DCS, 2003d). It is generally accepted that these soft zones in the ST1 and ST2 layers at the SRS formed as a result of dissolution of carbonate-rich, clastic sediments – a process that reduces the stiffness of the materials. In addition, as the materials lose stiffness during the dissolution process, they tend to compact. However, it is

speculated that due to the limited lateral extents of the isolated pockets of the soft zones, the overlying stiffer soils “arched” over these pockets of soft materials. The assumed arching supports the overlying soils, resulting in the soils in the pockets of soft zones being underconsolidated. A concern has been raised (Bechtel, 1998) that such arches might be broken during an earthquake, and, as a result, the soft zone soils would be exposed to the full overburden pressure of the overlying soils. In this case, consolidation settlement of the soils within the soft zones would occur under the increased vertical stresses, leading to additional post-earthquake settlement, which would ultimately spread to the ground surface.

This scenario involves a series of assumptions. Validation of each of the assumptions is discussed below.

8.2.3.1 Soil Arching

Arching of soils above the soft zones can be verified by comparing the strength of the soils within the assumed area of arching with the strength of the adjacent soils at the same elevation. If arching has occurred, the strength of the soil in the arched area should be greater than the strength (i.e., as measured by the CPT tip resistance) outside of the arched area. Should there be no significant difference in the strength of the soils in these areas, the formation of such an arch may lack physical support.

Comparison of soil strength was made at selected locations where a soft zone was identified. Figure 8-131 shows the CPT tip resistance values measured at CPT-106 and those measured at the CPTs adjacent to CPT-106. A soft zone of 2.1 feet thick was identified around elevation 182 feet at CPT-106 (DCS, 2003f). No soft zones were identified at this elevation in CPT-112, CPT-107, and CPT-51, which were located adjacent to CPT-106, as shown in Figure 8-131. The profiles of the CPT tip stresses in the figure indicate that the identified soft zone is within a weak soil layer from approximately El 185 ft to El 176 ft at CPT-106. The pattern of the tip stress profiles suggest that this weak layer stretches across this area; it is present from approximately El 182 ft to El 174.5 ft at CPT-112, from El 181 ft to El 173.5 ft at CPT-107, and from El 178 to El 172 ft at CPT-51. A strong soil layer exists immediately above the weak layer, extending approximately from El 185 ft to El 190 ft at CPT-106, from El 182 ft to El 188 ft at CPT-112, from El 181 ft to El 188 ft at CPT-107, and from El 178 to El 186 ft at CPT-51. The tip stresses measured in the strong layer at CPT-106 are slightly less than those measured in the strong layer at the adjacent CPTs outside the soft zone. This demonstrates that localized soil arching immediately above the soft zone noted in CPT-106 may not exist. At other locations a pattern of relatively higher tip stresses immediately above the identified soft zones could not be established.

8.2.3.2 Breakdown of Arches in Soils Above Soft Zones Due to Earthquake

The soils at the MFFF site immediately above the soft zones were classified as SC, SM, and SP-SM soils with various amounts of plastic or slightly plastic fines content. These types of soil, in general, have stronger interparticle bonds than clean sands, and they are not as vulnerable to

buildup of excess pore pressures due to seismic cyclic shearing. The computed cyclic stress ratios developed under the design earthquake at the depths of the assumed areas where arching may have occurred are less than 0.09, and the corresponding effective cyclic shear strains are less than 0.035%, based on DCS (2003a). Soils under such limited amounts of cyclic loading behave primarily as elastic materials. The magnitudes of cyclic stresses and strains are not sufficient to alter the static stress conditions within the soil mass. It is very unlikely that the soil structure would undergo drastic changes and break any "arches" that might exist at these depths during the design earthquake.

Another argument is that the MFFF site has experienced numerous historical earthquakes after the postulated formation of such soil arches. Some of these earthquakes had intensities that were close to the intensity of the design earthquake (DCS, 2000d). If arching had occurred over soft zones that had formed in the past and such arches could be broken by earthquake disturbance, this would have occurred a long time ago, and the current overburden pressure above the soft zones would be equal to that of the existing overburden soils.

Figure 8-77 shows the CPT tip stresses measured at CPT-106. Two soft zones are identified around El 182 ft and El 142 ft. Assume that soil arching occurred immediately above the soft zones, as represented by the reduction in tip stress at El 187 ft and El 146 ft. Also assume that the earthquake could break the soil arch immediately above this zone. In this case, it is expected that the overlying soils would create a new arch as the underlying soft zone soil settles. Because the soft zones are so deep at the MFFF site, it would be difficult for the earthquake to break all of the stronger soil layers above the soft zones; e.g., the thick stiff layer from El 150 ft to 170 ft with tip stresses on the order of 200 tsf and the stiff layers above El 195 ft with tip stresses on the order of 150 tsf.

Based on the reasoning presented above, it is concluded that the breaking of the postulated soil arches above the soft zones due to the design earthquake is not considered to be a realistic assumption.

8.2.4 Results of Post-Earthquake Settlement Analyses for the Generalized Soil Profile

8.2.4.1 Post-earthquake Settlement Based on PC-3+ Control Motion

The estimated post-earthquake settlements, computed using the PC-3+ motion for all of the CPTs and borings within the MFFF Structure Vicinity, are presented in Tables 8-2 and 8-3 and are posted at the locations of the respective borings and CPTs on the location plan that is included as Figure 8-132. The post-earthquake settlements calculated based on the CPTs are considered to provide a much more reliable estimate of the post-earthquake settlements than those based on the borings because of the robustness of the data collected. Therefore, the values computed for the borings are printed in a smaller, lighter font to distinguish them from those calculated based on the CPT data. In addition, the contours of post-earthquake settlement shown on this figure are based only on the results from the CPTs.

The CPTs provide a nearly continuous record of the strength of the soils, collecting data at a frequency of approximately one reading every 2 cm (< 1 inch interval of depth per reading) as the penetrometer is pushed into the subsurface soils. In addition, the CPT data are collected using instrumentation that is calibrated on a daily basis to ensure that the system is working correctly. On the other hand, the borings provide a snapshot of the strength of the soils, generally collecting one sample for every 5-ft depth interval penetrated as the boring is advanced into the subsurface soils. In addition, the SPT blowcount, which provides the strength of the soils required for the post-earthquake settlement calculation, is less robust because of the nature of the Standard Penetration Test. For example, the hammer drop may vary somewhat from the prescribed 30 inches, friction losses between the hammer and drill rods may affect the values obtained, and since these data are recorded manually, based on observations by the driller and the field inspector, it is possible that errors may be made in determining and recording the SPT N-value. Therefore, the CPTs collect far more detailed and higher quality data than do the borings, providing a much better estimate of the post-earthquake settlement.

As indicated in Table 8-3, the maximum post-earthquake settlement is estimated to be 1.47 inches, occurring at CPT-101, located approximately 50 ft east of the MFFF structure, under the northern end of the HVAC Chillers. The post-earthquake settlement at SCPT-94, located about 50 ft north of CPT-101, which is also about 50 ft east of the MFFF structure, is 1.43 inches. Directly beneath the MFFF structure, the maximum estimated post-earthquake settlement is 1.36 inches, occurring at CPT-60, located near the southern edge of the structure, just east of the centerline of the building. At CPT-55, located near the center of the MFFF structure, the estimated post-earthquake settlement is 1.3 inches. Elsewhere under the MFFF structure, the estimated post-earthquake settlements are fairly uniformly distributed about the average value of approximately 0.9 inches, as evidenced by the contours of post-earthquake settlements presented in Figure 8-132. The minimum post-earthquake settlements occurred at the northern-central portion of the MFFF structure, ranging from about 0.3 inches to 0.4 inches.

The maximum post-earthquake settlement of 1.47 inches occurs at CPT-101. This settlement includes 0.20 inches estimated for the 8-ft portion of engineering unit ST2 that was not penetrated by this CPT because the stiffness of the overlying materials precluded penetration to the target layer, the Congaree formation. This estimate is based on an overall average strain for all of the CPTs that penetrated engineering unit ST2. The post-earthquake settlement at SCPT-94, approximately 50 ft north of CPT-101, was 1.43 inches. SCPT-94 fully penetrated the ST1 and ST2 layers and, the post-earthquake volumetric strain in ST2 at CPT-94 was comparable to the average volumetric strain. Therefore, the estimated additional settlement applied to the calculated post-earthquake settlement based on the depth penetrated by CPT-101 to account for the portion of the ST2 layer that was not penetrated by that CPT seems reasonable. The plots of the variation of the factor safety against liquefaction, Figures 8-65 and 8-72, show that SCPT-94 and CPT-101 have comparatively more extensive zones with lower factors of safety (FS_L between 1.3 and 1.5) than at locations with less post-earthquake settlement. Since post-earthquake settlements increase as the factor of safety against liquefaction decreases, it is

reasonable that the post-earthquake settlements calculated for these CPTs would be greater than those calculated elsewhere at the site.

The lowest post-earthquake settlements of 0.26 inches and 0.28 inches occurred at CPT-110 and SCPT-75, respectively. Table 8-3 indicates that engineering units ST1 and ST2 were fully penetrated at both locations. Soft zones were not encountered at these locations, which contributed to the low post-earthquake settlements calculated for these CPTs. The primary reason these are low, however, is demonstrated by Figures 8-47 and 8-81, which show that these locations had very limited depth zones where the factor of safety against liquefaction was less than 1.5. CPT-112, located just south of this area, encountered a soft zone, but the extent of the soft zone was limited, which contributed the low post-earthquake settlement estimate of 0.4 inches at this location. The lowest volumetric strain for the CPTs that did penetrate the ST2 layer occurred at CPT-110, and it was about 1/3 of the average volumetric strain from all of the CPTs, indicating that the post-earthquake settlement increment applied to the portions of the ST2 layer that were not penetrated by the CPTs in the vicinity of this CPT might be overestimated.

8.2.4.2 Post-earthquake Settlement Based on 1886 Charleston (50th Percentile) Control Motion

The estimated post-earthquake settlements, computed based on all of the borings and CPTs performed within the MFFF Structure Vicinity, are presented in Table 8-4 (boring data) and Table 8-5 (CPT data) and are posted at the locations of the respective borings and CPTs on the location plan that is included as Figure 8-133. As discussed above, the post-earthquake settlements calculated based on the CPTs are considered to provide a much more reliable estimate of the post-earthquake settlements than those based on the borings because of the robustness of the data collected and, therefore, the contours of post-earthquake settlement shown on Figure 8-133 are based only on the results from the CPTs.

It should be recognized that the settlement contours shown in Figure 8-133 are based on estimated post-earthquake settlements that may occur within the soils found at depths ranging from 60 ft to 130 ft below the design foundation base at approximately El 270. These contours do not represent the estimated post-earthquake settlements expected to occur at the ground surface or at the foundation base level. Assuming that these estimated settlements are transmitted directly up to the base of the foundation provides a very conservative, upper-bound estimate of what the structure may experience as post-earthquake settlement due to the design earthquake. In reality, the great thickness of liquefaction-resistant soil layers above the soil layers that are susceptible to post-earthquake settlement will spread the estimated differences in settlements laterally, tending to smooth them out, so that the overall effect at the ground surface would be more uniform, minimizing the differential settlement that the structure may experience.

As indicated in Table 8-5, the maximum post-earthquake settlement is estimated to be 2.22 inches, occurring at CPT-117, located approximately 20 ft west of the eastern wall in the southeastern portion of the MFFF Building. The estimated post-earthquake settlement is 1.92 inches at CPT-55 located near the center of the MFFF Building. Elsewhere under the MFFF

Building, the estimated post-earthquake settlements are fairly uniformly distributed about the average value of approximately 1.4 inches, as evidenced by the contours of post-earthquake settlements presented in Figure 8-133.

The minimum post-earthquake settlements occurred at the northern-central portion of the MFFF structure, ranging from about 0.6 inches to 0.7 inches at CPT-110 and SCPT-75. This is contrary to what would be expected considering that the static settlements were larger in this area than elsewhere under the building due to the soft zones encountered at depth in some of the CPTs performed in this area. Soft zones were not encountered at the locations of these CPTs, which contributed to the low post-earthquake settlements calculated for these CPTs. In addition, Table 8-5 indicates that Engineering Units ST1 and ST2 were fully penetrated at both locations, so it was not necessary to estimate a portion of the post-earthquake settlement for this location based on the average value encountered elsewhere at the site. The primary reason these are low, however, is demonstrated by Figures 8-46 and 8-81, which show that these locations had very limited depth zones where the factor of safety against liquefaction was less than 1.5. Post-earthquake settlements are inversely related to the factor of safety against liquefaction; therefore, where FS_L is high, the estimated post-earthquake settlements will be low. CPT-112, located just south of this area, encountered a soft zone, but the extent of the soft zone was limited, which contributed the low post-earthquake settlement estimate of 0.75 inches at this location. In addition, this CPT fully penetrated the ST2 layer, so it was not necessary to estimate a portion of the post-earthquake settlement for this location based on the average value encountered elsewhere at the site.

8.2.4.3 Post-earthquake Settlements Occurring in Each Engineering Unit

On the basis of the elevations of the top of the engineering units, the calculated post-earthquake settlements at each CPT were analyzed to determine the portions of the settlement applicable to each engineering unit. The unit settlements were added for all of the CPTs to find the contribution of each engineering unit to the total settlement. The results, presented in the form of a bar chart in Figure 8-134, show that more than a third of the estimated post-earthquake settlement occurs in the ST2 layer, the deepest layer. Only seven percent of the estimated settlement occurs in the ST1 layer, which overlies the ST2 layer. The percentage of the settlement occurring in the other units that are below the design water table and which overlie the ST1 and ST2 layers, were approximately ten percent for TR3/4, twenty-two percent for DB1/3, and twenty-five percent for DB4/5.

These results, considering the variation in unit thickness, are consistent with the trend expected based on the average factor of safety against liquefaction presented in Figure 8-96 and Table 8-1. The post-earthquake settlements are inversely related to the factor of safety against liquefaction; therefore, where FS_L is lower, the post-earthquake settlement should be higher. This trend is apparent in Figure 8-134, where the greatest amount of post-earthquake settlement is attributed to the ST2 layer, which has the lowest FS_L , followed by the DB4/5 layer, which has the next lowest FS_L . The ST1 layer has the highest FS_L , and the percentage of the post-earthquake

settlement applicable for it is the smallest. The portion of the post-earthquake settlement occurring in the TR3/4 layer is less than that applicable for the DB1/3 layer in spite of FS_L being lower for the TR3/4 layer because the thickness of the TR3/4 layer is much less than that of the DB1/3 layer; i.e., the strains are higher in the TR3/4 layer, but they are applicable for thinner layer, resulting in less total settlement in the layer.

As discussed in Section 8.1.2.1, case histories show that the presence of liquefaction-resistant surface layers mask the observable effects of liquefaction of layers at depth. The design groundwater table is at El 210 and, with a site elevation of 270, there are approximately 60 feet of liquefaction-resistant material overlying Engineering Units TR3/4, DB1/3, DB4/5, ST1, and ST2. In addition, underlying the MFFF Building, there will be a 10-ft thick layer of engineered select structural fill, comprised of well-compacted crushed stone, which will provide a uniform, extremely dense zone of non-liquefiable material directly beneath the structure. This thick zone of non-liquefiable material will significantly reduce differential settlements due to the estimated post-earthquake settlements calculated on the basis of penetration resistances measured at individual CPT locations. In addition to the non-liquefiable zone above the water table, substantial sections of the layers do not undergo any post-earthquake settlement because of their high strengths, as evidenced by the CPT tip resistance values, plasticity, or fines content, and these liquefaction-resistant zones provide an additional basis for the expectation that localized differences in estimated settlements will be smoothed out before they reach the surface of the site.

About one-third of the estimated post-earthquake settlement occurs in the deepest of the engineering units under consideration for liquefaction, Engineering Unit ST2. This layer is overlain by ST1, a thicker layer with a very high factor of safety against liquefaction. The ST1 layer will moderate any post-earthquake settlement occurring in the ST2 layer, spreading it laterally, which will diminish its contribution to differential settlement at the surface of the profile.

Another thirty percent of the estimated settlements are from layers that have an average factor of safety against liquefaction of more than 2. Settlements in isolated sections of such materials are likely to be substantially moderated by adjoining sections of more competent materials, which will similarly tend to distribute the effects of the settlement laterally. This effect provides the basis for the expectation that localized differences in settlements following the earthquake will be significantly reduced at the ground surface. The interaction of layers with and without post-earthquake settlement potential mitigates differences that would have otherwise occurred over limited areas. Therefore, estimating the differential settlement the structures will experience from adjacent CPTs will yield overly conservative results. Rather, these results should be viewed as providing evidence that the post-earthquake settlements are likely to be more uniform, on the order of the average value, ~1.4 inches. As indicated in Figure 5-133, the 1.4-inch contour generally runs along a diagonal through the MFFF structure, from the southwest to the northeast. The post-earthquake settlements near the northwestern corner (~1.2 inches) are slightly less than this, and those in the southeastern corner (~1.8 inches) are slightly greater,

indicating that the MFFF structure may experience a slight tilting (~0.6 inches) from the northwestern corner to the southeastern corner, settling, at most, approximately 1.4 inches, ignoring the smoothing effects of the liquefaction-resistant layers above the soils at depth that may experience post-earthquake settlements..

8.2.5 Results of Post-Earthquake Settlement Analyses for the Individual Soil Profile

The estimated post-earthquake settlements using individual CSR profiles computed based on 18 SCPTs and 3 borings are summarized in Table 8-6. They range from 0.00 inches to 1.98 inches, with an average of 1.08 inches. The SRS site-specific volumetric strain and factor of safety against liquefaction relations, Figure 8-135, (WSRC, 1995a) were used to estimate these post-earthquake settlements (DCS, 2003j).

The post-earthquake settlements based on the generalized CSR profile were also computed using the SRS site-specific volumetric strain and factor of safety against liquefaction relations, and. As summarized in Table 8-6, they range from 0.05 inches to 2.11 inches, with an average of 1.18 inches.

Of the 18 SCPTs and 3 borings, the estimated settlements based on the individual profiles are higher than those by generalized profile at 10 locations, and they are lower than those by generalized profile at the other 11 locations. The greatest difference occurred at SCPT-81; 0.24" based on SCPT-81 vs 0.94" for the generalized profile. The CSR profile (Section 6.2.3.7) at SCPT-81 is significantly lower than the rest of the CSR profiles due to the soft materials encountered around elevation 150. As a result, the post-earthquake settlements estimated at and near SCPT-81 using individual CSR from SCPT-81 are also noticeably less than those using the generalized CSR. The differences between the individual and the generalized post-earthquake settlements, excluding SCPT-81, ranged from -0.57" at SCPT-83 to 0.28" at SCPT-78A.

8.2.6 Summary of Post-Earthquake Settlement Analyses

The estimated post-earthquake settlements at the 18 seismic CPTs and 3 borings ranges from 0.00 inches to 1.98 inches using the individual profiles. The comparable estimated post-earthquake settlements using the generalized profile range from 0.05 inches to 2.11 inches. The averages of the settlements are 1.08 inches and 1.18 inches, respectively for the individual profiles and the generalized profile, as summarized in Table 8-6. There does not appear to be a systematic variation in the settlements from the individual profiles and the generalized profiles. These results demonstrate that the estimated post-earthquake settlements using either individual soil profiles or generalized soil profile are not significantly different and yield the same order of magnitude of settlements. This supports the application of the CSR profile from the generalized soil column to all the 95 CPTs and 14 borings across the MFFF site, as performed in DCS (2003f and 2003q), suggesting that the approach adopted in DCS, 2003c those analyses is appropriate and yields post-earthquake settlement estimates for the MFFF site with reasonable accuracy.

In general, the site within the vicinity of the MFFF structures is expected to experience very little post-earthquake settlement as a result of the design earthquake. The estimated settlements at the locations of the borings in the area are summarized in Table 8-2, and the estimated settlements at locations of the CPTs in the area are summarized in Table 8-3. As indicated in Tables 8-2 and 8-3, the post-earthquake settlements range from 0.00 to 1.47 inches, respectively, with an average value of approximately 0.9 inches. The post-earthquake settlements are also posted at the locations of the borings and CPTs in Figure 8-130. These values are based on the PC-3+ control motion. The corresponding post-earthquake settlement values for the Charleston 50th percentile control motion range from 0.0 to 2.2 inches, with an average value of 1.4 inches.

Because these settlements are the result of volumetric strains that might occur at depths of 60 feet to 130 feet below ground surface, it is anticipated that the settlement manifested at the ground surface would be fairly uniform, approximately equal to the predicted average value of 0.9 inches for the PC-3+ motion (or 1.4 inches for the Charleston 50th percentile earthquake). Differential settlements due to post-earthquake settlements of this magnitude would be much less than these values and are not considered detrimental to the structures.

As shown in Figures 5-2 through 5-7, the thick layer of structural fill overlying the strong TR2A TR2B layers, provide a significant stiff soil layer (over 40 feet thick) between the deep, potentially liquefiable zone and the mat foundations for the MFFF and BEG Buildings. These strong soil units will successfully redistribute any post-earthquake settlements that might occur such that an abrupt differential settlement will not occur at the foundation base elevation. The redistribution of settlement at depth beneath the MFFF and BEG foundation levels is demonstrated by the FLAC analyses, which are described in Section 7.4.3.6. The effects of post-earthquake settlement redistribution in the upward direction from deep potentially liquefiable pockets of weaker soils would be analogous to the redistribution of settlements due to static loads observed in the FLAC settlement analyses.

Consequently, such post-earthquake settlements will not result in any adverse differential settlement to the MFFF or BEG Buildings.

The hypothetical breakdown of soil arches over the soft zones due to shaking caused by the design earthquake is not considered to be realistic. This conclusion is based on the discussion presented above in Section 8.2.3, which is summarized as follows. The CPTs measured very high tip resistances for substantial thicknesses of the soil layers above the soft zones, which typically are at depths of 90 to 140 ft below grade. If the soils above the soft zones experienced arching, such arching would lead to higher tip resistances in those layers directly above the soft zones. As discussed in Section 8.2.3 and as shown by the CPT data presented in Figure 8-131, such a phenomenon was not observed. In our opinion, if such a phenomenon were possible, it would have already occurred due to historical earthquakes that have occurred in the area.

8.2.7 Static and Post-earthquake Settlement

Static settlement analyses were performed for the MFFF and BEG Buildings using the FLAC computer program in Calculation G-00017-C (DCS, 2003d). Settlements of 2.7 inches to 3.5 inches were estimated for the MFFF Building. The estimated settlements for the BEG Building ranged from 1.1 to 1.6 inches. The effect on the buildings of the post-earthquake settlements occurring after these structures have undergone the estimated static settlements is discussed below.

The static settlements at the CPT locations were estimated from the contour map of settlements from static loads (Figure 7-6). These were added to the post-earthquake settlements calculated in DCS (2003k), and the results are presented as contours of static + post-earthquake settlement in Figure 8-136. The combined static and post-earthquake settlements are posted at the CPT locations on the contour map. As stated above in Section 8.2.4, it should be recognized that the settlement contours shown in this figure are based on estimated post-earthquake settlements that may occur within the soils found at depths ranging from 60 ft to 130 ft below the design foundation base at El 270. These contours do not represent the estimated post-earthquake settlements expected to occur at the ground surface or at the foundation base level. Assuming that these estimated settlements are transmitted directly up to the base of the foundation provides a very conservative, upper-bound estimate of what the structure may experience as post-earthquake settlement due to the design earthquake. In reality, the great thickness of liquefaction-resistant soil layers above the soil layers that are susceptible to post-earthquake settlement will distribute the estimated settlements laterally, tending to smooth out these contours, so that the overall effect at the ground surface would be more uniform, minimizing the differential settlement that the structure may experience.

The post-earthquake settlement, should it occur, is expected to be a general ground movement and should have no impact on the effect of the differential settlement of the buildings with respect to the immediate surroundings; i.e., the yard area, as the yard areas should experience similar post-earthquake settlements.

Contours of the combined static and post-earthquake settlements are plotted in Figure 8-136. The maximum and minimum combined settlements at the MFFF Building are 5.3 inches and 3.7 inches, respectively. The static + post-earthquake settlement at the BEG Building is 3 inches. A conservative estimate of the maximum differential settlement of the MFFF Building due to the combined static and post-earthquake settlements is 1.6 inches. This settlement occurs over a distance of approximately 220 feet. In the north-central part of the MFFF Building, a differential settlement of ~0.7 inches is indicated between CPT-112 and CPT-107, located ~20 ft to the south. This differential settlement, calculated based on conservatively accumulating all of the post-earthquake settlement occurring at depth within the profile vertically without distributing it laterally, translates into a worst-case angular distortion of $\sim 1/342$ (i.e., 0.7" / 20 ft), or 0.00292ℓ. This value is within the limiting factor of 0.003ℓ for allowable differential settlements identified in Table 14.1 of Lambe and Whitman (1969) for reinforced concrete building curtain walls.

Therefore, such differential settlements are not unreasonable for structures such as these. However, structural analyses should be performed to confirm that the structure can tolerate such movements. Should these conservatively estimated values cause distress to the structure, then further refined analyses can be performed to address the propagation of the post-earthquake settlement from depth up through the profile to the base of the structure. Such analyses are expected to distribute the vertical settlements laterally, which would tend to smooth out the contours shown in Figures 8-132 and 133. Individual profile post-earthquake settlement results from SCPT-69, SCPT-85, SCPT87A, and SCPT-75 were sufficiently close to a north-south section (Section E on Figure 5-1) to allow an approximate estimate of the surface manifestation of the post-earthquake settlement for the individual profile, providing a better estimate of the differential settlements that the structure will actually experience, which will be less than the conservatively determined values discussed above.

The procedures outlined in Section 7.4.3.6 to analyze the postulated collapse of soil arches overlying the soft zones with FLAC were used to estimate the surface distribution of the calculated post-earthquake settlement at depth. The settlement at the ground surface due to calculated post-earthquake settlements of Engineering Units TR3/4, DB1/3, DB4/5, ST1, and ST2 were computed by incrementally pulling down the top of each engineering unit. The results indicated that the surface movement is a smooth average of the settlement troughs and peaks predicted by the calculated post-earthquake settlements.

These results were used as a guideline to smooth out the post-earthquake settlement contours for the Charleston 50th percentile control motion shown in Figure 8-133. As expected, differential settlements over shorter distances were eliminated and angular distortions were reduced. The results showed variations of up to 0.5 inches in the individual surface settlement and the generalized surface settlement along the section, with less differential settlement occurring based on the individual profile. However, the differences are not considered significant in evaluating the post-earthquake settlement of structures at the MFFF site, and the generalized profile should provide a reasonable estimate of the surface post-earthquake settlement. Using the FLAC results as a guideline to smooth out the calculated post-earthquake settlements, the order of magnitude of the differential settlement of the combined static and post-earthquake settlement is approximately 1", resulting in a maximum angular distortion of approximately 0.001 ℓ .

8.3 SOFT ZONE SETTLEMENT

Soft zone conditions identified at the MFFF site are discussed in Section 5.2. The soft zones identified within the influence of critical structure foundation systems were evaluated for both static and dynamic loading conditions. Settlement from static loading is discussed in Section 7.4.3, and it does not result in any adverse total or differential settlement. The soft zones were evaluated in the liquefaction and post-earthquake settlement analyses and the results are discussed in Sections 8.1 and 8.2. The soft zones are isolated with respect to static and dynamic loads and, therefore, are considered stable and are not anticipated to cause any adverse affect to the foundations for the MFFF and BEG Buildings. The soft zones do not present any subsurface

stability problems, because they are limited in lateral and vertical extents and are surrounded by competent materials. Furthermore, as evidenced by computed factors of safety against liquefaction that exceed 1 for all of the CPT tip measurements made at the MFFF site, the materials in the soft zones are not liquefiable.

8.4 FAULTING

Studies at SRS have indicated that identified faults at or near SRS are not capable; therefore, faults do not present a subsurface stability problem for the MFFF site. Refer to Section 3.3 for more detail.

8.5 SLOPE STABILITY

There are no slopes in the vicinity of the safety-related structures (i.e., MFFF and BEG Buildings) whose failure could adversely affect the MFFF. The closest slopes to these critical structures are associated with the yard area civil work (i.e., detention ponds) and are located over 800 feet to the south and east of the MFFF site. These slopes are Quality Level 4 structures, not important to safety. Therefore, slope stability is not an issue for the MFFF.

9. CONCLUSIONS

The geotechnical investigations and analyses performed of the subsurface conditions existing at the MFFF site indicate that this site is suitable for design and construction of the MFFF and BEG Buildings. The subsurface conditions encountered at the MFFF site demonstrate consistency with subsurface conditions found throughout the F-Area, which is located adjacent to the site proposed for location of the MFFF at SRS. No unusual subsurface conditions have been identified. All soft zones and loose soil deposits identified at depth are consistent with those identified in the adjacent F-Area, and the geotechnical analyses demonstrate that their presence will not have an adverse effect on the MFFF and BEG Buildings. All of the soft zones and loose soil zones identified at the MFFF site are deep, isolated, have a limited lateral extent, and are overlain and surrounded by far more competent materials. No unusual soft conditions were found at the locations proposed for construction of the MFFF and BEG Buildings.

The exploration and testing programs performed for the site are considered adequate to define the subsurface conditions and to establish the geotechnical design criteria required for the MFFF. All subsurface conditions identified during this geotechnical program indicate that the underlying geology at the MFFF site is consistent with conditions described in WSRC (2000a). The regional and SRS-specific hydrology, geology, and seismology descriptions presented in Sections 1.4.2, 1.4.4, and 1.4.4 of WSRC (2000a), respectively, are applicable for use at the MFFF site.

An assessment of the subsurface conditions indicates that an engineered select structural fill is required beneath the MFFF and BEG Buildings. Due to the variability of the subsurface soils at the foundation grade proposed for these structures, the current design recommends removal of approximately 5 to 10 ft of subgrade materials. Approximately 10 feet of select structural fill will be required beneath the MFFF and the BEG Buildings will require approximately 5 feet of engineered select structural fill. This select structural fill will provide adequate support for the high concentrated edge pressure due to static loading (Figure 7-2) and the high edge bearing pressures anticipated during seismic loading. In addition, this select structural fill will minimize adverse effects of any differential settlement that the structures may experience. Settlement analyses included evaluation of the effects of the soft zones, and the results indicate that the MFFF and BEG Buildings will not experience any detrimental differential settlements. The total and differential settlements estimated are considered within the limits that these structures can tolerate. Further structural analysis will be performed during design to accommodate these anticipated static and post-earthquake settlements.

The results of the dynamic analyses indicate that the soils underlying the MFFF site will not liquefy due to cyclic loadings from the design level earthquakes, including the PC-3+ and 1886 Charleston events. In addition, post-earthquake settlements are expected to be minimal, averaging less than 1 inch for the PC-3+ earthquake and less than 1.5 inches for the Charleston earthquake. Differential settlements due to post-earthquake settlements of this magnitude would be much less than these values because the presence of the stronger soil units that overlie the



deep zones that contribute to most of the post-earthquake settlement. These stronger zones will successfully redistribute any post-earthquake settlements that might occur over a wider area of the mat foundations of the MFFF and BEG Buildings such that an abrupt differential settlement will not occur at the foundation base elevation.

The present location for the MFFF and Emergency Generator Buildings is considered appropriate for design and construction of the planned facilities.

10. REFERENCES

Aadland, R.K., Gellici, J.A., and Thayer, P.A., 1995, "Hydrogeological Framework of West-Central South Carolina," State of South Carolina Department of Natural Resources, Water Resources Division, Report 5.

American Society for Testing and Materials (ASTM), ASTM Construction Standards, 1916 Race Street, Philadelphia, PA.

American Society of Civil Engineers, 2000, "Seismic Analysis of Safety Related Nuclear Structures and Commentary," Document No. ASCE 4-98, October.

ARA, 2000, "Cone Penetration Testing at the Mixed Oxide Fuel Fabrication Facility (MFFF), Savannah River Site, Aiken, South Carolina," Final Report, prepared by Applied Research Associates, Inc, for Duke Cogema Stone & Webster, LLC, ARA Report No. 0198, October.

ARA, 2003, "Phase II Cone Penetration Testing at the Mixed Oxide Fuel Fabrication Facility (MFFF), Savannah River Site, Aiken, South Carolina," Final Report, prepared by Applied Research Associates, Inc, for Duke Cogema Stone & Webster, LLC, ARA Report No. 0198-1, January.

Bay Geophysical, 2001, "Seismic Downhole Surveying for the Mixed Oxide Fuel Fabrication Facility at the Savannah River Site, Aiken, SC," Final Report, prepared for Duke Cogema Stone & Webster, April.

Bechtel Corp, 1998, "SRS-APSF Soft Zone Settlement Analysis," Calculation No. 20216-395-03, Rev. 0, April; also see Westinghouse Savannah River Company (1998), "APSF Soft Zone Settlement Analysis (U)," Calculation No. K-CLC-F-00034, Rev. 0, June

Bowles, Joseph E., 1996, Foundation Analysis and Design, Fifth Edition, McGraw-Hill, Inc., New York.

Das, B.M., 1993, Principles of Soil Dynamics, PWS-KENT.

Department of Energy, 1996, DOE Standard-Natural Phenomena Hazards Design and Evaluation Criteria for Department of Energy Facilities," DOE-STP-1020-94, April 1994, Change Notice #1, January 1996.

DCS, 2000a, DCS01-WRS-DS-SPE-G-00001-A, "Specification for Cone Penetration Testing of Soil," Duke Cogema Stone & Webster.

DCS, 2000b, DCS01-WRS-DS-SPE-G-00002-A, "Specification for Geotechnical Test Borings and Sampling," Duke Cogema Stone & Webster.

DCS, 2000c, DCS01-WRS-DS-SPE-G-00003-A, "Specification for Laboratory Testing of Soils Quality," Duke Cogema Stone & Webster.

DCS, 2000d, DCS01-WWJ-DS-CAL-H-38316-A, "Selection of Extreme Natural Phenomena For MOX Design," Duke Cogema Stone & Webster.

- DCS, 2000e, Project Procedure 9-19, Rev. 0, "Geotechnical Exploration and Testing," Duke Cogema Stone & Webster.
- DCS, 2001a, DCS01-WRS-DS-CAL-G-00008-A, "Development of Subsurface Stratigraphy Across MFFF Site," Duke Cogema Stone & Webster.
- DCS, 2001b, DCS01-WRS-DS-CAL-G-00012-A, "Determination of Shear Modulus Reduction Curves and Damping Ratio," Duke Cogema Stone & Webster.
- DCS, 2001c, DCS01-WRS-DS-CAL-G-00021-A, "Development of Engineering Data Summary Table", Duke Cogema Stone & Webster.
- DCS, 2001d, DCS01-WRS-DS-CAL-G-00023-A, "Validation of ProShake Version 1.1," Duke Cogema Stone & Webster.
- DCS, 2001e, DCS01-WRS-DS-CAL-G-00031-A, "Calculation of Post Earthquake Settlement of ST-1 and ST-2 Engineering Units," Duke Cogema Stone & Webster.
- DCS, 2001f, DCS01-WRS-DS-NTE-G-00005-C, "MOX Fuel Fabrication Facility Site Geotechnical Report," Duke Cogema Stone & Webster.
- DCS, 2001g, DCS01-WRS-DS-SPE-G-00001-B, "Specification for Cone Penetration Testing of Soil," Duke Cogema Stone & Webster.
- DCS, 2001h, DCS01-WRS-DS-SPE-G-00002-B, "Specification for Geotechnical Test Borings and Sampling," Duke Cogema Stone & Webster.
- DCS, 2002, DCS01-WRS-DS-CAL-G-00019-C, "Determination of Consolidation Settlement and Recompression Indices," Duke Cogema Stone & Webster.
- DCS, 2003a, DCS01-WRS-DS-CAL-G-00011-C, "One-Dimensional Free-Field Site Response Analyses," Duke Cogema Stone & Webster.
- DCS, 2003b, DCS01-WRS-DS-CAL-G-00015-B, "Determination of Dynamic Poisson's Ratio Using Shear and Compression Wave Velocity Data," Duke Cogema Stone & Webster.
- DCS, 2003c, DCS01-WRS-DS-CAL-G-00016-B, "Seismic Liquefaction and Post-Liquefaction Settlement Analyses for the Mixed Oxide Fuel Fabrication Facility (MFFF)," Duke Cogema Stone & Webster.
- DCS, 2003d, DCS01-WRS-DS-CAL-G-00017-C, "Estimates of Static Settlement of MFFF Structures Using FLAC Model," Duke Cogema Stone & Webster.
- DCS, 2003e, DCS01-WRS-DS-CAL-G-00018-B, "One-Dimensional Free-Field Site Response Analysis of MFFF Site for the 1886 Charleston (50th Percentile) Control Motion," Duke Cogema Stone & Webster.
- DCS, 2003f, DCS01-WRS-DS-CAL-G-00020-C, "Soft Zone Summary Table," Duke Cogema Stone & Webster.

DCS, 2003g, DCS01-WRS-DS-CAL-G-00022-B, "Determination of Safety Factor Against Bearing Capacity Failure for MFFF and BEG Buildings," Duke Cogema Stone & Webster.

DCS, 2003h, DCS01-WRS-DS-CAL-G-00025-B, "One-Dimensional Free-Field Site Response Analysis by Individual Seismic CPT," Duke Cogema Stone & Webster.

DCS, 2003j, DCS01-WRS-DS-CAL-G-00026-B, "Seismic Liquefaction and Post-Earthquake Settlement Analyses by Individual Seismic CPT," Duke Cogema Stone & Webster.

DCS, 2003k, DCS01-WRS-DS-CAL-G-00030-B, "Seismic Liquefaction and Post-Earthquake Settlement Analyses for the MFFF Site with 1886 Charleston Control Motion," Duke Cogema Stone & Webster.

DCS, 2003m, DCS01-WRS-DS-CAL-G-00045-A, "Engineering Properties of Select Structural Fill," Duke Cogema Stone & Webster.

DCS, 2003n, DCS01-WRS-DS-CAL-G-00046-A, "Development of Boring Logs for BH-14 Through BH-20 and Documentation of Field Logs," Duke Cogema Stone & Webster.

DCS, 2003p, DCS01-WRS-DS-CAL-G-00047-B, "Development of Subsurface Stratigraphy Across the MFFF Site, 2002 Geotechnical Investigation," Duke Cogema Stone & Webster.

DCS, 2003q, DCS01-WRS-DS-CAL-G-00048-A, "Engineering Properties of Soft Zones and Soft Materials – 2002 Supplemental Geotechnical Investigations," Duke Cogema Stone & Webster.

DCS, 2003r, DCS01-WRS-DS-CAL-G-00050-A, "Summary of Laboratory Test Results, 2002 Supplemental Geotechnical Investigations," Duke Cogema Stone & Webster.

Geomatrix Consultants, Inc. 1997, Calculation No. 06957-G-010-0, "Free-field Site Response Analyses – Actinide Packaging and Storage Facility, Savannah River Site," September.

Geomatrix Consultants, 1997a, Calculation No. 06957-G-018-0, "Estimation of Settlement for the MAA Bldg. and Truck Dock, APSF," September.

Geomatrix Consultants, Inc. 1998, "Final Geotechnical Study Report – Actinide Packaging and Storage Facility, Savannah River Site," prepared for Stone & Webster Engineering Corporation, Project No. 3984.02, January.

Gutierrez, B.J., 1999, "Revised Envelope of the Site Specific PC-3 Surface Ground Motion," Letter from DOE to L.A. Salamone and F. Loceff, September 1999.

Idriss, I. M., and Sun, J. I. 1992, "User's Manual for SHAKE91: A Computer Program for Conducting Equivalent Linear Seismic Response Analyses of Horizontally Layered Soil Deposits," University of California, Davis, November.

Ishihara, K. and Yoshimine, M., 1990, "Evaluation of Settlements in Sand Deposits Following Liquefaction During Earthquakes," Soil and Foundations, Japanese Society of Soil Mechanics and Foundation Engineering, Vol. 32, No.1.

Itasca Consulting Group, Inc., 2000b, FLAC Fast Lagrangian Analysis of Continua User's Guide, Fluid-Mechanical Interaction.

Itasca Consulting Group, Inc., 2001, FLAC Fast Lagrangian Analysis of Continua Theory and Background.

Itasca Consulting Group, Inc., August 2000a, "Fast Lagrangian Analysis of Continua," Second Edition.

LawGibb Group, 2001, Laboratory Test Results from May-July 2000 Field Investigation, MOX Fuel Fabrication Facility, prepared for Duke Cogema Stone & Webster (DCS), DCS Subcontract No.:DCS-0023, Atlanta, Georgia.

Leonards, G. A., 1976, "Estimating Consolidation Settlements of Shallow Foundations on Overconsolidated Clay," in "Manual of Practice - Estimation of Consolidation Settlement," Transportation Research Board Special Report 163, National Academy of Sciences, Washington, D.C.

MACTEC, 2003, Laboratory Test Results for 2002 Supplemental Geotechnical Investigation, MOX Fuel Fabrication Facility, prepared for Duke Cogema Stone & Webster by MACTEC Engineering and Consulting of Georgia, Inc., f/k/a Law Engineering and Environmental Services, Inc., Atlanta, GA.

National Center for Earthquake Engineering Research, 1997, "Proceedings of the NCEER Workshop on Evaluation of Liquefaction Resistance of Soils," Technical Report No. NCEER-97-0022, State University of New York at Buffalo, New York, December 31.

Raymond Concrete Pile Division 1973, "Test Boring Report," prepared for E. J. Du Pont De Nemours & Co. and transmitted to Meuser, Rutledge, Wentworth & Jackson, February 20.

Robertson, P. K., and Wride (Fear), C. E. 1997 "Cyclic Liquefaction and its Evaluation based on SPT and CPT," Proceeding of the NCEER Workshop on Evaluation of Liquefaction Resistance of Soils, pp. 41 - 87.

Seed, H. B., Idriss, I. M., Arango, I., 1983, "Evaluation of Liquefaction Potential Using Field Performance Data," Journal of the Geotechnical Engineering Division, Proceedings of ASCE, New York, NY, Vol. 109, No. 3, pp 458-482.

SRS Engineering Practices Manual No. 02224-G, Rev. 1, 2001, "Excavation, Backfill, Placement of Low Permeability Soil and Grading (U)," Manual WSRC-IM-95-58, July.

United States Nuclear Regulatory Commission (USNRC), Office of Nuclear Regulatory Research, 2001, Draft Regulatory Guide DG-1105, "Procedures and Criteria for Assessing Seismic Soil Liquefaction at Nuclear Power Plant Sites," March.

Wang, W.S. 1979, "Some Findings on Soil Liquefaction," Water Conservancy and Hydroelectric Power Scientific Research Institute, Beijing, China

WSRC, 1994, "Estimated Settlement of Tanks 48, 49, 50, and 51 (U)," Calculation No. K-CLC-H-00057, In-Tank Precipitation (ITP) Facility Project, Westinghouse Savannah River Company, July 28.

WSRC, 1995a, "RCRA Facility Investigation/Remedial Investigation Report, Rev. 1, For the Old F-Area Seepage Basin (904-49-G)(U)," Report No. WSRC RP 94 942, Westinghouse Savannah River Company, June.

WSRC, 1995b, "In-Tank Precipitation Facility (ITP) and H-Tank Farm (HTF) Geotechnical Report", WSRC-TR-95-0057, Rev. 0, Westinghouse Savannah River Company, September.

WSRC, 1996a, "Investigation of Non-linear Dynamic Soil Properties at the Savannah River Site," Document No. WSRC-TR-96-0062, Rev. 0, Westinghouse Savannah River Company, March.

WSRC, 1996b, "F-Area Geotechnical Characterization Report," Document No. WSRC-TR-96-0069, Rev. 0, Westinghouse Savannah River Company, September.

WSRC, 1997, Savannah River Site Response Analysis and Design Basis Guidelines," Document No. WSRC-TR-97-0085, Rev. 0, Westinghouse Savannah River Company, March.

WSRC, 1998, "Actinide Packaging and Storage Facility Spectrum Compatible Time Histories," Calculation No. K-CLC-G-00053, Rev. 0, by Richard C. Lee, Westinghouse Savannah River Company.

WSRC, 1998a, "APSF Confirmatory Drilling Program Results," Interoffice Memorandum, Document No. PECD-SGS-98-0115, Westinghouse Savannah River Company, June 18.

WSRC, 1998b, "APSF Borros Heave Point Measurements and Effective Overburden Removal Graphs," electronic file borros.jpg, Westinghouse Savannah River Company.

WSRC, 1999a, "F-Area Northeast Expansion Report (U)," Report No. K TRT F 00001, Rev. 0, Westinghouse Savannah River Company, June.

WSRC, 1999b, "Significance of Soft Zone Sediments at the Savannah River Site – Historical Review of Significant Investigations and Current Understanding of Soft Zone Origin, Extent and Stability," Report No. WRSC TR 99 4083, Rev. 0, Westinghouse Savannah River Company, September.

WSRC, 2000, "Probability of Liquefaction for F-Area, Savannah River Site," Report No. WSRC TR 2000-00039, Rev. 0, Westinghouse Savannah River Company, August 31, 2000.

WSRC, 2000a, "Natural Phenomena Hazards (NPH) and Design Criteria and Other Characterization Information for the Mixed Oxide (MOX) Fuel Fabrication Facility at Savannah River Site (U)," Report No. WSRC TR 2000 00454, Rev. 0, Westinghouse Savannah River Company, November.

WSRC, 2000b, "2000 RCRA Part B permit Renewal Application (U) Mixed Waste Management Facility (MWMF) Postclosure," Report No. WSRC IM 98 30, Westinghouse Savannah River Company, March.

WSRC, 2000c, "WSRC Action Items from November 16, 2000 Meeting," Interoffice Memorandum, Document No. PED-SGS-2000-00124, Westinghouse Savannah River Company, November.

WSRC, 2001a, "Probability of Liquefaction F-Area and MOX Fuel Fabrication Facility (MFFF) Site – Savannah River Site," Document No. WSRC-TR-2001-00043, Rev. 0, Westinghouse Savannah River Company, January.

WSRC, 2001b, "Settlement Summary for H-Area Tanks and Selected Structures (U)," Report K-ESR-H-00015, Revision 1, Westinghouse Savannah River Company.

WSRC, 2002a, "Work Task Authorization 06; Summary of Groundwater Quality at the Mixed Oxide Fuel Fabrication Facility Site (U)," Westinghouse Savannah River Company.

WSRC, 2002b, "Settlement of Defense Waste Processing Facility (U)," Report No. K-ESR-S-00005, Rev. 0, Westinghouse Savannah River Company, September.

Wood, David Muir, 1990, Soil Behaviour and Critical State Soil Mechanics, Cambridge University Press.



TABLES

TABLE 5-1 CORRELATION OF ENGINEERING AND GEOLOGIC STRATIGRAPHIC UNITS FOR MFFF SITE

"Geologic" Unit	"Engineering" Unit	Thickness (feet)	Average Top Elevation (feet)	Materials
Tobacco Road Formation	TR1	1 to 19	272 to 286	Medium dense to dense poorly sorted sands, clayey sands, and silty sands, occasional fine gravel
	TR1A	1 to 17	270	Medium dense to dense poorly sorted sands, clayey sands, and silty sands
	TR2A	12 to 35	263	Medium dense to dense poorly sorted sands and clayey sands
	TR2B	18 to 34	237	Medium dense to dense sands and clayey sands
	TR3/4	3 to 17	212	Stiff clay and sandy clay interbedded with loose to medium dense clayey sands and sandy silts; isolated soft clays (less than 2 to 3 feet in thickness)
Dry Branch Formation	DB1/3	12 to 32	204	Medium dense poorly sorted sands and silty sands with widely interspersed thin sandy clay and clayey sand layers, widely interspersed pockets of loose and dense to very dense sands; isolated soft clays (less than 2 to 3 feet in thickness)
	DB4/5	4 to 16	183	Loose to medium dense clayey and silty sands; some soft zones
Tinker/Santee Formation	ST1	17 to 26	174	Dense to very dense poorly sorted sands and silty sands
	ST2	6 to 16	153	Loose to medium dense poorly sorted sands and silty sands
Warley Hill Formation	GC	1 to 7	141	Medium dense to dense clayey sands, silty sands, sandy silts, and stiff to very stiff sandy clays; isolated soft silty clay zones (less than 2 to 3 feet in thickness)
Congaree Formation and Coastal Sedimentary Deposits	CG	725	137	Very dense sand to very hard sedimentary deposits
Paleozoic Bedrock	Bedrock	NA	-585	Paleozoic crystalline bedrock

TABLE 5-2 TOP ELEVATIONS OF ENGINEERING UNITS

ID	Engineering Unit Top Elevation from 2000 Investigation (feet)											
	FILL	TR1	TR1A	TR1B	TR2B	TR3/4	DB1/3	DB4/5	ST-1	ST-2	GC	CG
CPT-4	No Fill	273	267	257	238	216	212	180	176	155	143	138
CPT-7	No Fill	280		262	241	214	208	185	175			
CPT-8	No Fill	273	267	260	239	211	205	183	174	154	141	136
CPT-9	No Fill	266		255	243	216	213	189	180	159	146	141
CPT-13	297	281	262	260	228	202	197	177	168	146	136	131
CPT-14	No Fill	276	268	260	235	205	201	185	175	153	139	134
CPT-18	No Fill	277	269	260	237	209	198	181	170			
CPT-21	295	274	269	260	235	208	201	179	165			
CPT-22	297	276	275	258	230	202	191	168	159			
CPT-33	No Fill	277	272	263	237	208	192	179	170			
CPT-27	278	275	267	260	235	210	205	174	167			
CPT-28	279	277		263	237	206	202	173	168	151	138	131
CPT-29	No Fill	276	270	257	236	212	206	180	172			
CPT-40	No Fill	275		258	239	211	203	180	174			
CPT-44	No Fill	285	275	274	240	214	207	184	174			
CPT-45	No Fill	281		271	240	216	210	188	181	159	145	
CPT-46	285	284	281	274	240	211	206	189	178	158		
CPT-47	No Fill	284	282	271	241	214	208	185	175			
CPT-48	No Fill	281	276	271	238	217	205	184	177			
CPT-49	292	278	270	260	235	213	208	186	174			
CPT-50	294	282		265	232	211	206	185	169			
CPT-51	296	281	271	263	228	205	198	179	168			
CPT-52	293	277	272	262	238	215	210	188	176			
CPT-53	293	279	268	261	238	215	210	189	178			
CPT-54	294	275	269	261	237	213	209	184	174			

TABLE 5-2 TOP ELEVATIONS OF ENGINEERING UNITS (CONTINUED)

ID	Engineering Unit Top Elevation from 2000 Investigation (feet)											
	Fill	TR1	TR1A	TR1B	TR2B	TR3/4	DB1/3	DB4/5	ST-1	ST-2	GC	CG
CPT-55	294	280	264	258	230	207	201	176	167			
CPT-56	294	275	268	259	240	217	210	185	176			
CPT-57	294	278	270	258	235	211	205	183	173			
CPT-58	295	272	267	260	241	217	212	186	176			
CPT-59	296	272	266	258	237	215	210	188	177			
CPT-60	296	275	267	262	231	208	192	178	170			
CPT-61	279	273	269	260	237	209	198	181	170			
CPT-62	279	273	264	257	239	211	200	184	174			
CPT-63	279	272	267	258	238	210	200	181	172			
CPT-64	280	272		261	237	210	200	174	169	148	142	139

TABLE 5-2 TOP ELEVATIONS OF ENGINEERING UNITS (CONTINUED)

ID	Engineering Unit Top Elevation from 2002 Investigation (feet)										
	Fill	TR1/TR1A	TR2A	TR2B	TR3/4	DB1/3	DB4/5	ST-1	ST-2	GC	CG
SCPT-65	287	276	267	237	214	209	184	175	154	142	136
SCPT-66	287	275	265	237	215	209	184	177			
SCPT-67	287	273	259	240	211	200	185	176	154	141	137
SCPT-68	286	273	260	236	210	203	184	174	153	141	136
SCPT-69	286	272	259	239	210	194	181	171	151	138	133
SCPT-70	286	275	261	239	211	196	176	168	149	137	131
SCPT-71	286	277	265	239	210	192	178	167	151	139	134
SCPT-72	286	279	259	231	203	192	181	171	151	138	134
SCPT-73	286	279	255	231	202	195	180	170	150	139	134
SCPT-74	286	279	260	230	205	197	181	171	153	142	136
SCPT-75	No Fill	286	264	239	206	203	179	171	153	145	141
SCPT-76	No Fill	286	276	246	216	213	192	184	158	152	150
SCPT-77	286	281	271	239	216	210	190	176	158	142	139
SCPT-78A	286	279	260	236	213	204	189	174	156	149	146
SCPT-79	286	278	267	240	218	214	189	179	159	148	147
SCPT-80	286	280	269	244	215	202	186	177	157	143	139
SCPT-81	296	278	264	237	209	204	187	180	156	143	139
CPT-82							189	177			
SCPT-83							189	176	154	140	137
SCPT-84							185	174			
SCPT-85							180	168	151	137	133
SCPT-86							178	169	150	140	134
SCPT-87A	295	281	261	234	213	209	183	171	150	139	133

TABLE 5-2 TOP ELEVATIONS OF ENGINEERING UNITS (CONTINUED)

ID	Engineering Unit Top Elevation from 2002 Investigation (feet)										
	FILL	TR1/TR1A	TR2A	TR2B	TR3/4	DB1/3	DB4/5	ST-1	ST-2	GC	CG
SCPT-88							187	174	153	141	137
SCPT-89A	292	282	265	237	224	205	188	182			
SCPT-90							189	176			
CPT-91	No Fill	279	264	237	213	204	185	177			
CPT-92	No Fill	279	261	237	220	213	189	181			
CPT-93									154	140	137
SCPT-94	No Fill	276	261	237	210	203	182	172	152	140	135
CPT-95	No Fill	276	266	238	205	194	180	172			
SCPT-96	293	277	263	235	212	207	187	174			
SCPT-97	286	281	264	233	212	204	188	174	154	142	136
CPT-98	286	280	264	246	212	203	188	176	157	144	139
CPT-99	297	279	267	234	216	211	187	175	156	143	139
CPT-100	294	277	265	236	214	207	185	171	152	140	135
CPT-101	No Fill	276	261	236	209	195	181	170			
CPT-102	300	279	261	229	207	191	179	169	151	145	141
CPT-103	287	274	259	237	214	202	186	175	154	142	137
CPT-104	286	276	263	237	211	196	177	169	150	138	133
CPT-105	296	284	263	237	210	205	183	173			
CPT-106	298	281	267	238	210	205	185	172	152	138	133
CPT-107	297	281	267	235	208	202	182	174	151	141	134
CPT-108	295	282	263	238	214	207	187	174	153	139	135
CPT-109	292	281	263	243	217	212	190	177	156	144	139
CPT-110	294	285	266	231	212	207	188	174	154	147	145
CPT-111	293	281	261	234	216	210	191	177			

TABLE 5-2 TOP ELEVATIONS OF ENGINEERING UNITS (CONTINUED)

ID	Engineering Unit Top Elevation from 2002 Investigation (feet)										
	FIII	TR1/TR1A	TR2A	TR2B	TR3/4	DB1/3	DB4/5	ST-1	ST-2	GC	CG
CPT-112	297	282	267	237	210	205	183	170	149	135	131
CPT-113	286	280	265	231	210	205	187	172			
CPT-114	293	280	260	236	213	207	185	177	151	136	134
CPT-115	296	280	261	234	211	205	182	170	151	139	134
CPT-116	292	280	264	238	215	212	188	175			
CPT-117	286	279	258	229	208	198	182	171	152	139	134
CPT-118	297	274	262	237	215	212	186	180			
CPT-119	286	278	263	234	210	192	179	170	153	139	135
CPT-120	277	273	263	237	210	203	175	170	150	142	139
CPT-121	294	278	263	237	212	207	187	176			
CPT-122	286	275	260	237	209	198	178	169	151	140	134
CPT-123	285	277	262	235	211	204	179	170			
CPT-124	286	283	265	239	217	213	191	177			

TABLE 5-3 SOFT ZONES AND SOFT MATERIALS FOUND IN BORINGS AND CPTS

Boring ID	Soft Zone/Soft Material Information ^{1,2,3}				
	Top Elevation (feet)	Bottom Elevation (feet)	Approximate Total Thickness ⁵ (feet)	Average Tip Stress (tsf)	Engineering Unit
BH-11	142.0	140.0	2.0	NA	GC ⁹
BH-13	182.0	180.0	2.0	NA	DB4/5
BH-15	156.7	154.7	2.0	NA	ST1
BH-16	181.5	180.5	2.0	NA	DB4/5
BH-18	178.8	176.8	2.0	NA	DB4/5
BH-20	174.9	172.9	2.0	NA	DB4/5
	149.9	147.9	2.0	NA	ST2
	139.9	137.9	2.0	NA	ST2

CPT ID	Soft Zone/Soft Material Information ^{1,2,3}				
	Top Elevation (feet)	Bottom Elevation (feet)	Approximate Total Thickness ^{3,4} (feet)	Average Tip Stress (tsf)	Engineering Unit
CPT-45	187.2	182.0	5.0	8.9	DB4/5
	151.0	147.9	2.7	11.1	ST2
CPT-46	182.8	179.6	2.9	11.1	DB4/5
	156.0	149.2	6.5	13.0	ST2
	145.8	142.2	3.0	13.6	ST2
CPT-50	184.7	180.8	3.2	9.7	DB4/5
CPT-54	198.1	195.9	2.1	11.6	DB1/3 ⁶
CPT-55	190.1	186.2	3.3	9.8	DB1/3 ⁶
CPT-61	185.4	181.0	4.3	9.8	DB4/5
	180.0	175.6	4.3	5.2	DB4/5
CPT-65	145.7	141.9	3.7	11.8	ST2
CPT-70	175.3	171.7	2.2	14.1	DB4/5
	170.7	167.9	2.1	11.9	DB4/5
CPT-71	177.4	170.6	6.1	10.2	DB4/5
CPT-72	177.6	174.9	2.7	13.0	DB4/5
	141.5	138.4	3.1	9.8	ST2
CPT-77	180.6	177.6	2.6	11.7	DB4/5
	152.1	149.2	2.9	13.2	ST2
	147.8	142.5	5.2	8.6	ST2
CPT-80	181.5	178.2	2.4	13.4	DB4/5
CPT-81	154.8	143.0	11.8	7.3	ST2

TABLE 5-3 SOFT ZONES AND SOFT MATERIALS FOUND IN CPTs AND BORINGS (CONT'D)

CPT ID	Soft Zone/Soft Material Information ^{1,2,3}				
	Top Elevation (feet)	Bottom Elevation (feet)	Approximate Total Thickness ^{3,4} (feet)	Average Tip Stress (tsf)	Engineering Unit
CPT-87	200.0	194.3	5.6	10.7	DB1/3 ⁶
	174.8	171.3	2.1	12.6	DB4/5
CPT-87A	199.3	192.3	6.4	10.2	DB1/3 ⁶
	174.5	171.1	3.3	10.4	DB4/5
CPT-98	146.7	144.4	2.3	13.8	ST2
CPT-103	185.6	177.7	4.8	12.3	DB4/5
CPT-105	177.3	175.3	2.1	8.1	DB4/5
CPT-106	182.9	180.2	2.1	12.0	DB4/5
	144.1	140.3	3.5	9.8	ST2
CPT-108	186.3	183.4	2.2	9.2	DB4/5
CPT-112	208.3	204.8	3.1	10.6	TR3/4 ⁶
CPT-114	182.2	177.5	4.5	11.9	DB4/5
CPT-119	172.6	170.1	2.2	12.3	DB4/5
Average ⁷	173.6	169.4	3.7	11.0	
Maximum ⁷	208.3	204.8	11.8	14.1	
Minimum ⁷	141.5	138.4	2.1	5.2	
Std. Deviation ⁷	18.4	18.5	2.0	2.0	

Notes:

- Soft Zones are soils within the DB4/5, ST1, and ST2 engineering units with a corrected CPT cone tip resistance equal to or less than 15 tsf or SPT N-values equal to or less than 5 blows/ft over a continuous interval of at least 2 feet.
- Soft Materials are soils within engineering units other than DB4/5, ST1, or ST2 that otherwise conform to the criteria indicated in Note 1 for Soft Zones.
- If two or more layers with CPT cone tip resistances equal to or less than 15 tsf or SPT N-values equal to or less than 5 blows/ft are separated by less than one foot of firmer soil, they are considered a soft zone/soft material if the total aggregate thickness of the soft layers is greater than 2 feet.
- The "Approximate Total Thickness" is the sum of the thickness of all adjacent layers within the indicated elevations conforming to the criteria of Notes 1, 2, and 3.
- Standard Penetration Tests (SPTs) in boreholes generally were conducted at 5 foot depths and the samplers were driven 18 inches as indicated by ASTM D 1586. Therefore, total thicknesses of materials with an SPT N-value less than 5 blows/ft could not be determined. The Soft Zone thicknesses shown for the boreholes were estimated from the thickness of soft material at approximately the same elevation and in the same engineering units in nearby CPTs. The estimated thicknesses in the boreholes are conservative (actual thicknesses are likely less than 2 feet).
- Indicated layer is Soft Material, as described in Note 2.
- Average, maximum, minimum, and standard deviation values based on CPT data.

TABLE 5-4 GROUNDWATER ELEVATIONS FROM CPT DISSIPATION TESTS

CPT	Groundwater Elevation (feet)	CPT	Groundwater Elevation (feet)
4	199.0	74	190.2
7	200.6	75	189.4
8	193.9	77	192.2
9	198.8	79	193.1
13	197.5	80	194.3
14	198.8	81	195.6
18	203.2	82	194.6
21	198.3	84	193.0
22	197.0	85	182.0
27	205.6	86	176.2
28	202.8	87	190.4
29	207.3	89A	188.1
40	202.7	90	175.0
44	198.9	92	176.0
45	198.0	93	191.3
48	198.8	94	190.5
49	200.9	95	191.1
50	187.5	96	192.2
51	200.6	97	186.6
52	198.6	98	187.6
53	202.7	99	197.4
54	200.8	100	194.0
55	200.1	101	184.3
56	201.8	102	198.5
57	201.8	103	195.3
58	207.3	104	203.3
61	203.1	105	196.6
62	202.7	106	196.2
65	205.7	107	197.6
66	198.7	108	192.7
67	199.3	109	195.4
68	188.8	110	192.4
69	198.1	111	195.3
70	197.5	116	192.0
71	198.0	117	179.3
72	193.0	119	190.8
73	190.7	121	195.4
Average Groundwater Surface Elevation			195

TABLE 6-1 AVERAGE CPT AND SPT TEST RESULTS

	AVE ENGR	AVE TOP EL. ^[1] (MSL)	AVE SPT N VALUE	AVE q _{cor} /N VALUE	AVE f _s (tsf)	AVE q _{cor} (tsf)	AVE R _f ^[2] (%)	AVE Pore Press. (tsf)	SHEAR WAVE VELOCITY (ft/sec)
F-Area	TR1 ^[3]		25	3.6		91			
NE Exp.		291	31	3.1		95	3.0		1544
APSF		289	33	4.3		142	2.0		1637
MOX FFF		276	17	6.6	1.8	112	1.6	0.18	1541
F-Area	TR1A ^[3]	278	25	4.8		120			
NE Exp.		278	31	3.3		103	3.0		1454
APSF		273	27	2.5		68	4.0		1464
MOX FFF		267	18	6.0	2.1	108	1.9	0.36	1488
F-Area	TR2A	261	28	5.3		147			
NE Exp.		262	37	3.9		146	1.0		1257
APSF		260	34	4.0		136	1.0		1284
MOX FFF		255	23	5.4	1.2	124	1.0	0.07	1281
F-Area	TR2B	233	36	5.6		201			
NE Exp.		236	39	4.2		164	1.0		1165
APSF		233	38	4.1		154	1.0		1215
MOX FFF		235	33	4.7	1.2	156	0.8	0.15	1264
F-Area	TR3/4	213	18	3.1		55			
NE Exp.		213	27	2.7		73	2.0		1056
APSF		211	19	1.9		37	2.0		1020
MOX FFF		212	24	1.9	1.0	45	2.2	2.80	1050
F-Area	DB1/3	204	33	5.2		172			
NE Exp.		206	37	5.2		194	1.0		1176
APSF		203	50	3.3		166	1.0		1197
MOX FFF		205	26	4.2	1.0	110	0.9	0.38	1107
F-Area	DB4/5	175	28	2.2		61			
NE Exp.		178	29	2.3		67	2.0		1180
APSF		175	21	2.5		52	2.0		1231
MOX FFF		183	24	1.7	1.0	40	2.5	3.76	1073
F-Area	ST1 ^[4]	167	47	2.8		131			
NE Exp.		172	43	3.2		138	1.0		1273
APSF		168	46	3.0		137	1.0		1223
MOX FFF		174	63	3.7	2.4	231	1.0	0.89	1164
F-Area	ST2 ^[4]	152							
NE Exp.		152							
APSF									
MOX FFF		157	22	1.5	0.8	34	2.4	5.85	1066
F-Area	GC	138	21	2.8		58			
NE Exp.		141	39	2.5		97	2.0		1319
APSF		143	49	1.6		79	2.0		1160
MOX FFF		146	36	1.3	1.0	46	2.2	9.95	1125
F-Area	CG								
NE Exp.		134				-	-		
APSF		134				-	-		
MOX FFF		141	92	2.3	2.0	213	0.9	6.65	

[1] NE Expansion values include APSF data.

[2] Friction Ratio = sleeve (f_s) / q_{cor} ratio.

[3] Surface effects have not been accounted for.

[4] The Northeast Expansion report does not separate ST1 and ST2.

TABLE 6-2 AVERAGE CLASSIFICATION AND PHYSICAL TEST RESULTS

	ENGR UNIT	AVE. THICK. ^[1] (ft)	AVE PI ^[2] (%)	LIQUID LIMIT ^[3] (%)	MOISTURE CONTENT (%)	AVE % SAND (%)	AVE -NO. 200 (%)	AVE % SILT (%)	AVE % CLAY (%)	USCS CLASS.	MOIST DENSITY (pcf)	DRY DENSITY (pcf)
F-Area	TR1	25	17	38	15	67	33		18.3		122	106
NE Exp.		13	23	48	18	66	34					
APSF		16	11	30	16	75	25					
MOX FFF		1-19								SM		
F-Area	TR1A	19	14	36	19	70	30		32.5		114	96
NE Exp.		16.0	20	35	19	70	30					
APSF		14	22	46	20	63	37				123	101
MOX FFF		7	16	39	15	66	34	18	23	SM		
F-Area	TR2A	25	10	33	17	83	17		10.1		122	101
NE Exp.		26	9	28	17	86	14					
APSF		27	10	33	21	84	16					
MOX FFF		26	17	37	18	83	16	4	13	SC	129	105
F-Area	TR2B	19	18	41	22	81	19		8.3		123	99
NE Exp.		23	12	24	18	90	10					
APSF		22	NP	NP	24	89	11				124	102
MOX FFF		25			17	91	9			SP-SM		
F-Area	TR3/4	10	58	96	51	36	64		39.6		108	76
NE Exp.		7	19	54	34	64	36					
APSF		8	19	54	42	66	34				115	89
MOX FFF		8	37	71	32	72	27	7	21	SC	117	91
F-Area	DB1/3	28	19	44	27	86	14		12.1		124	99
NE Exp.		28	16	11	25	89	11					
APSF		28	NP	NP	27	91	9				122	98
MOX FFF		21	30	63	32	82	18	5	17	SC-SM	115	91
F-Area	DB4/5	7	15	48	39	78	22		20.1		118	86
NE Exp.		6	11	45	36	80	20					
APSF		7	11	45	38	79	21				115	87
MOX FFF		9	38	73	37	70	29	8	21	SC-SM	104	76
F-Area	ST1 ^[2]	19	18	40	29	71	29		23.9		116	87
NE Exp.		20	14	23	30	81	19					
APSF			25	49	30	82	18					
MOX FFF		21	22	52	29	88	12	5	13	SP-SM		
F-Area	ST2 ^[2]											
NE Exp.		11										
APSF												
MOX FFF		12	19	47	30	66	84	19	16	SM	118	98
F-Area	GC	7	47	83	32	61	39		2.8		121	92
NE Exp.		7	27	42	32	67	33					
APSF		9	30	57	28	48	52					
MOX FFF		4	30	57	31	46	55	29	26	SP-SM	110	81

Notes: [1] NE Expansion values include APSF data.

[2] The Northeast Expansion Report does not separate ST1 and ST2.

[3] Atterberg limits determined from fraction of soil sample smaller than No. 200 sieve were not used in determining average liquid limit and plasticity index values.

TABLE 6-3 AVERAGE STRENGTH TEST RESULTS

	ENGR UNIT	AVE. THICK. ^[1] (ft)	AVE TOP EL. ^[1] (MSL)	AVE Triaxial C (ksf)	AVE Triaxial ϕ (degree)	AVE Triaxial C' (ksf)	AVE Triaxial ϕ' (degree)
F-Area	TR1	25					34
NE Exp.		13	291				
APSF		16	289				
MOX FFF		9	276				
F-Area	TR1A	19	278				32
NE Exp.		16.0	278				
APSF		14	273	0	28		33
MOX FFF		12	267				
F-Area	TR2A	25	261				32
NE Exp.		26	262				
APSF		27	260				
MOX FFF		20	255	0.6	28	0	33
F-Area	TR2B	19	233				31
NE Exp.		23	236				
APSF		22	233				
MOX FFF		23	235			0	36
F-Area	TR3/4	10	213	0.75	13	0	30
NE Exp.		7	213				
APSF		8	211	0.9	12	0	29
MOX FFF		7	212	1.5	12	0	33
F-Area	DB1/3	28	204				34
NE Exp.		28	206				
APSF		28	203				
MOX FFF		22	205				
F-Area	DB4/5	7	175		17		26
NE Exp.		6	178				
APSF		7	175				34
MOX FFF		9	183	0.2	11	0	29
F-Area	ST1 ^[2]	19	167				31
NE Exp.		20	172				
APSF			168				
MOX FFF		17	174				
F-Area	ST2 ^[2]	11	152				
NE Exp.		11	152				
APSF							
MOX FFF		11	157	1.1	9	1	24
F-Area	GC	7	138				28
NE Exp.		7	141				
APSF		9	143				
MOX FFF		5	146				
F-Area	CG						
NE Exp.			134				
APSF			134				
MOX FFF			141				

[1] NE Expansion values include APSF data.

[2] The Northeast Expansion report does not separate ST1 and ST2.

TABLE 6-4 AVERAGE CONSOLIDATION TEST RESULTS

	ENGR UNIT	AVE. THICK. ^[1] (ft)	AVE TOP EL. ^[1] (MSL)	VOID RATIO	C _c	C _r	P _c (ksf)
F-Area	TR1	25		0.68	0.12	0.011	6.2
NE Exp.		13	291				
APSF		16	289				
MOX FFF		9	276				
F-Area	TR1A	19	278	0.74	0.08	0.009	6.3
NE Exp.		16	278				
APSF		14	273	0.66	0.12	0.100	
MOX FFF		12	267				
F-Area	TR2A	25	261	0.69	0.07	0.011	5.0
NE Exp.		26	262				
APSF		27	260				
MOX FFF		20	255	0.65	0.12	0.011 (0.010)	8.0 (8.2)
F-Area	TR2B	19	233	0.80	0.05		12.0
NE Exp.		23	236				
APSF		22	233				
MOX FFF		23	235				
F-Area	TR3/4	10	213	1.39	0.85	0.138	14.8
NE Exp.		7	213				
APSF		8	211	0.89	0.28	0.160	
MOX FFF		7	212	0.94	0.41 (0.34)	0.021 (0.021)	5.8 (9.6)
F-Area	DB1/3	28	204	0.75	0.27	0.109	13.9
NE Exp.		28	206				
APSF		28	203				
MOX FFF		22	205	0.83	0.10	0.011 (0.010)	4.0 (9.3)
F-Area	DB4/5	7	175	1.04	0.55	0.053	10.7
NE Exp.		6	178				
APSF		7	175	1.03	0.25	0.009	
MOX FFF		9	183	1.19	0.45	0.035 (0.021)	7.9 (10.3)
F-Area	ST1 ^[2]	19	167	0.98	0.31	0.042	14.8
NE Exp.		20	172				
APSF			168				
MOX FFF		17	174	0.96	0.15	0.017 (0.016)	9.1 (9.2)
F-Area	ST2 ^[2]						
NE Exp.		11	152				
APSF							
MOX FFF		12	157	0.99	0.28	0.024 (0.016)	8.4 (10.3)
F-Area	GC	7	138	0.83	0.31	0.035	11.5
NE Exp.		7	141				
APSF		9	143				
MOX FFF		5	146	0.87	0.21	0.045 (0.015)	9.6 (12.0)

[1] NE Expansion values include APSF data.

[2] The Northeast Expansion report does not separate ST1 and ST2.

[3] Average values of C_c, C_r, and P_c for MFFF from DCS (2002a). Values in parentheses based on DCS interpretation of results reported by LawGibb (2001).

TABLE 6-5 GENERALIZED SUBSURFACE PROFILE

Geologic Formation	Engineering Unit	Top Elevation (ft, MSL)
Tobacco Road	TR1A	270
Tobacco Road	TR2A	263
Tobacco Road	TR2B	237
Tobacco Road	TR3/4	212
Dry Branch	DB1/3	204
Dry Branch	DB4/5	183
Santee	ST1	174
Santee	ST2	153
Warley Hill "Green Clay"	GC	141
Congaree	CG	137
Fourmile	FM	85
Steel Creek	SC1	-2
Steel Creek	SC2	-50
Black Creek	BC1	-120
Black Creek	BC2	-280
Black Creek	BC3	-310
Middendorf	MD1	-380
Middendorf	MD2	-438
Middendorf	MD3	-496
Cape Fear	CF	-534
Basement	BM	-595

Note: Top elevations for units in shallow profile (Units TR1A through CG) are from Table 5-2. Top elevations for units in deep profile are from Geomatrix (1997a).

TABLE 6-6 SEISMIC CPTS USED TO DEVELOP INDIVIDUAL SOIL PROFILES

SCPT-67	SCPT-76
SCPT-68	SCPT-77
SCPT-69	SCPT-78A
SCPT-70	SCPT-81
SCPT-71	SCPT-83
SCPT-72	SCPT-85
SCPT-73	SCPT-86
SCPT-74	SCPT-87A
SCPT-75	SCPT-97

TABLE 6-7 STATISTICAL SUMMARY OF SEISMIC CPT SHEAR WAVE VELOCITY DATA

Engineering Unit	Top El (ft, MSL)	Average V_s (fps)	No. of Data Points	Max	Min	Std Dev	Ave. + 1 Std Dev	Ave. - 1 Std Dev
TR1A	270	1488.2	13	1845.6	1106.9	226.4	1714.6	1261.7
TR2A	263	1280.7	64	1505.4	1041.3	111.4	1392.1	1169.4
TR2B	237	1263.8	72	1704.2	956.7	130.6	1394.4	1133.2
TR3/4	212	1050.4	28	1452.2	823.4	138.5	1188.9	911.9
DB1/3	204	1106.9	83	1504.7	635.3	165.2	1272.2	941.7
DB4/5	183	1073.3	58	1429.4	815.8	118.4	1191.7	954.9
ST1	173	1163.7	107	1873.8	681.7	164.4	1328.0	999.3
ST2	153	1065.7	54	1545.5	468.2	206.9	1272.6	858.8
GC	141	1125.0	7	1358.1	860.8	170.4	1295.4	954.6
CG	137	No Data						

TABLE 6-8 SHEAR MODULUS REDUCTION VALUES FOR USE AT MFFF SITE

Soil Type	Stiff Upland Sands	Tobacco Road	Snapp Sands	Dry Branch/Santee	Shallow Sand	Shallow Clay	Deep Sand	Deep Clay
Depth Range (ft)	0-30	30-70	280-300	70-250	<300	<300	>300	>300
ϵ_r^1	0.021	0.044	0.044	0.077	0.066	0.148	0.111	0.23
Strain (ϵ)								
0.0001	0.99526	0.99773	0.99773	0.9987	0.99849	0.99932	0.9991	0.99957
0.0002	0.99057	0.99548	0.99548	0.99741	0.99698	0.99865	0.9982	0.99913
0.0003	0.98592	0.99323	0.99323	0.99612	0.99548	0.99798	0.9973	0.9987
0.0005	0.97674	0.98876	0.98876	0.99355	0.99248	0.99663	0.99552	0.99783
0.001	0.95455	0.97778	0.97778	0.98718	0.98507	0.99329	0.99107	0.99567
0.002	0.91304	0.95652	0.95652	0.97468	0.97059	0.98667	0.9823	0.99138
0.003	0.875	0.93617	0.93617	0.9625	0.95652	0.98013	0.97368	0.98712
0.005	0.80769	0.89796	0.89796	0.93902	0.92958	0.96732	0.9569	0.97872
0.01	0.67742	0.81481	0.81481	0.88506	0.86842	0.93671	0.91736	0.95833
0.02	0.5122	0.6875	0.6875	0.79381	0.76744	0.88095	0.84733	0.92
0.03	0.41176	0.59459	0.59459	0.71963	0.6875	0.83146	0.78723	0.88462
0.05	0.29577	0.46809	0.46809	0.6063	0.56897	0.74747	0.68944	0.82143
0.1	0.17355	0.30556	0.30556	0.43503	0.39759	0.59677	0.52607	0.69697
0.2	0.09502	0.18033	0.18033	0.27798	0.24812	0.42529	0.35691	0.53488
0.3	0.06542	0.12791	0.12791	0.20424	0.18033	0.33036	0.27007	0.43396
0.5	0.04031	0.08088	0.08088	0.13345	0.11661	0.2284	0.18167	0.31507
1	0.02057	0.04215	0.04215	0.07149	0.06191	0.12892	0.09991	0.18699
2	0.01039	0.02153	0.02153	0.03707	0.03195	0.0689	0.05258	0.10314
3	0.00695	0.01445	0.01445	0.02502	0.02153	0.04701	0.03568	0.07121
5	0.00418	0.00872	0.00872	0.01517	0.01303	0.02875	0.02172	0.04398
10	0.0021	0.00438	0.00438	0.00764	0.00656	0.01458	0.01098	0.02248

Source: WSRC (1996a)

¹ ϵ_r is the reference strain in the relationship $G/G_{max} = 1/(1+\epsilon/\epsilon_r)$

TABLE 6-9 DAMPING RATIOS RECOMMENDED FOR USE AT MFFF SITE

Soil Type	Stiff Upland Sands	Tobacco Road	Snapp Sands	Dry Branch/Santee	Shallow Sand	Shallow Clay	Deep Sand	Deep Clay
Depth Range (ft)	0-30	30-70	280-300	70-250	<300	<300	>300	>300
Strain (%)								
0.0001	1.059	0.625	0.625	0.825	0.674	1.296	0.489	0.992
0.0002	1.103	0.647	0.647	0.835	0.687	1.292	0.497	0.99
0.0003	1.151	0.67	0.67	0.846	0.702	1.293	0.505	0.991
0.0005	1.248	0.717	0.717	0.871	0.733	1.3	0.524	0.995
0.001	1.493	0.835	0.835	0.936	0.811	1.326	0.57	1.103
0.002	1.973	1.07	1.07	1.07	0.97	1.389	0.665	1.054
0.003	2.434	1.3	1.3	1.205	1.127	1.456	0.759	1.097
0.005	3.302	1.747	1.747	1.47	1.435	1.594	0.945	1.186
0.01	5.201	2.79	2.79	2.108	2.171	1.938	1.398	1.41
0.02	8.165	4.605	4.605	3.281	3.505	2.603	2.251	1.851
0.03	10.407	6.139	6.139	4.336	4.686	3.233	3.039	2.276
0.05	13.639	8.614	8.614	6.162	6.692	4.392	4.453	3.08
0.1	18.317	12.799	12.799	9.605	10.363	6.82	7.289	4.856
0.2		17.425	17.425	13.951	14.825	10.356	11.179	7.671
0.3				16.683		12.844	13.799	9.833
0.5						16.317	17.21	12.955

Source: WSRC (1996a)

**TABLE 6-10 SEISMIC CPTs WITH PAIRS OF COMPRESSION AND SHEAR WAVE
VELOCITY DATA**

CPT Performed in 2000	CPT Performed in 2002
CPT-1S	SCPT-72
CPT-3S	SCPT-73
CPT-5S	SCPT-75
CPT-8S	SCPT-76
CPT-11S	SCPT-77
CPT-13S	SCPT-78A
CPT-16S	SCPT-81
CPT-19S	SCPT-94
CPT-23S	
CPT-26S	
CPT-31S	
CPT-34S	
CPT-35S	
CPT-37S	

TABLE 6-11 SUMMARY OF FILTERED DYNAMIC POISSON'S RATIOS BASED ON SEISMIC CPTs

Engineering Unit	Number of data	Average	Minimum	Maximum	Standard Deviation
TR2A	27	0.29	0.21	0.39	0.04
TR2B	29	0.30	0.21	0.38	0.05
TR3/4	6	0.31	0.25	0.38	0.04
DB1/3	10	0.33	0.25	0.39	0.05

Note: Due to the limited amount of data collected for Engineering Units TR1 and TR1A, these two units are excluded from this table. Values of Poisson's ratio for TR1 and TR1A provided by Geomatrix (1997a) for the APSF site, located ~500 ft south of the MFFF area, are recommended for use for the MFFF site.

TABLE 6-12 RECOMMENDED VALUES OF DYNAMIC POISSON'S RATIO FOR THE MFFF SITE

Engineering Unit	Poisson's Ratio
TR1	0.37
TR1A	0.34
TR2A	0.29
TR2B	0.30
TR3/4 (above water table)	0.31
DB1/3 (above water table)	0.33
Others (below water table)	0.47

Note: Values of Poisson's ratio for TR1 and TR1A are from Geomatrix (1997a) – See note above.

**TABLE 6-13 PROFILES OF LOW-STRAIN SHEAR WAVE VELOCITY, DENSITY,
AND DYNAMIC POISSON'S RATIO FOR THE MFFF AREA**

Unit ID	Top Elevation (ft)	Depth (ft)	Moist Unit Weight (pcf)	Shear Wave Velocity (fps)			Dynamic Poisson's Ratio
				Best Estimate	Upper Bound	Lower Bound	
TR1A	270	0	123	1488.2	1822.6	1215.1	0.34
TR2A	263	7	120	1280.7	1568.6	1045.7	0.29
TR2B	237	33	118	1263.8	1547.8	1031.9	0.30
TR3/4	212	58	115	1050.4	1286.5	857.7	0.31
DB1/3	204	66	119	1106.9	1355.7	903.8	0.47
DB1/3	200	70	119	1106.3	1354.9	903.2	0.47
DB4/5	183	87	108	1073.3	1314.5	876.4	0.47
ST1	173	97	113	1163.7	1425.2	950.1	0.47
ST2	153	117	113	1065.7	1305.3	870.2	0.47
GC	141	129	114	1125.0	1377.9	918.6	0.47
CG	137	133	125	1364	1670	1114	0.47
FM	85	185	125	1467	1796	1198	0.47
SC1	-2	272	125	1818	2226	1485	0.47
SC2	-50	320	130	2124	2601	1734	0.47
BC1	-120	390	125	2230	2731	1821	0.47
BC2	-280	550	130	2712	3321	2215	0.47
BC3	-310	580	130	2457	3009	2006	0.47
MD1	-380	650	135	2460	3013	2009	0.47
MD2	-438	708	135	2741	3357	2238	0.47
MD3	-496	766	135	2980	3649	2433	0.47
CF	-534	804	135	2744	3360	2241	0.47
BM	-595	865	150	11000	11000	11000	0.26

Notes: Assume ground surface at El 270 ft.

Assume groundwater table at El 210 ft.

Values of moist unit weight are from DCS, 2003p.

Values for dynamic Poisson,'s ratio are from DCS, 2003f.

Values of upper-bound $v_s = \sqrt{1.5} \times (\text{best-estimate})$, except for BM.

Values of lower-bound $v_s = (\text{best-estimate}) / \sqrt{1.5}$, except for BM.

TABLE 6-14 STRAIN-COMPATIBLE SHEAR WAVE VELOCITIES, SHEAR MODULI, AND DAMPING RATIOS – PC-3 ROCK MOTION SCALED UP BY 1.25

Center El. (ft)	Shear Wave Velocity (fps)			Shear Moduli (ksf)			Damping Ratio (%)		
	Best Estimate	Upper Bound	Lower Bound	Best Estimate	Upper Bound	Lower Bound	Best Estimate	Upper Bound	Lower Bound
268.0	1480.7	1816.6	1207.1	8382	12,616	5570	0.69	0.67	0.72
264.5	1469.4	1804.9	1194.0	8254	12,454	5450	0.86	0.80	0.94
260.0	1241.0	1529.4	1001.7	5744	8,724	3742	1.26	1.08	1.46
254.0	1210.3	1509.9	973.9	5464	8,503	3537	1.67	1.38	2.01
247.5	1185.6	1480.0	954.0	5243	8,169	3394	2.16	1.70	2.53
240.5	1166.4	1457.1	931.0	5074	7,919	3233	2.57	2.07	3.08
234.0	1124.9	1418.5	885.2	4641	7,379	2874	3.08	2.42	3.82
228.0	1100.5	1408.0	865.1	4441	7,271	2745	3.53	2.60	4.25
221.5	1076.8	1398.3	848.8	4252	7,170	2642	3.95	2.77	4.6
215.0	1057.4	1377.6	837.2	4100	6,960	2570	4.29	3.09	4.94
208.0	972.5	1214.1	785.1	3380	5,269	2203	2.82	2.40	3.13
200.5	960.7	1219.9	762.8	3414	5,504	2152	3.75	2.96	4.45
193.5	956.2	1212.5	751.9	3382	5,437	2091	3.88	3.07	4.75
186.5	952.4	1204.7	743.0	3355	5,368	2042	3.98	3.18	5
178.0	893.7	1139.8	680.3	2681	4,361	1553	4.73	3.78	6.11
168.0	1002.6	1263.0	773.2	3530	5,602	2100	3.94	3.23	5.2
158.0	999.7	1255.8	767.8	3510	5,539	2071	4.02	3.35	5.34
150.0	877.0	1121.1	666.2	2701	4,414	1559	4.98	4.03	6.43
144.0	871.4	1119.5	667.5	2667	4,402	1565	5.11	4.06	6.38
139.0	944.5	1199.0	732.6	3161	5,094	1902	4.56	3.69	5.6
111.0	1216.5	1534.8	974.9	5749	9,152	3692	3.12	2.57	3.53
72.0	1269.7	1670.7	1016.2	6263	10,844	4012	3.60	2.21	4.11
28.5	1241.7	1628.8	1026.9	5990	10,307	4097	4.17	2.72	3.85
-26.0	1767.4	2182.5	1443.2	12136	18,506	8092	1.54	1.38	1.53
-85.0	2044.0	2509.6	1666.6	16880	25,447	11222	1.28	1.21	1.31
-200.0	2187.8	2689.8	1785.3	18595	28,108	12383	1.35	1.25	1.37
-295.0	2624.7	3250.9	2146.6	27835	42,703	18619	1.13	0.88	1.08
-345.0	2362.7	2925.1	1932.5	22556	34,573	15090	1.30	1.01	1.25
-409.0	2417.1	2971.2	1970.8	24514	37,041	16298	1.31	1.22	1.35
-467.0	2650.4	3271.8	2162.2	29475	44,916	19616	1.15	0.94	1.17
-515.0	2890.0	3566.3	2360.3	35046	53,366	23375	1.07	0.91	1.07
-564.5	2646.9	3265.6	2161.2	29397	44,746	19599	1.21	1.02	1.21
-595.0	11000.0	11000.0	11000.0	564120	564,120	564120	0.01	0.01	0.01

TABLE 6-15 BEST-ESTIMATE STRAIN-COMPATIBLE CYCLIC STRESS RATIO, EFFECTIVE SHEAR STRAIN, PEAK SHEAR STRAIN, PEAK SHEAR STRESS, AND PEAK GROUND ACCELERATION – PC-3 ROCK MOTION SCALED UP BY 1.25

Center Elevation (ft)	Cyclic Stress Ratio	Effective Shear Strain (%)	Peak Shear Strain (%)	Peak Shear Stress (psf)	Top Elevation (ft)	Peak Ground Acceleration (g)
268.0	0.132	0.0004	0.0006	50.3	270	0.20
264.5	0.132	0.0011	0.0017	137.0	266	0.20
260.0	0.131	0.0028	0.0043	246.4	263	0.20
254.0	0.129	0.0046	0.0071	386.3	257	0.19
247.5	0.127	0.0066	0.0101	530.6	251	0.19
240.5	0.123	0.0086	0.0133	674.9	244	0.18
234.0	0.120	0.0112	0.0172	799.2	237	0.17
228.0	0.117	0.0133	0.0204	906.5	231	0.17
221.5	0.114	0.0156	0.0240	1019.2	225	0.15
215.0	0.111	0.0177	0.0273	1118.6	218	0.13
208.0	0.107	0.0229	0.0353	1193.3	212	0.12
200.5	0.107	0.0240	0.0369	1259.7	204	0.13
193.5	0.105	0.0251	0.0387	1307.8	197	0.15
186.5	0.104	0.0261	0.0402	1349.4	190	0.15
178.0	0.101	0.0335	0.0516	1383.3	183	0.16
168.0	0.097	0.0258	0.0397	1401.9	173	0.20
158.0	0.094	0.0265	0.0408	1433.6	163	0.19
150.0	0.094	0.0359	0.0552	1491.8	153	0.16
144.0	0.094	0.0372	0.0573	1527.6	147	0.16
139.0	0.093	0.0319	0.0491	1552.7	141	0.17
111.0	0.083	0.0181	0.0279	1604.6	137	0.17
72.0	0.086	0.0206	0.0318	1988.7	85	0.15
28.5	0.085	0.0252	0.0387	2319.4	59	0.15
-26.0	0.070	0.0122	0.0187	2274.2	-2	0.14
-85.0	0.056	0.0083	0.0128	2155.6	-50	0.13
-200.0	0.048	0.0084	0.0129	2406.2	-120	0.12
-295.0	0.048	0.0066	0.0102	2836.4	-280	0.13
-345.0	0.046	0.0085	0.0131	2963.8	-310	0.13
-409.0	0.039	0.0074	0.0114	2802.0	-380	0.12
-467.0	0.040	0.0069	0.0106	3109.6	-438	0.12
-515.0	0.040	0.0061	0.0094	3283.8	-496	0.12
-564.5	0.039	0.0076	0.0116	3415.9	-534	0.11
-595.0	0.037	0.0004	0.0006	3384.7	-595	0.11

Note: 1. Peak ground acceleration is output at top of layer.

TABLE 6-16 BEST-ESTIMATE STRAIN-COMPATIBLE CYCLIC STRESS RATIO, EFFECTIVE SHEAR STRAIN, PEAK SHEAR STRAIN, PEAK SHEAR STRESS, AND PEAK GROUND ACCELERATION – 1886 CHARLESTON (50TH PERCENTILE) CONTROL MOTION

Center Elevation (ft)	Cyclic Stress Ratio	Effective Shear Strain (%)	Peak Shear Strain (%)	Peak Shear Stress (psf)	Top Elevation (ft)	Peak Ground Acceleration (g)
268.0	0.0694	0.0002	0.0003	26.1	270	0.11
264.5	0.0692	0.0006	0.0009	71.7	266	0.11
260.0	0.0685	0.0014	0.0022	128.6	263	0.11
254.0	0.0669	0.0022	0.0035	199.9	257	0.10
247.5	0.0649	0.0031	0.0048	271.7	251	0.09
240.5	0.0623	0.0040	0.0062	341.3	244	0.09
234.0	0.0595	0.0050	0.0077	397.2	237	0.09
228.0	0.0579	0.0057	0.0088	449.0	231	0.09
221.5	0.0571	0.0066	0.0102	510.7	225	0.08
215.0	0.0563	0.0075	0.0115	570.0	218	0.08
208.0	0.0566	0.0113	0.0173	632.7	212	0.08
200.5	0.0588	0.0115	0.0178	694.9	204	0.08
193.5	0.0603	0.0126	0.0195	749.0	197	0.08
186.5	0.0613	0.0137	0.0210	798.0	190	0.08
178.0	0.0627	0.0181	0.0279	857.9	183	0.08
168.0	0.0642	0.0154	0.0238	926.2	173	0.09
158.0	0.0648	0.0166	0.0256	984.6	163	0.10
150.0	0.0645	0.0217	0.0333	1021.4	153	0.10
144.0	0.0640	0.0222	0.0342	1042.5	147	0.09
139.0	0.0633	0.0195	0.0300	1055.7	141	0.08
111.0	0.0636	0.0131	0.0202	1230.4	137	0.08
72.0	0.0608	0.0133	0.0204	1404.1	85	0.09
28.5	0.0572	0.0152	0.0234	1561.9	59	0.08
-26.0	0.0499	0.0085	0.0132	1624.5	-2	0.08
-85.0	0.0473	0.0069	0.0107	1820.7	-50	0.07
-200.0	0.0446	0.0078	0.0119	2222.9	-120	0.06
-295.0	0.0397	0.0054	0.0084	2350.0	-280	0.06
-345.0	0.0406	0.0075	0.0115	2609.3	-310	0.06
-409.0	0.0383	0.0072	0.0111	2723.1	-380	0.07
-467.0	0.0350	0.0060	0.0092	2719.0	-438	0.07
-515.0	0.0339	0.0052	0.0080	2812.3	-496	0.06
-564.5	0.0330	0.0064	0.0099	2925.3	-534	0.05
-595.0	0.0333	0.0004	0.0005	3046.2	-595	0.05

TABLE 6-17 SOFT SOIL LAYER CLASSIFICATION AND ENGINEERING PROPERTIES AT MFFF AND BEG BUILDING LOCATIONS

Geotechnical Criteria	General Soil Description	USCS	SBT Class	q _t (tsf)	Sand %	Fines Content %	LL	PL	PI	w _n %
Recommendations Initial Static Design	Predominantly Silty and Clayey Fine Sand to Fine Sand	SM-SC		11	70	30	55	30	25	35
WSRC (1999b)	Predominantly Silty and Clayey Fine Sand to Fine Sand	Varies As Above					50-100		20-90	25-75

Geotechnical Criteria	General Soil Description	γ _s (pcf)	γ _w (pcf)	S _u (tsf)	φ'	C _c	C _r	Void Ratio (e _o)	OCR	V _s (fps)
Recommendations Initial Static Design	Predominantly Silty and Clayey Fine Sand to Fine Sand	90	120	0.5	19°	0.5	0.07	0.85-1.0	1	500 (low value)
WSRC (1999b)	Predominantly Silty and Clayey Fine Sand to Fine Sand	50-80	90-110			0.15 - 1.2		0.3-1.4	0.3 - 1.0 Recommends (0.7)	250 (low value)

TABLE 7-1 SUMMARY OF SOIL PARAMETERS FOR FLAC CAM-CLAY MODEL

Material	Dry Unit Weight		Moist Unit Weight		Void Ratio (e)	Porosity (n)	Shear Wave Velocity (V _s) (fps)	Poisson's Ratio (μ)	Shear Modulus (G) (kips/ft ²)	Bulk Modulus (K) (kips/ft ²)	Friction Angle ^{1,2} (φ) (degrees)	Frictional Constant ² (M)	Specific Volume (v) (1 + e)	Preconsolidation Pressure (P _c) (psf)		Compression Index		Recompression Index	
	(γ _d) (pcf)	(ρ) (slug/ft ³)	(γ _m) (pcf)	ρ (slug/ft ³)										(P _c) (psf)		(C _c)	(λ)	(C _R)	(K)
														Laboratory	Model				
Structural Fill	126	3.91	145	4.50	0.34	NA	1600	0.30	11528	24977	40	1.64	1.34	20000	20000	0.040	0.017	0.004	0.0017
TR1	101	3.14	123	3.82	0.67	NA	1476	0.34	8322	23232	32	1.29	1.67	6300	20000	0.100	0.043	0.011	0.0048
TR1A	101	3.14	123	3.82	0.67	NA	1476	0.34	8322	23232	32	1.29	1.67	6300	20000	0.100	0.043	0.011	0.0048
TR2A	100	3.11	120	3.73	0.68	NA	1324	0.25	6533	10888	32	1.29	1.68	8000	20000	0.095	0.041	0.011	0.0048
TR2B	103	3.20	118	3.66	0.64	NA	1253	0.31	5753	13223	31	1.24	1.64	12000	20000	0.110	0.048	0.011	0.0048
TR3/4	89	2.76	115	3.57	0.89	0.47	1016	0.30	3687	7988	30	1.20	1.89	14800	20000	0.250	0.109	0.021	0.0091
DB1/3	95	2.95	119	3.70	0.77	0.44	1126	0.30	4686	10152	30	1.20	1.77	13900	20000	0.100	0.043	0.011	0.0048
DB4/5	78	2.42	108	3.35	1.16	0.54	1104	0.30	4088	8857	26	1.03	2.16	10700	20000	0.450	0.195	0.035	0.0152
ST1	83	2.58	113	3.51	1.03	0.51	1129	0.30	4473	9692	31	1.24	2.03	14800	20000	0.150	0.065	0.017	0.0074
ST2	85	2.64	113	3.51	0.98	0.50	1068	0.30	4003	8673	30	1.20	1.98	See Note 2	20000	0.280	0.122	0.024	0.0104
GC	91	2.83	114	3.54	0.85	0.46	1217	0.30	5244	11361	28	1.11	1.85	See Note 2	20000	0.210	0.091	0.045	0.0195
CG	109	3.39	125	3.88	0.55	0.35	1364	0.30	7222	15649	35	1.42	1.55	20000	20000	0.099	0.043	0.009	0.0039
Soft Materials ³	85	2.64	100	3.11	0.98	0.50	500	0.30	776	1682	15	0.57	1.98	See Note 2	See Note 2	0.500	0.217	0.170	0.0734
Soft Zones ³	85	2.64	100	3.11	0.98	0.5	500	0.30	116	252	15	0.57	1.98	See Note 2	See Note 2	0.500	0.217	0.100	0.0434

Notes:

- Friction angles of 32°, 33°, and 34° were used for some cases for the engineering unit soils. Frictional constants of 1.29, 1.33, and 1.37, respectively were used for those cases.
- The preconsolidation pressure input into the FLAC model is the existing overburden pressure calculated assuming the ground surface is at Elevation 269 feet MSL, moist densities as shown in the table, and a groundwater surface at elevation 210 feet MSL.
- Soft Material parameters are used for Soft Material and Soft Zone soils for the settlement analysis for static loads. The Soft Zone parameters are used for the soft zone soils for the earthquake induced soft soil settlement models for underconsolidated soils.

TABLE 7-2 SUMMARY OF SOIL PARAMETERS FOR FLAC MOHR-COULOMB COLLAPSE MODEL

Material	Dry Unit Weight	(p)	Moist Unit Weight	(p)	Effective Cohesion	Tensile Strength	Shear Wave Velocity	Poisson's Ratio	Shear Modulus ¹	Bulk Modulus ¹	Effective Friction Angle	Dilation Angle
	(γ_d) (pcf)		(γ_m) (pcf)									
	(pcf)	(slug/ft ³)	(pcf)	(slug/ft ³)	(psf)	(psf)	(fps)	(μ)	(G) (kips/ft ²)	(K) (kips/ft ²)	(ϕ') (degrees)	(Ψ) (degrees)
Structural Fill	126	3.91	145	4.50	100	0	1600	0.30	11528	24977	40	15
TR1	101	3.14	123	3.82	100	0	1476	0.34	8322	23232	32	14
TR1A	101	3.14	123	3.82	100	0	1476	0.34	8322	23232	32	14
TR2A	100	3.11	120	3.73	100	0	1324	0.25	6533	10888	32	13
TR2B	103	3.20	118	3.66	100	0	1253	0.31	5753	13223	31	13
TR3/4	89	2.76	115	3.57	100	0	1016	0.30	3687	7988	30	13
DB1/3	95	2.95	119	3.70	100	0	1126	0.30	4686	10152	30	13
DB4/5	78	2.42	108	3.35	100	0	1104	0.30	4088	8857	26	11
ST1	83	2.58	113	3.51	100	0	1129	0.30	4473	9692	31	13
ST2	85	2.64	113	3.51	100	0	1068	0.30	4003	8673	30	13
GC	91	2.83	114	3.54	100	0	1217	0.30	5244	11361	28	12
CG	109	3.39	125	3.88	100	0	1364	0.30	7222	15649	35	15
Soft Zones/ Materials	85	2.64	100	3.11	100	0	500	0.30	776	1682	15	0

NOTES:

1. The shear modulus and bulk modulus used for some of the analysis was 15 percent of the values shown.
2. Definitions, sources and derivation of parameters are discussed in DCS (2003d).

TABLE 7-3 MEASURED SETTLEMENTS AT S-AREA STRUCTURES

Structure	Bearing Pressure (ksf)	Maximum Settlement (inches)
221-S Vitrification Building	5.5	3
292-S Glass Waste Storage Building	2.5	0.7
294-S Fan House	2	0.9
210-S Sand Filter Building	0.8	0.8

WSRC (2002b)

**TABLE 8-1 AVERAGE FACTOR OF SAFETY AGAINST LIQUEFACTION BY
ENGINEERING UNIT**

Engineering Unit	Thickness (feet)	Factor of Safety Against Liquefaction
TR3/4	8.0	1.7
DB1/3	21.0	2.2
DB4/5	10.0	1.4
ST1	20.0	4.4
ST2	12.0	1.3

**TABLE 8-2 SUMMARY OF ESTIMATED POST-EARTHQUAKE SETTLEMENTS
BASED ON BORINGS DUE TO PC-3+ MOTION**

Series No.	Boring ID	Estimated Settlement (inches)
1	BH1	0.06
2	BH4	0.00
3	BH7	0.27
4	BH8	0.00
5	BH11	0.30
6	BH12	0.02
7	BH13	0.18
8	BH14	0.00
9	BH15	0.12
10	BH16	0.33
11	BH17	0.00
12	BH18	0.34
13	BH19	0.02
14	BH20	0.32

TABLE 8-3 TOTAL POST-EARTHQUAKE SETTLEMENTS BASED ON CPT DATA – PC-3+ MOTION

ID	Total Depth (feet)	Estimated Settlement to Bottom of CPT (Inches)	Penetrated Portion of ST1 (feet)	Portion of ST1 <i>not</i> Penetrated (feet)	Penetrated Portion of ST2 (feet)	Portion of ST2 <i>not</i> Penetrated (feet)	Additional Settlement of ST1 (Inches)	Additional Settlement of ST2 (Inches)	Estimated Total Settlement (Inches)
CPT-4	135	0.66	-	-	-	-	-	-	0.66
CPT-7	114	0.70	8.3	12.7	0	9	0.02	0.22	0.94
CPT-8	140	0.99	-	-	-	-	-	-	0.99
CPT-9	126	0.84	-	-	-	-	-	-	0.84
CPT-13	166	0.60	-	-	-	-	-	-	0.60
CPT-14	142	1.09	-	-	-	-	-	-	1.09
CPT-18	120	0.70	13.2	6.8	0	8	0.01	0.20	0.90
CPT-21	139	0.87	8.2	4.8	0	12	0.01	0.30	1.17
CPT-22	153	0.92	14.2	0.0	0	3	0.00	0.07	0.99
CPT-23	124	0.75	16.5	3.5	0	8	0.00	0.20	0.95
CPT-27	128	1.15	17.8	0.0	0	7	0.00	0.17	1.32
CPT-28	150	0.64	-	-	-	-	-	-	0.64
CPT-29	118	0.68	13.6	7.4	0	13	0.01	0.32	1.02
CPT-40	113	0.47	11.7	11.3	0	13	0.01	0.32	0.80
CPT-44	118	0.34	7.3	10.7	0	10	0.01	0.25	0.60
CPT-45	142	0.66	-	-	-	-	-	-	0.66
CPT-46	147	0.87	-	-	-	-	-	-	0.87
CPT-47	116	0.28	6.9	12.1	0	10	0.02	0.25	0.55
CPT-48	111	0.64	6.3	12.7	0	11	0.02	0.27	0.93
CPT-49	123	0.32	4.5	13.5	0	10	0.02	0.25	0.59
CPT-50	134	0.44	8.7	8.3	0	10	0.01	0.25	0.70
CPT-51	139	0.85	11.2	7.8	0	13	0.01	0.32	1.18
CPT-52	120	0.50	2.1	16.9	0	14	0.02	0.35	0.87

TABLE 8-3 TOTAL POST-EARTHQUAKE SETTLEMENTS BASED ON CPT DATA – PC-3+ MOTION

ID	Total Depth (feet)	Estimated Settlement to Bottom of CPT (inches)	Penetrated Portion of ST1 (feet)	Portion of ST1 not Penetrated (feet)	Penetrated Portion of ST2 (feet)	Portion of ST2 not Penetrated (feet)	Additional Settlement of ST1 (inches)	Additional Settlement of ST2 (inches)	Estimated Total Settlement (inches)
CPT-53	119	0.63	10.0	17.0	0	15	0.02	0.37	1.03
CPT-54	123	0.65	3.4	14.6	0	15	0.02	0.37	1.04
CPT-55	136	0.97	9.0	7.0	0	13	0.01	0.32	1.30
CPT-56	120	0.33	1.8	19.2	0	15	0.02	0.37	0.73
CPT-57	129	0.58	7.9	12.1	0	13	0.02	0.32	0.91
CPT-58	122	0.36	2.5	20.5	0	13	0.03	0.32	0.71
CPT-59	126	0.70	7.0	16.0	0	14	0.02	0.35	1.07
CPT-60	141	1.03	15.4	3.6	0	13	0.00	0.32	1.36
CPT-61	116	0.38	6.9	9.1	0	12	0.01	0.30	0.69
CPT-62	116	0.91	11.0	9.0	0	12	0.01	0.30	1.22
CPT-63	119	0.67	11.2	12.8	0	6	0.02	0.15	0.84
CPT-64	141	0.82	-	-	-	-	-	-	0.82
SCPT-65	151	0.86	-	-	-	-	-	-	0.86
SCPT-66	116	0.31	6.3	17.0	0	12	0.02	0.30	0.63
SCPT-67	150	0.61	-	-	-	-	-	-	0.61
SCPT-68	151	1.13	-	-	-	-	-	-	1.13
SCPT-69	154	1.01	-	-	-	-	-	-	1.01
SCPT-70	155	0.80	-	-	-	-	-	-	0.80
SCPT-71	152	0.66	-	-	-	-	-	-	0.66
SCPT-72	153	1.17	-	-	-	-	-	-	1.17
SCPT-73	152	1.29	-	-	-	-	-	-	1.29
SCPT-74	150	0.82	-	-	-	-	-	-	0.82
SCPT-75	145	0.28	-	-	-	-	-	-	0.28

TABLE 8-3 TOTAL POST-EARTHQUAKE SETTLEMENTS BASED ON CPT DATA – PC-3+ MOTION

ID	Total Depth (feet)	Estimated Settlement to Bottom of CPT (inches)	Penetrated Portion of ST1 (feet)	Portion of ST1 <i>not</i> Penetrated (feet)	Penetrated Portion of ST2 (feet)	Portion of ST2 <i>not</i> Penetrated (feet)	Additional Settlement of ST1 (inches)	Additional Settlement of ST2 (inches)	Estimated Total Settlement (inches)
SCPT-76	137	0.51	-	-	-	-	-	-	0.51
SCPT-77	147	0.63	-	-	-	-	-	-	0.63
SCPT-78A	141	0.97	-	-	-	-	-	-	0.97
SCPT-79	139	0.60	-	-	-	-	-	-	0.60
SCPT-80	147	0.69	-	-	-	-	-	-	0.69
SCPT-81	157	0.58	-	-	-	-	-	-	0.58
CPT-82	131	0.40	13.3	9.8	0	14	0.01	0.35	0.76
SCPT-83	158	0.90	-	-	-	-	-	-	0.90
SCPT-84	138	0.56	17.6	2.2	0	12	0.00	0.30	0.86
SCPT-85	165	0.67	-	-	-	-	-	-	0.67
SCPT-86	164	1.19	-	-	-	-	-	-	1.19
SCPT-87A	163	0.84	-	-	-	-	-	-	0.84
SCPT-88	157	0.69	-	-	-	-	-	-	0.69
SCPT-89A	120	0.72	10.0	15.7	0	12	0.02	0.30	1.04
SCPT-90	126	0.43	9.2	10.6	0	10	0.01	0.25	0.69
CPT-91	116	0.20	13.9	3.9	0	11	0.01	0.27	0.48
CPT-92	105	0.44	6.8	16.3	0	10	0.02	0.25	0.71
CPT-93	138	0.45	-	-	-	-	-	-	0.45
SCPT-94	141	1.43	-	-	-	-	-	-	1.43
CPT-95	121	0.98	17.2	5.0	0	8	0.01	0.20	1.19
SCPT-96	129	0.69	10.9	9.5	0	12	0.01	0.30	1.00
SCPT-97	151	1.00	-	-	-	-	-	-	1.00
CPT-98	147	0.94	-	-	-	-	-	-	0.94

TABLE 8-3 TOTAL POST-EARTHQUAKE SETTLEMENTS BASED ON CPT DATA – PC-3+ MOTION

ID	Total Depth (feet)	Estimated Settlement to Bottom of CPT (inches)	Penetrated Portion of ST1 (feet)	Portion of ST1 <i>not</i> Penetrated (feet)	Penetrated Portion of ST2 (feet)	Portion of ST2 <i>not</i> Penetrated (feet)	Additional Settlement of ST1 (inches)	Additional Settlement of ST2 (inches)	Estimated Total Settlement (inches)
CPT-99	158	0.86	-	-	-	-	-	-	0.86
CPT-100	160	0.93	-	-	-	-	-	-	0.93
CPT-101	123	1.27	17.6	2.7		8	0.00	0.20	1.47
CPT-102	160	1.07	-	-	-	-	-	-	1.07
CPT-103	150	0.60	-	-	-	-	-	-	0.60
CPT-104	153	1.10	-	-	-	-	-	-	1.10
CPT-105	135	0.44	12.2	9.0	0	15	0.01	0.37	0.83
CPT-106	164	0.91	-	-	-	-	-	-	0.91
CPT-107	163	0.87	-	-	-	-	-	-	0.87
CPT-108	161	1.03	-	-	-	-	-	-	1.03
CPT-109	153	0.95	-	-	-	-	-	-	0.95
CPT-110	149	0.26	-	-	-	-	-	-	0.26
CPT-111	125	0.45	9.1	13.6	0	12	0.02	0.30	0.76
CPT-112	166	0.40	-	-	-	-	-	-	0.40
CPT-113	129	0.81	14.8	4.0	0	11	0.01	0.27	1.09
CPT-114	160	0.96	-	-	-	-	-	-	0.96
CPT-115	162	1.07	-	-	-	-	-	-	1.07
CPT-116	125	0.58	7.6	10.9	0	11	0.01	0.27	0.87
CPT-117	152	1.38	-	-	-	-	-	-	1.38
CPT-118	124	0.45	6.1	19.5	0	14	0.03	0.35	0.82
CPT-119	152	1.06	-	-	-	-	-	-	1.06
CPT-120	140	1.12	-	-	-	-	-	-	1.12
CPT-121	124	0.39	6.0	14.5	0	9	0.02	0.22	0.63

TABLE 8-3 TOTAL POST-EARTHQUAKE SETTLEMENTS BASED ON CPT DATA – PC-3+ MOTION

ID	Total Depth (feet)	Estimated Settlement to Bottom of CPT (inches)	Penetrated Portion of ST1 (feet)	Portion of ST1 <i>not</i> Penetrated (feet)	Penetrated Portion of ST2 (feet)	Portion of ST2 <i>not</i> Penetrated (feet)	Additional Settlement of ST1 (inches)	Additional Settlement of ST2 (inches)	Estimated Total Settlement (inches)
CPT-122	153	1.21	-	-	-	-	-	-	1.21
CPT-123	130	0.65	14.7	4.2	0	13	0.01	0.32	0.98
CPT-124	122	0.55	12.5	8.6	0	11	0.01	0.27	0.83

Maximum Settlement	= 1.47 inches
Minimum Settlement	= 0.26 inches
Average Settlement	= 0.88 inches

C04

**TABLE 8-4 SUMMARY OF ESTIMATED POST-EARTHQUAKE SETTLEMENTS
 BASED ON BORINGS DUE TO 1886 CHARLESTON 50TH PERCENTILE MOTION**

Series No.	Boring ID	Estimated Settlement (inches)
1	BH-1	0.14
2	BH-4	0.00
3	BH-7	0.52
4	BH-8	0.00
5	BH-11	0.52
6	BH-12	0.02
7	BH-13	0.31
8	BH-14	0.03
9	BH-15	0.41
10	BH-16	0.37
11	BH-17	0.00
12	BH-18	0.48
13	BH-19	0.11
14	BH-20	0.78

TABLE 8-5 TOTAL POST-EARTHQUAKE SETTLEMENTS BASED ON CPT DATA – 1886 CHARLESTON 50TH PERCENTILE MOTION

ID	Total Depth (feet)	Estimated Settlement to Bottom of CPT (Inches)	Penetrated Portion of ST1 (feet)	Portion of ST1 not Penetrated (feet)	Penetrated Portion of ST2 (feet)	Portion of ST2 not Penetrated (feet)	Additional Settlement of ST1 (Inches)	Additional Settlement of ST2 (Inches)	Estimated Total Settlement (Inches)
CPT-4	135	1.12	-	-	-	-	-	-	1.12
CPT-7	114	0.82	8.3	12.7	0	9	0.06	0.39	1.27
CPT-8	140	1.56	-	-	-	-	-	-	1.56
CPT-9	126	1.45	-	-	-	-	-	-	1.45
CPT-13	166	1.15	-	-	-	-	-	-	1.15
CPT-14	142	1.75	-	-	-	-	-	-	1.75
CPT-18	120	0.89	13.2	6.8	0	8	0.03	0.34	1.27
CPT-21	139	1.23	8.2	4.8	0	12	0.02	0.51	1.77
CPT-22	153	1.56	14.2	0.0	0	3	0.00	0.12	1.68
CPT-23	124	0.99	16.5	3.5	0	8	0.02	0.34	1.35
CPT-27	128	1.55	17.8	0.0	0	7	0.00	0.30	1.85
CPT-28	150	1.22	-	-	-	-	-	-	1.22
CPT-29	118	0.85	13.6	7.4	0	13	0.04	0.56	1.44
CPT-40	113	0.61	11.7	11.3	0	13	0.06	0.56	1.23
CPT-44	118	0.46	7.3	10.7	0	10	0.05	0.43	0.94
CPT-45	142	1.13	-	-	-	-	-	-	1.13
CPT-46	147	1.17	-	-	-	-	-	-	1.17
CPT-47	116	0.34	6.9	12.1	0	10	0.06	0.43	0.83
CPT-48	111	0.76	6.3	12.7	0	11	0.06	0.47	1.29
CPT-49	123	0.48	4.5	13.5	0	10	0.07	0.43	0.98
CPT-50	134	0.67	8.7	8.3	0	10	0.04	0.43	1.14
CPT-51	139	1.15	11.2	7.8	0	13	0.04	0.56	1.75

TABLE 8-5 TOTAL POST-EARTHQUAKE SETTLEMENTS BASED ON CPT DATA – 1886 CHARLESTON 50TH
PERCENTILE MOTION

ID	Total Depth (feet)	Estimated Settlement to Bottom of CPT (inches)	Penetrated Portion of ST1 (feet)	Portion of ST1 not Penetrated (feet)	Penetrated Portion of ST2 (feet)	Portion of ST2 not Penetrated (feet)	Additional Settlement of ST1 (inches)	Additional Settlement of ST2 (inches)	Estimated Total Settlement (inches)
CPT-52	120	0.66	2.1	16.9	0	14	0.09	0.60	1.34
CPT-53	119	0.75	10.0	17.0	0	15	0.09	0.64	1.48
CPT-54	123	0.89	3.4	14.6	0	15	0.07	0.64	1.61
CPT-55	136	1.33	9.0	7.0	0	13	0.04	0.56	1.92
CPT-56	120	0.45	1.8	19.2	0	15	0.10	0.64	1.19
CPT-57	129	0.83	7.9	12.1	0	13	0.06	0.56	1.44
CPT-58	122	0.50	2.5	20.5	0	13	0.10	0.56	1.16
CPT-59	126	0.90	7.0	16.0	0	14	0.08	0.60	1.58
CPT-60	141	1.32	15.4	3.6	0	13	0.02	0.56	1.90
CPT-61	116	0.50	6.9	9.1	0	12	0.05	0.51	1.06
CPT-62	116	1.15	11.0	9.0	0	12	0.05	0.51	1.71
CPT-63	119	0.90	11.2	12.8	0	6	0.06	0.26	1.22
CPT-64	141	1.22	-	-	-	-	-	-	1.22
SCPT-65	151	1.44	-	-	-	-	-	-	1.44
SCPT-66	116	0.48	6.3	17.0	0	12	0.09	0.51	1.08
SCPT-67	150	1.15	-	-	-	-	-	-	1.15
SCPT-68	151	1.80	-	-	-	-	-	-	1.80
SCPT-69	154	1.54	-	-	-	-	-	-	1.54
SCPT-70	155	1.22	-	-	-	-	-	-	1.22
SCPT-71	152	0.84	-	-	-	-	-	-	0.84
SCPT-72	153	1.64	-	-	-	-	-	-	1.64
SCPT-73	152	2.08	-	-	-	-	-	-	2.08

TABLE 8-5 TOTAL POST-EARTHQUAKE SETTLEMENTS BASED ON CPT DATA – 1886 CHARLESTON 50TH PERCENTILE MOTION

ID	Total Depth (feet)	Estimated Settlement to Bottom of CPT (inches)	Penetrated Portion of ST1 (feet)	Portion of ST1 not Penetrated (feet)	Penetrated Portion of ST2 (feet)	Portion of ST2 not Penetrated (feet)	Additional Settlement of ST1 (inches)	Additional Settlement of ST2 (inches)	Estimated Total Settlement (inches)
SCPT-74	150	1.43	-	-	-	-	-	-	1.43
SCPT-75	145	0.66	-	-	-	-	-	-	0.66
SCPT-76	137	0.82	-	-	-	-	-	-	0.82
SCPT-77	147	0.88	-	-	-	-	-	-	0.88
SCPT-78A	141	1.51	-	-	-	-	-	-	1.51
SCPT-79	139	0.97	-	-	-	-	-	-	0.97
SCPT-80	147	1.22	-	-	-	-	-	-	1.22
SCPT-81	157	1.01	-	-	-	-	-	-	1.01
CPT-82	131	0.54	13.3	9.8	0	14	0.05	0.60	1.19
SCPT-83	158	1.50	-	-	-	-	-	-	1.50
SCPT-84	138	0.82	17.6	2.2	0	12	0.01	0.51	1.35
SCPT-85	165	1.23	-	-	-	-	-	-	1.23
SCPT-86	164	1.91	-	-	-	-	-	-	1.91
SCPT-87	132	0.57	8.4	12.4	0	11.2	0.06	0.48	1.11
SCPT-87A	163	1.29	-	-	-	-	-	-	1.29
SCPT-88	157	1.36	-	-	-	-	-	-	1.36
SCPT-89A	120	0.90	10.0	15.7	0	12	0.08	0.51	1.49
SCPT-90	126	0.66	9.2	10.6	0	10	0.05	0.43	1.14
CPT-91	116	0.30	13.9	3.9	0	11	0.02	0.47	0.79
CPT-92	105	0.58	6.8	16.3	0	10	0.08	0.43	1.09
CPT-93	138	0.95	-	-	-	-	-	-	0.95
SCPT-94	141	2.17	-	-	-	-	-	-	2.17

TABLE 8-5 TOTAL POST-EARTHQUAKE SETTLEMENTS BASED ON CPT DATA – 1886 CHARLESTON 50TH PERCENTILE MOTION

ID	Total Depth (feet)	Estimated Settlement to Bottom of CPT (inches)	Penetrated Portion of ST1 (feet)	Portion of ST1 not Penetrated (feet)	Penetrated Portion of ST2 (feet)	Portion of ST2 not Penetrated (feet)	Additional Settlement of ST1 (inches)	Additional Settlement of ST2 (inches)	Estimated Total Settlement (inches)
CPT-95	121	1.33	17.2	5.0	0	8	0.03	0.34	1.70
SCPT-96	129	0.92	10.9	9.5	0	12	0.05	0.51	1.48
SCPT-97	151	1.46	-	-	-	-	-	-	1.46
CPT-98	147	1.63	-	-	-	-	-	-	1.63
CPT-99	158	1.50	-	-	-	-	-	-	1.50
CPT-100	160	1.54	-	-	-	-	-	-	1.54
CPT-101	123	1.79	17.6	2.7	-	8	0.01	0.34	2.14
CPT-102	160	1.71	-	-	-	-	-	-	1.71
CPT-103	150	1.12	-	-	-	-	-	-	1.12
CPT-104	153	1.67	-	-	-	-	-	-	1.67
CPT-105	135	0.59	12.2	9.0	0	15	0.05	0.64	1.28
CPT-106	164	1.43	-	-	-	-	-	-	1.43
CPT-107	163	1.38	-	-	-	-	-	-	1.38
CPT-108	161	1.52	-	-	-	-	-	-	1.52
CPT-109	153	1.55	-	-	-	-	-	-	1.55
CPT-110	149	0.61	-	-	-	-	-	-	0.61
CPT-111	125	0.64	9.1	13.6	0	12	0.07	0.51	1.22
CPT-112	166	0.75	-	-	-	-	-	-	0.75
CPT-113	129	1.02	14.8	4.0	0	11	0.02	0.47	1.51
CPT-114	160	1.35	-	-	-	-	-	-	1.35
CPT-115	162	1.61	-	-	-	-	-	-	1.61
CPT-116	125	0.69	7.6	10.9	0	11	0.05	0.47	1.22

TABLE 8-5 TOTAL POST-EARTHQUAKE SETTLEMENTS BASED ON CPT DATA – 1886 CHARLESTON 50TH PERCENTILE MOTION

ID	Total Depth (feet)	Estimated Settlement to Bottom of CPT (inches)	Penetrated Portion of ST1 (feet)	Portion of ST1 <i>not</i> Penetrated (feet)	Penetrated Portion of ST2 (feet)	Portion of ST2 <i>not</i> Penetrated (feet)	Additional Settlement of ST1 (inches)	Additional Settlement of ST2 (inches)	Estimated Total Settlement (inches)
CPT-117	152	2.22	-	-	-	-	-	-	2.22
CPT-118	124	0.56	6.1	19.5	0	14	0.10	0.60	1.25
CPT-119	152	1.63	-	-	-	-	-	-	1.63
CPT-120	140	1.85	-	-	-	-	-	-	1.85
CPT-121	124	0.50	6.0	14.5	0	9	0.07	0.39	0.96
CPT-122	153	1.86	-	-	-	-	-	-	1.86
CPT-123	130	0.87	14.7	4.2	0	13	0.02	0.56	1.45

Maximum Settlement	= 1.47 inches
Minimum Settlement	= 0.26 inches
Average Settlement	= 0.88 inches

**TABLE 8-6 SUMMARY OF ESTIMATED POST-EARTHQUAKE SETTLEMENTS -
1886 CHARLESTON 50TH PERCENTILE MOTION**

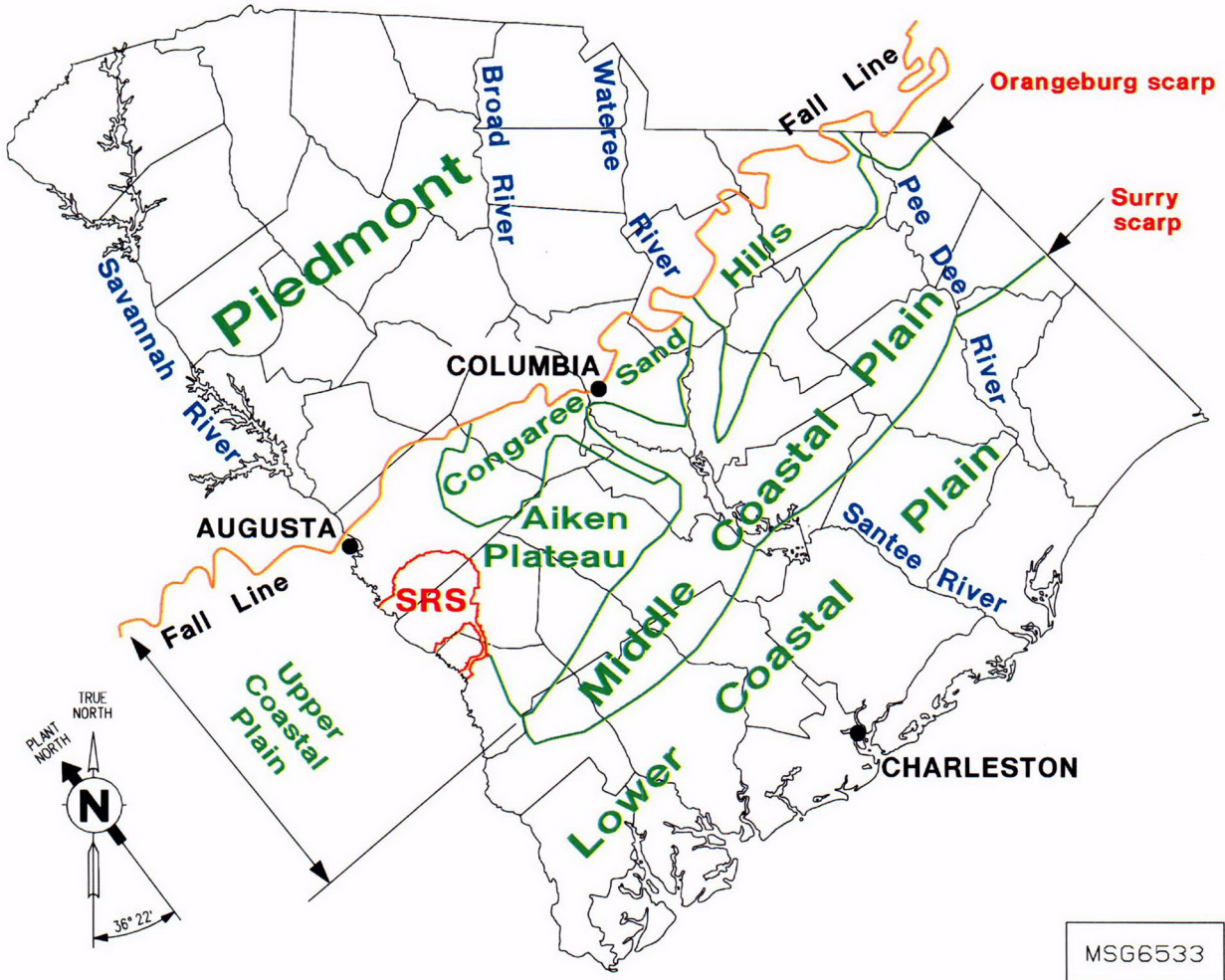
ID	Estimated Post-earthquake Settlement	
	Individual Profiles (in.)	Generalized Profile (in.)
SCPT-67	1.29	1.13
SCPT-68	1.98	1.80
SCPT-69	1.71	1.51
SCPT-70	0.78	1.15
SCPT-71	0.62	0.89
SCPT-72	1.29	1.64
SCPT-73	1.67	2.11
SCPT-74	1.57	1.31
SCPT-75	0.65	0.54
SCPT-76	0.95	0.73
SCPT-77	0.56	0.84
SCPT-78A	1.66	1.39
SCPT-81	0.24	0.94
SCPT-83	1.03	1.60
SCPT-85	0.72	1.18
SCPT-86	1.83	2.08
SCPT-87A	1.36	1.24
SCPT-97	1.67	1.43
BH-14	0.00	0.05
BH-16	0.51	0.45
BH-20	0.53	0.74
Average	1.08	1.18

TABLE 8-7 SUMMARY OF ESTIMATED TOTAL AND DIFFERENTIAL SETTLEMENTS OF THE MFFF BUILDING

Settlement (Inches)	Minimum	Maximum	Differential	Refer to Figure
Static	2.7	3.5	0.8	Fig. 7-6
Post-earthquake – 1886 Charleston 50 th Percentile Motion*	0.6 @ CPT-110	2.2 @ CPT-117	1.8	Fig. 8-133
Secondary Consolidation	0.5	0.5	0.0	N/A
Soft Zones: Mohr-Coulomb Model with Collapse of Overlying “Arches”	0	2.6	2.6	Fig. 7-13
Soft Zones: Cam-Clay Model with Underconsolidated Soft Zones (OCR = 0.7), No Structures	0	0.2	0.2	N/A

* Post-earthquake settlements at depth. The presence of liquefaction-resistant layers above the soil layers where these settlements may occur will smooth out variations throughout the area, so that resulting surface manifestation of these settlements will have smaller differentials. Using the FLAC results as a guideline to smooth out the calculated post-earthquake settlements as they pass to the surface of the site through the overlying liquefaction-resistant layers, the order of magnitude of the differential settlement of the combined static + post-earthquake settlement is about 1”, resulting in a maximum angular distortion of approximately 0.0001ℓ.

FIGURES



WSRC (2000a)

FIGURE 3-1 PHYSIOGRAPHY OF THE SRS AREA

COB

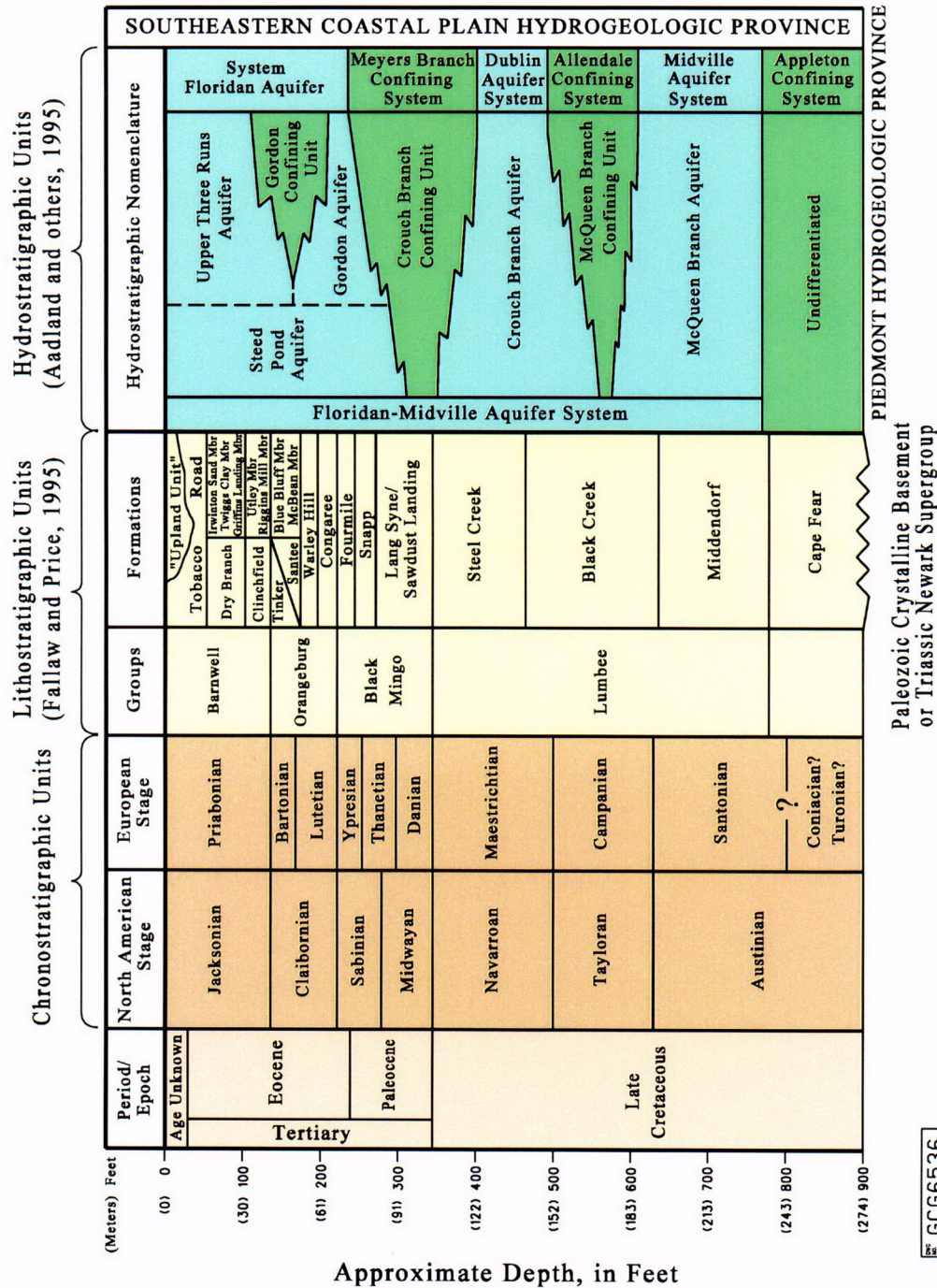
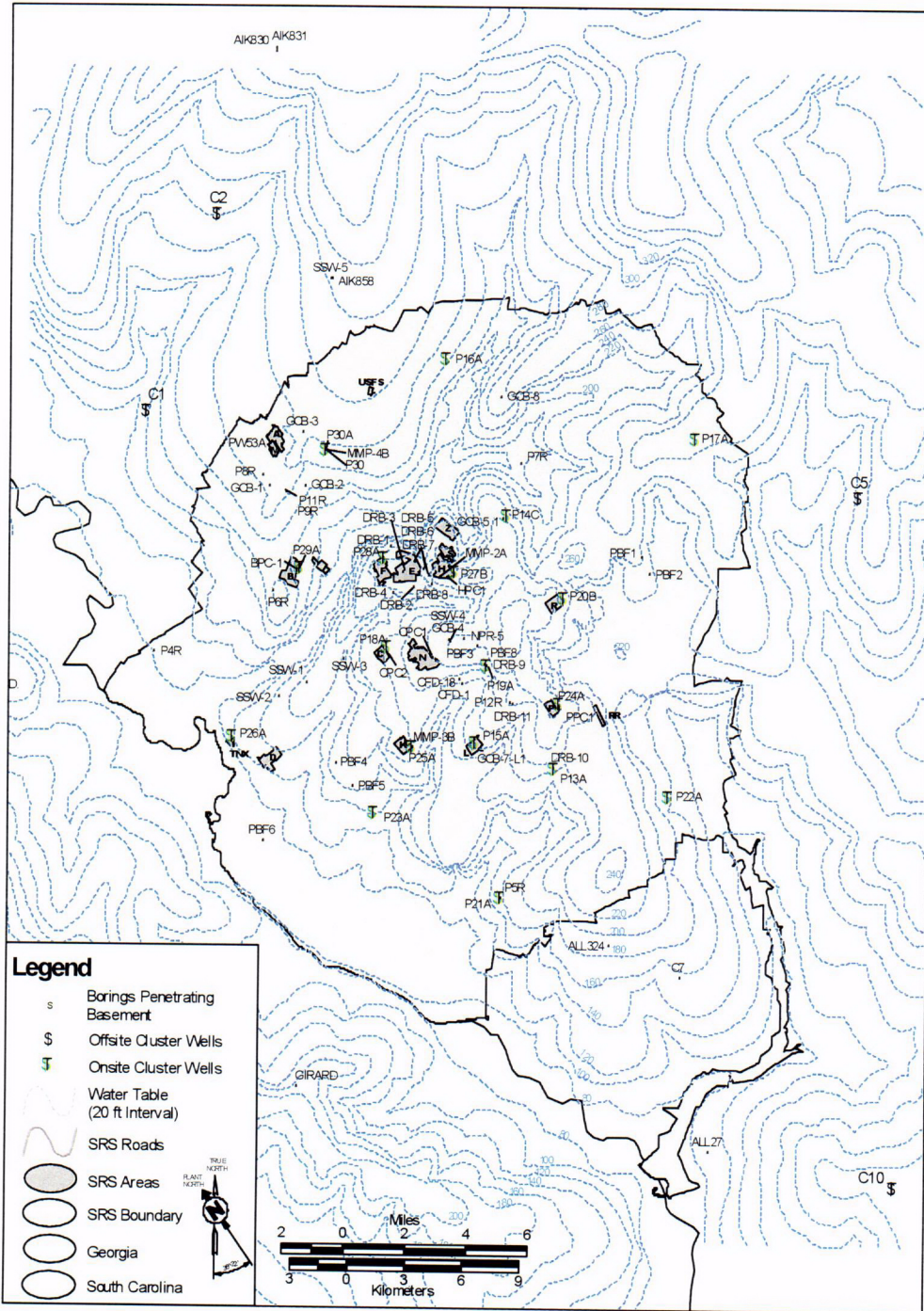


FIGURE 3-2 COMPARISON OF CHRONOSTRATIGRAPHIC, LITHOSTRATIGRAPHIC, AND HYDROSTRATIGRAPHIC UNITS IN THE SRS REGION

CO9



WSRC (2000a)

FIGURE 3-3 LOCATION OF TYPE AND REFERENCE WELLS FOR GEOLOGIC UNITS AT SRS

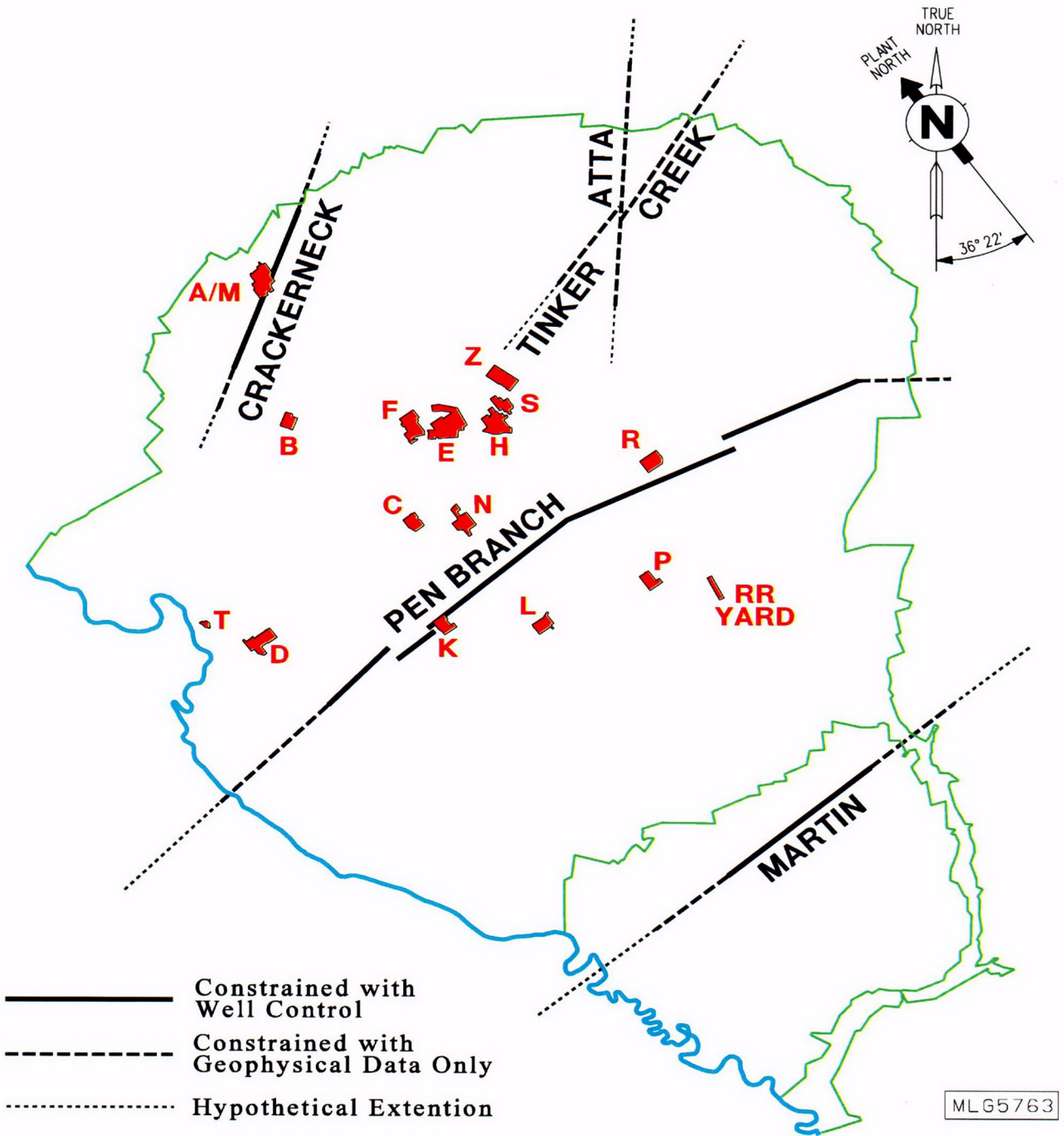
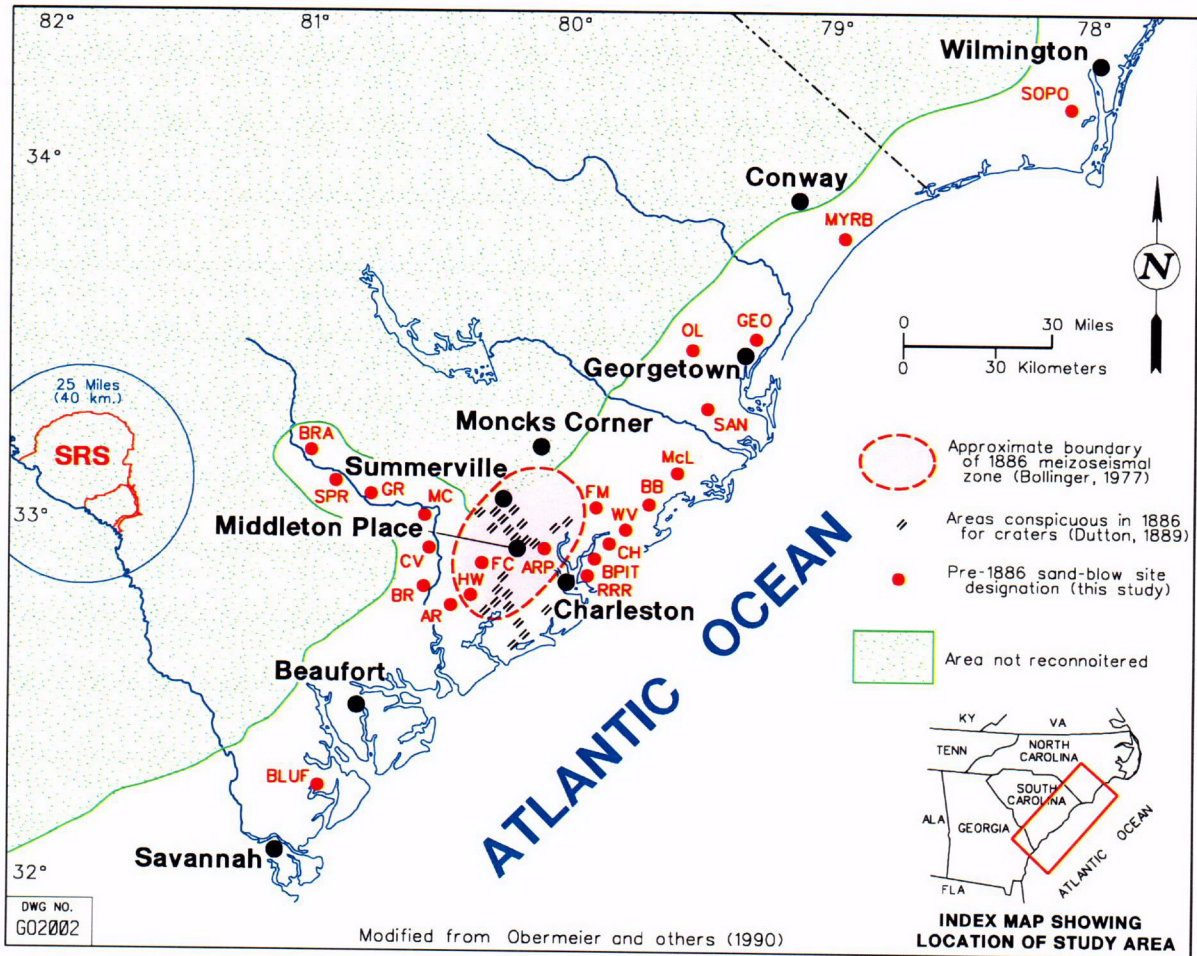


FIGURE 3-4 REGIONAL SCALE FAULTS FOR SRS AND VICINITY



WSRC 2000a

FIGURE 3-5 LOCATION OF SAND BLOWS

Comparison of DOE Revised PC-3 Design Basis Spectrum (Gutierrez, 1999) to PC-3 Design Spectrum (WSRC, 1997)

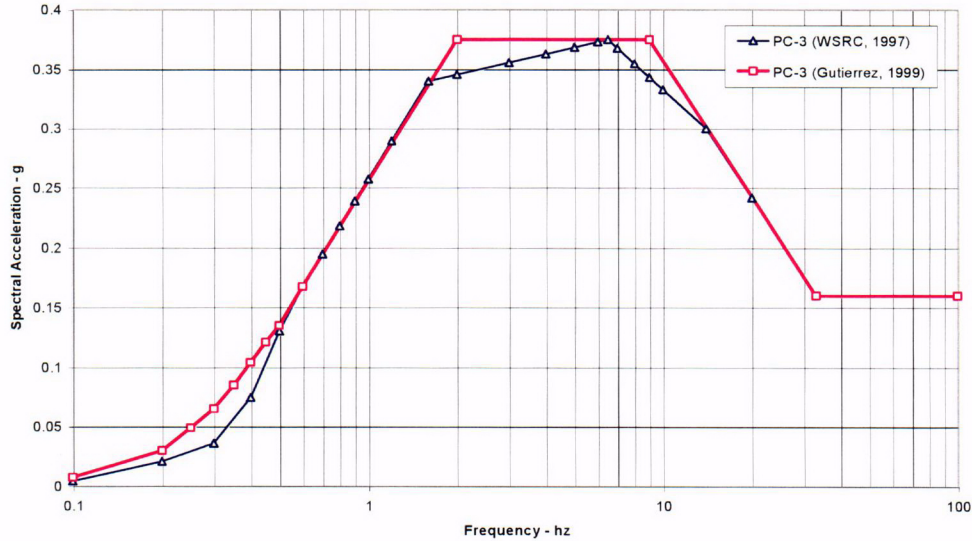
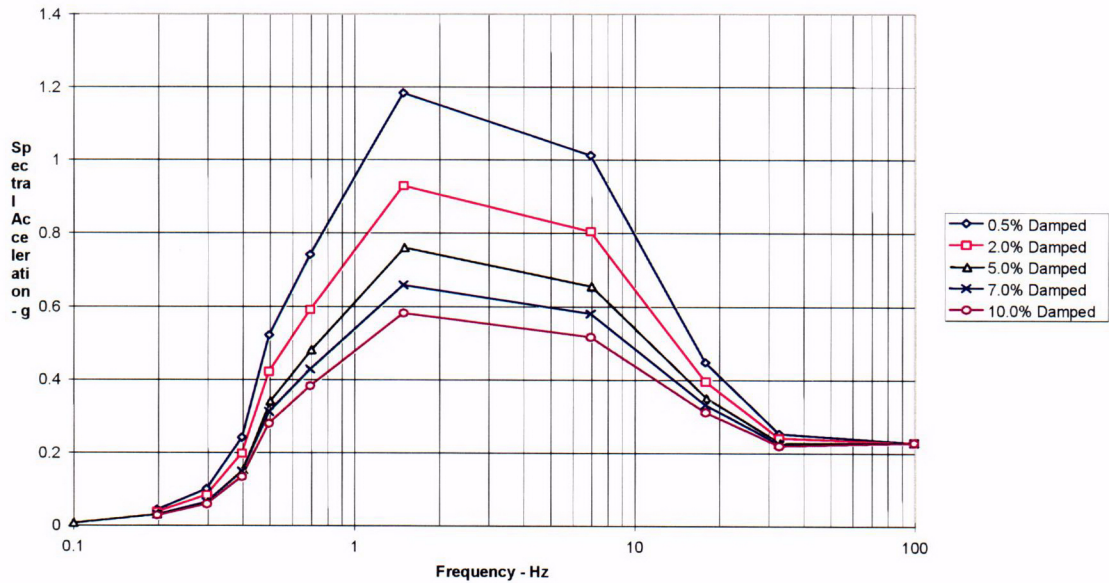


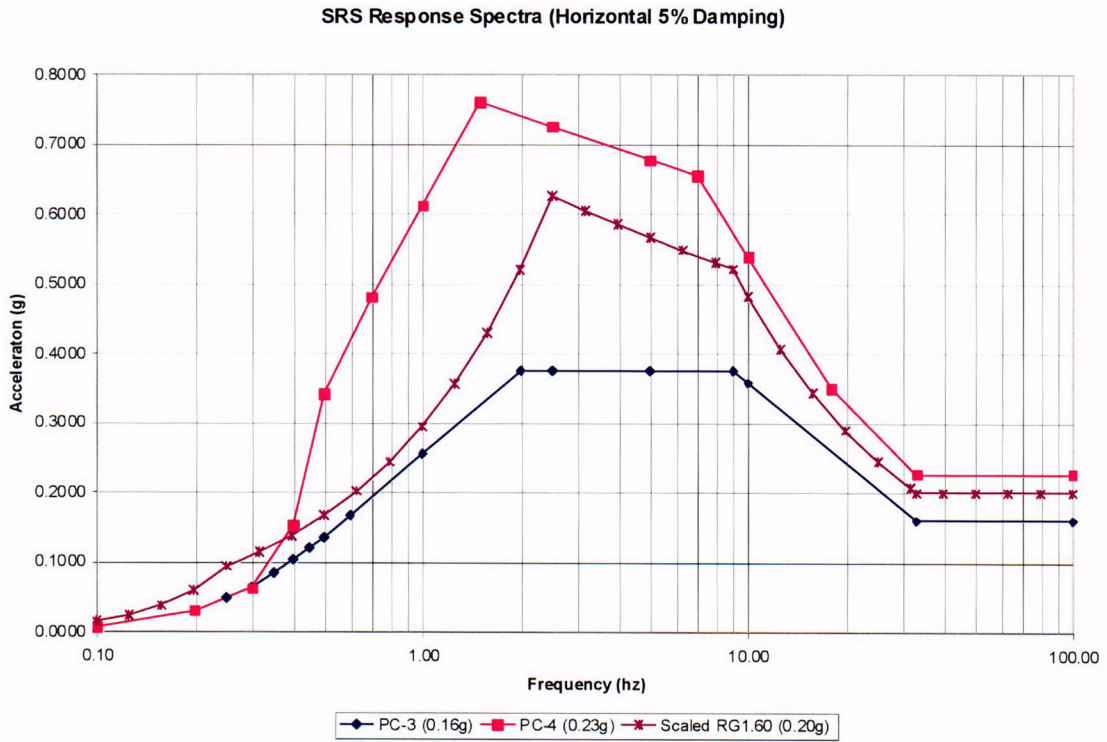
FIGURE 3-6 SRS PC-3 DESIGN BASIS SURFACE RESPONSE SPECTRUM (DAMPED 5%) – REVISED 1999

PC-4 Response Spectra Envelopes



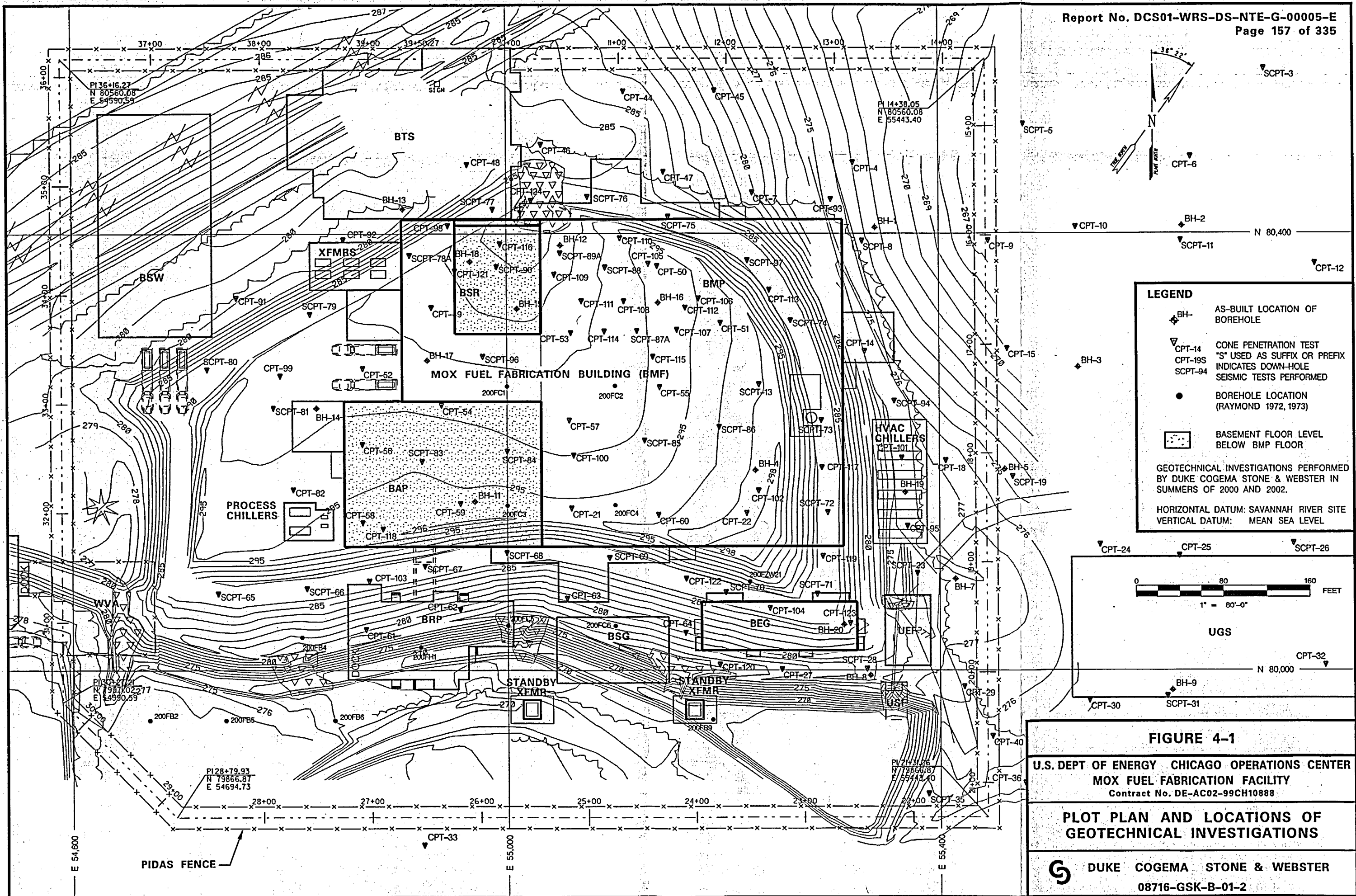
WSRC (1997)

FIGURE 3-7 PC-4 SURFACE RESPONSE SPECTRA ENVELOPES



DCS (2000z)

FIGURE 3-8 COMPARISON OF 0.2G REGULATORY GUIDE 1.60 SPECTRUM TO PC-3 AND PC-4 SURFACE RESPONSE SPECTRA



LEGEND

- AS-BUILT LOCATION OF BOREHOLE
- CONE PENETRATION TEST
"S" USED AS SUFFIX OR PREFIX
INDICATES DOWN-HOLE
SEISMIC TESTS PERFORMED
- BOREHOLE LOCATION
(RAYMOND 1972, 1973)
- BASEMENT FLOOR LEVEL
BELOW BMP FLOOR

GEOTECHNICAL INVESTIGATIONS PERFORMED
BY DUKE COGEMA STONE & WEBSTER IN
SUMMERS OF 2000 AND 2002.

HORIZONTAL DATUM: SAVANNAH RIVER SITE
VERTICAL DATUM: MEAN SEA LEVEL

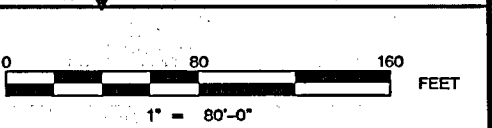
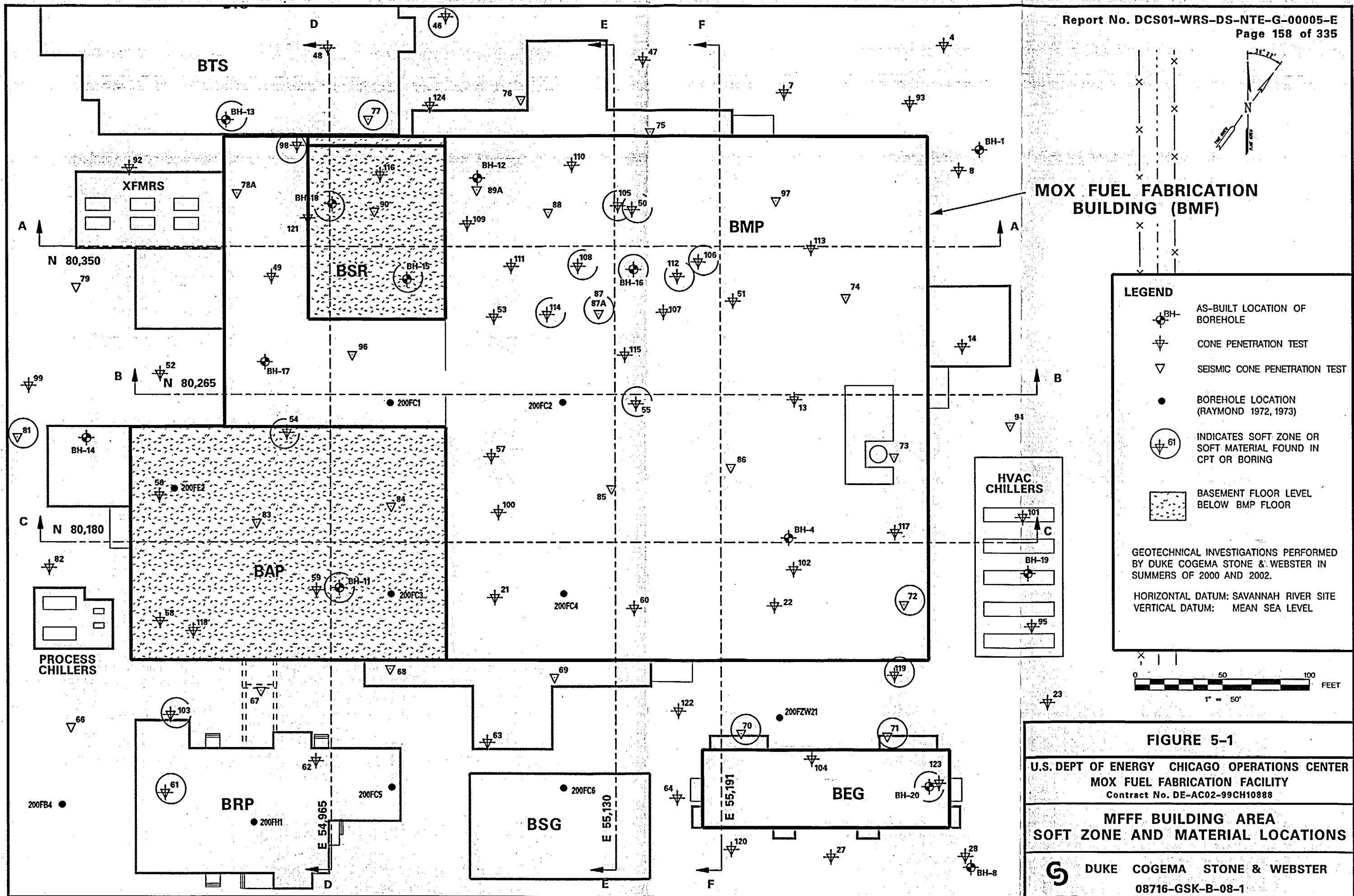


FIGURE 4-1

**U.S. DEPT OF ENERGY CHICAGO OPERATIONS CENTER
MOX FUEL FABRICATION FACILITY**
Contract No. DE-AC02-99CH10888

**PLOT PLAN AND LOCATIONS OF
GEOTECHNICAL INVESTIGATIONS**

DUKE COGEMA STONE & WEBSTER
08716-GSK-B-01-2



LEGEND

- AS-BUILT LOCATION OF BOREHOLE
- CONE PENETRATION TEST
- SEISMIC CONE PENETRATION TEST
- BOREHOLE LOCATION (RAYMOND 1972, 1973)
- INDICATES SOFT ZONE OR SOFT MATERIAL FOUND IN CPT OR BORING
- BASEMENT FLOOR LEVEL BELOW BMP FLOOR

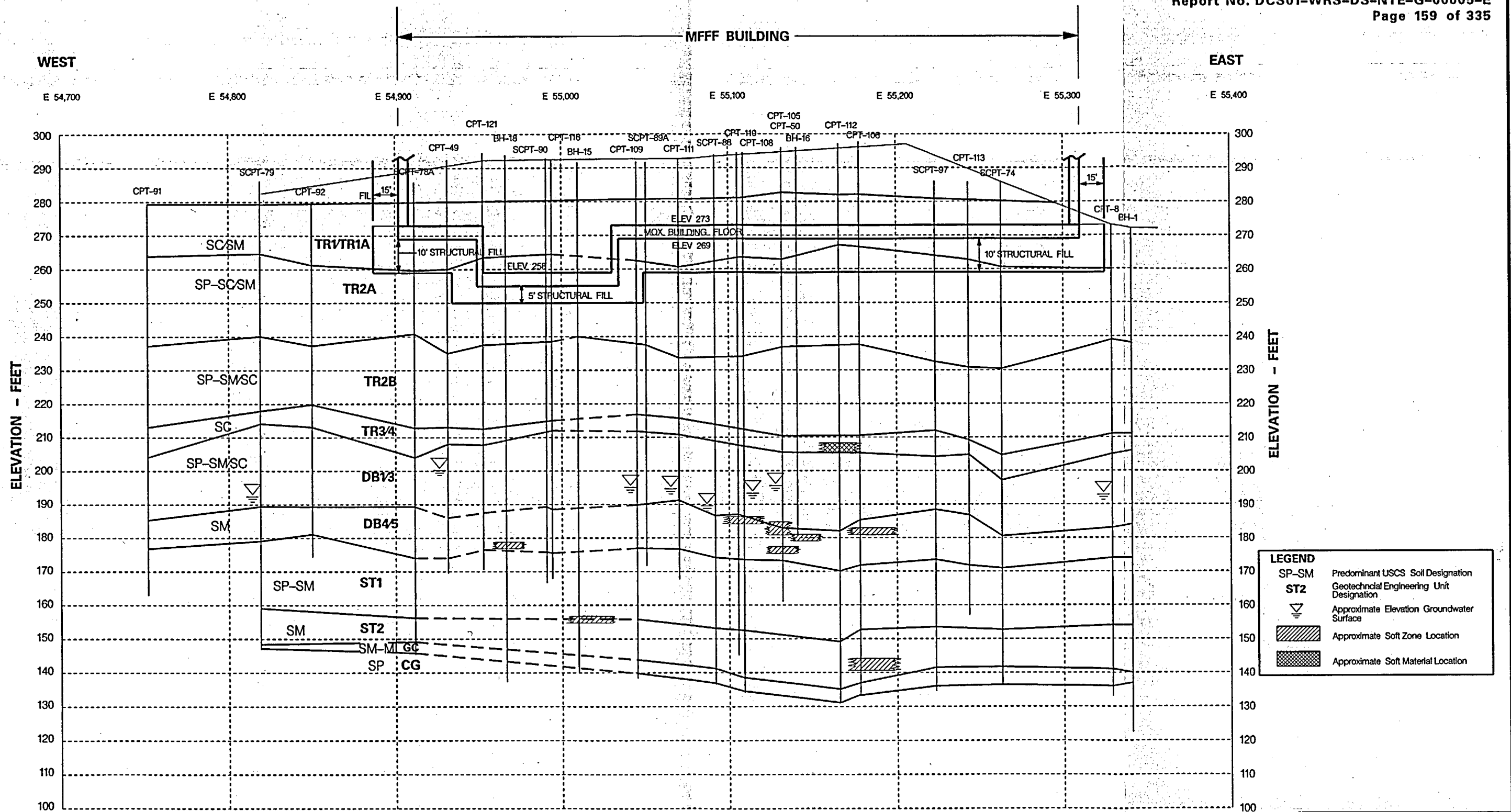
GEOTECHNICAL INVESTIGATIONS PERFORMED BY DUKE COGEMA STONE & WEBSTER IN SUMMERS OF 2000 AND 2002.

HORIZONTAL DATUM: SAVANNAH RIVER SITE
VERTICAL DATUM: MEAN SEA LEVEL

FIGURE 5-1
U.S. DEPT OF ENERGY CHICAGO OPERATIONS CENTER
MOX FUEL FABRICATION FACILITY
Contract No. DE-AC02-99CH10888

**MFF BUILDING AREA
SOFT ZONE AND MATERIAL LOCATIONS**

DUKE COGEMA STONE & WEBSTER
08716-GSK-B-08-1



EAST - WEST SECTION AT N 80,350

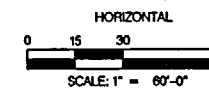
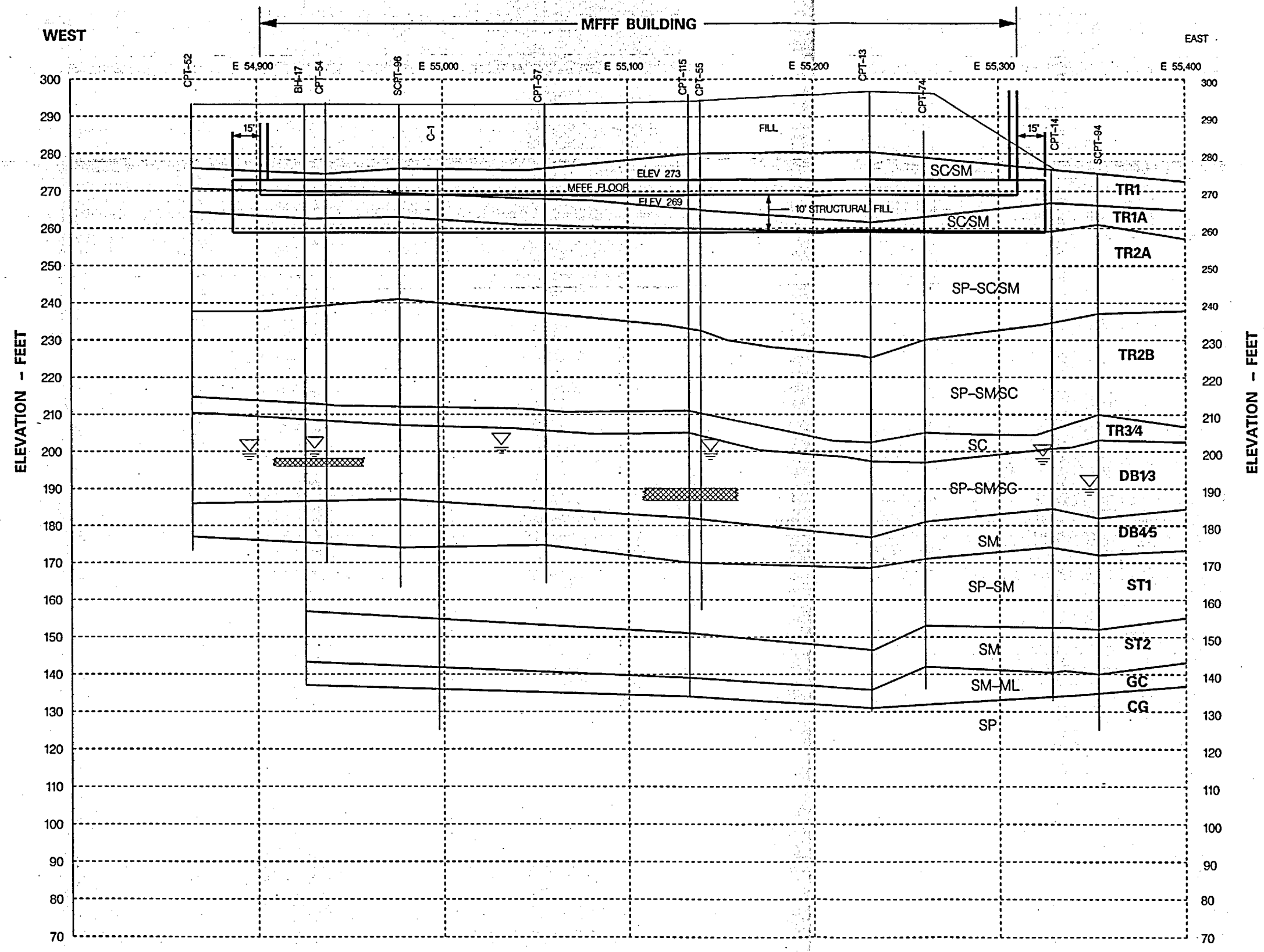


FIGURE 5-2

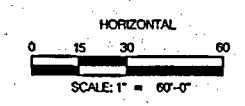
U.S. DEPT OF ENERGY CHICAGO OPERATIONS CENTER
MOX FUEL FABRICATION FACILITY
Contract No. DE-AC02-99CH10888

MFFF BUILDING AREA
GEOTECHNICAL SECTION A

 DUKE COGEMA STONE & WEBSTER
08716-GSK-B-09-1



EAST - WEST SECTION AT N 80,265



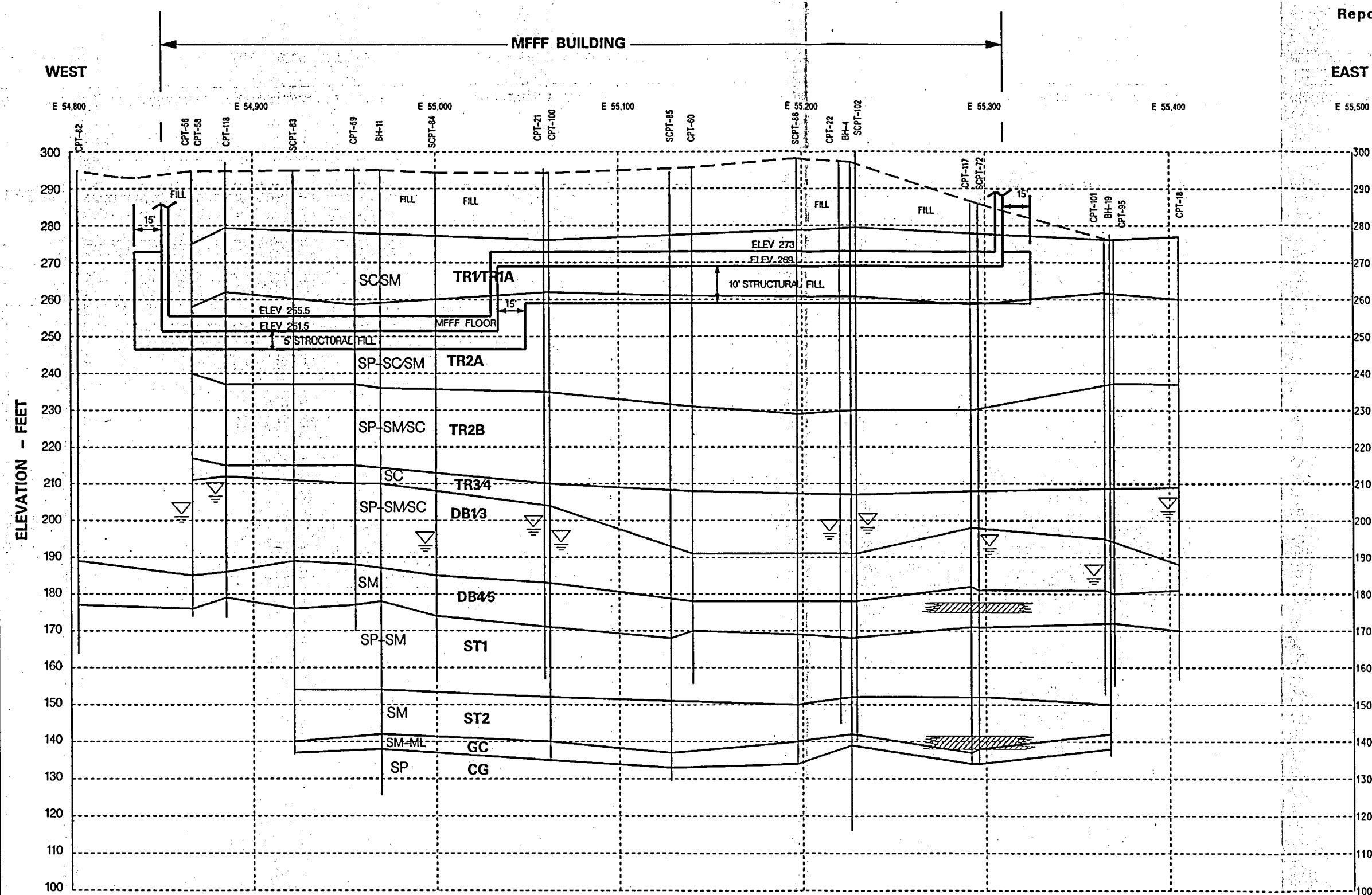
LEGEND	
SP-SM	Predominant USCS Soil Designation
ST2	Geotechnical Engineering Unit Designation
	Approximate Elevation Groundwater Surface
	Approximate Soft Zone Location
	Approximate Soft Material Location

FIGURE 5-3

U.S. DEPT OF ENERGY CHICAGO OPERATIONS CENTER
MOX FUEL FABRICATION FACILITY
Contract No. DE-AC02-99CH10888

**MFFF BUILDING AREA
GEOTECHNICAL SECTION B**

DUKE COGEMA STONE & WEBSTER
08716-GSK-B-10-1



LEGEND

- SP-SM Predominant USCS Soil Designation
- ST2 Geotechnical Engineering Unit Designation
- Approximate Elevation Groundwater Surface
- Approximate Soft Zone Location
- Approximate Soft Material Location

EAST - WEST SECTION AT N 80,180

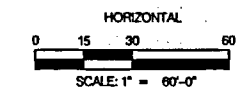
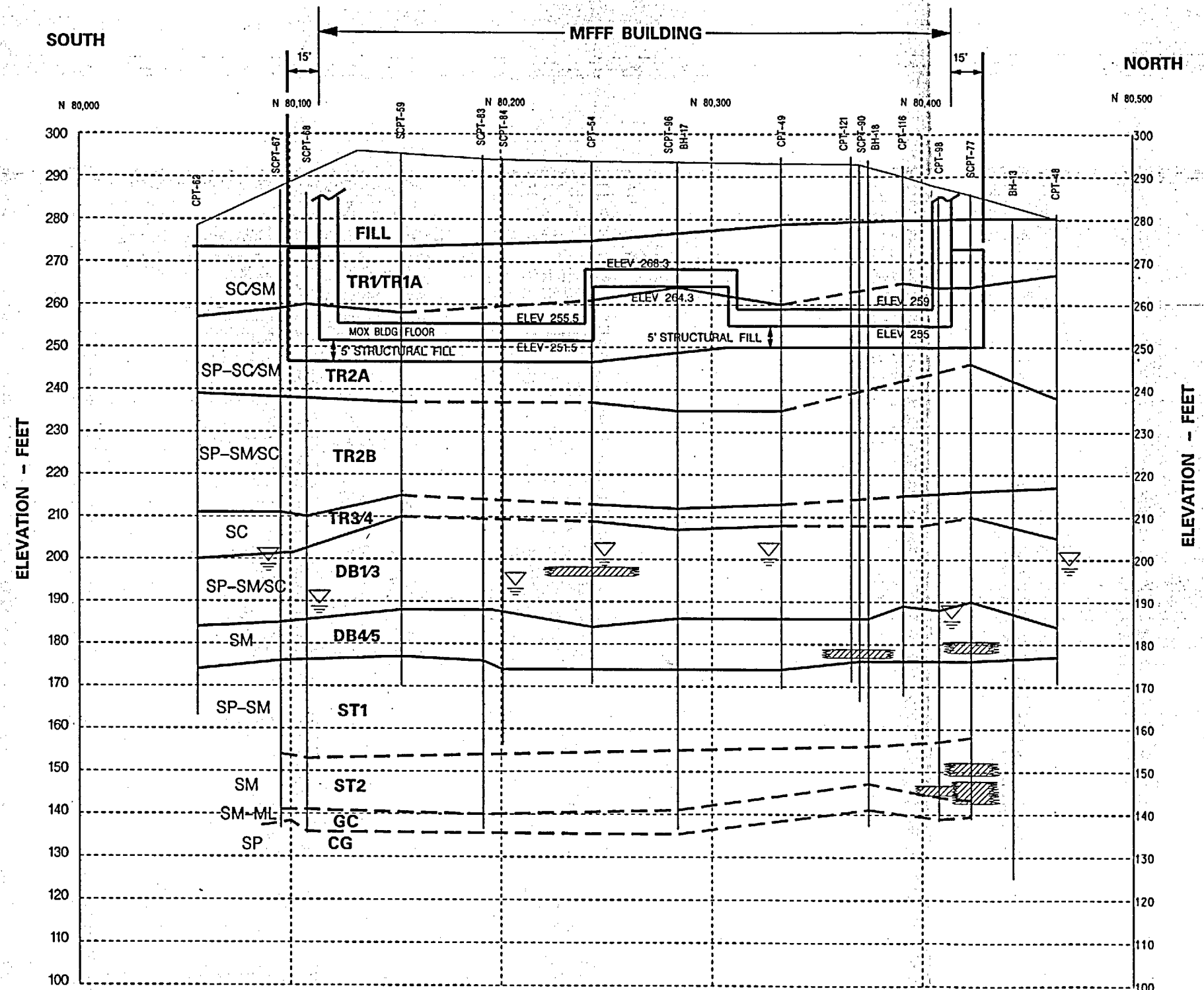


FIGURE 5-4

U.S. DEPT OF ENERGY CHICAGO OPERATIONS CENTER
MOX FUEL FABRICATION FACILITY
Contract No. DE-AC02-99CH10888

**MFFF BUILDING AREA
GEOTECHNICAL SECTION C**

DUKE COGEMA STONE & WEBSTER
08716-GSK-B-11-1



LEGEND	
SP-SM	Predominant USCS Soil Designation
ST2	Geotechnical Engineering Unit Designation
	Approximate Elevation Groundwater Surface
	Approximate Soft Zone Location
	Approximate Soft Material Location

NORTH - SOUTH SECTION AT E 54,965

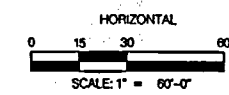
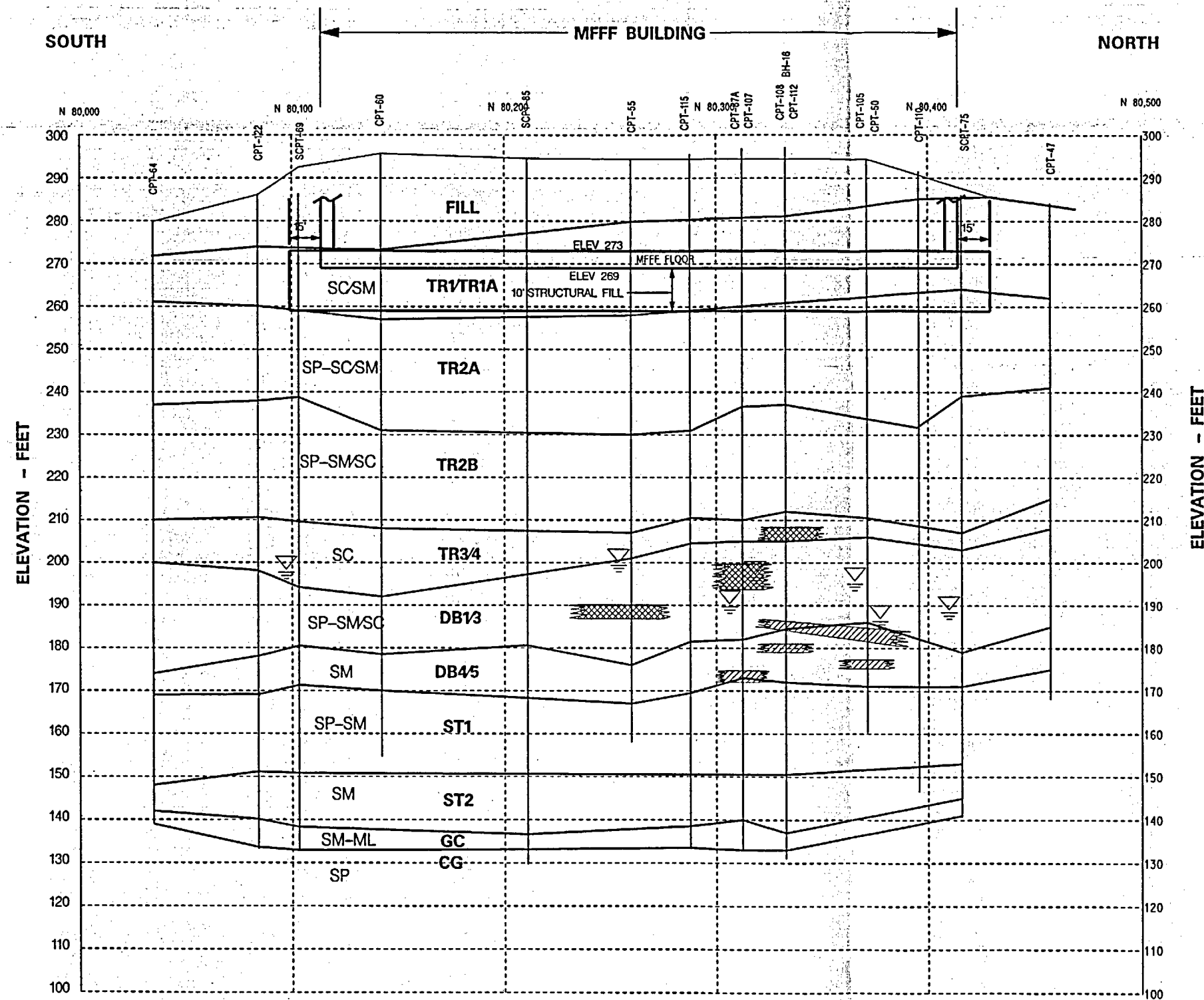


FIGURE 5-5

U.S. DEPT OF ENERGY CHICAGO OPERATIONS CENTER
 MOX FUEL FABRICATION FACILITY
 Contract No. DE-AC02-99CH10888

**MFFF BUILDING AREA
 GEOTECHNICAL SECTION D**

DUKE COGEMA STONE & WEBSTER
 08716-GSK-B-12-1



NORTH - SOUTH SECTION AT E 55,130

LEGEND	
SP-SM	Predominant USCS Soil Designation
ST2	Geotechnical Engineering Unit Designation
	Approximate Elevation Groundwater Surface
	Approximate Soft Zone Location
	Approximate Soft Material Location

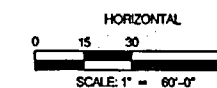
FIGURE 5-6

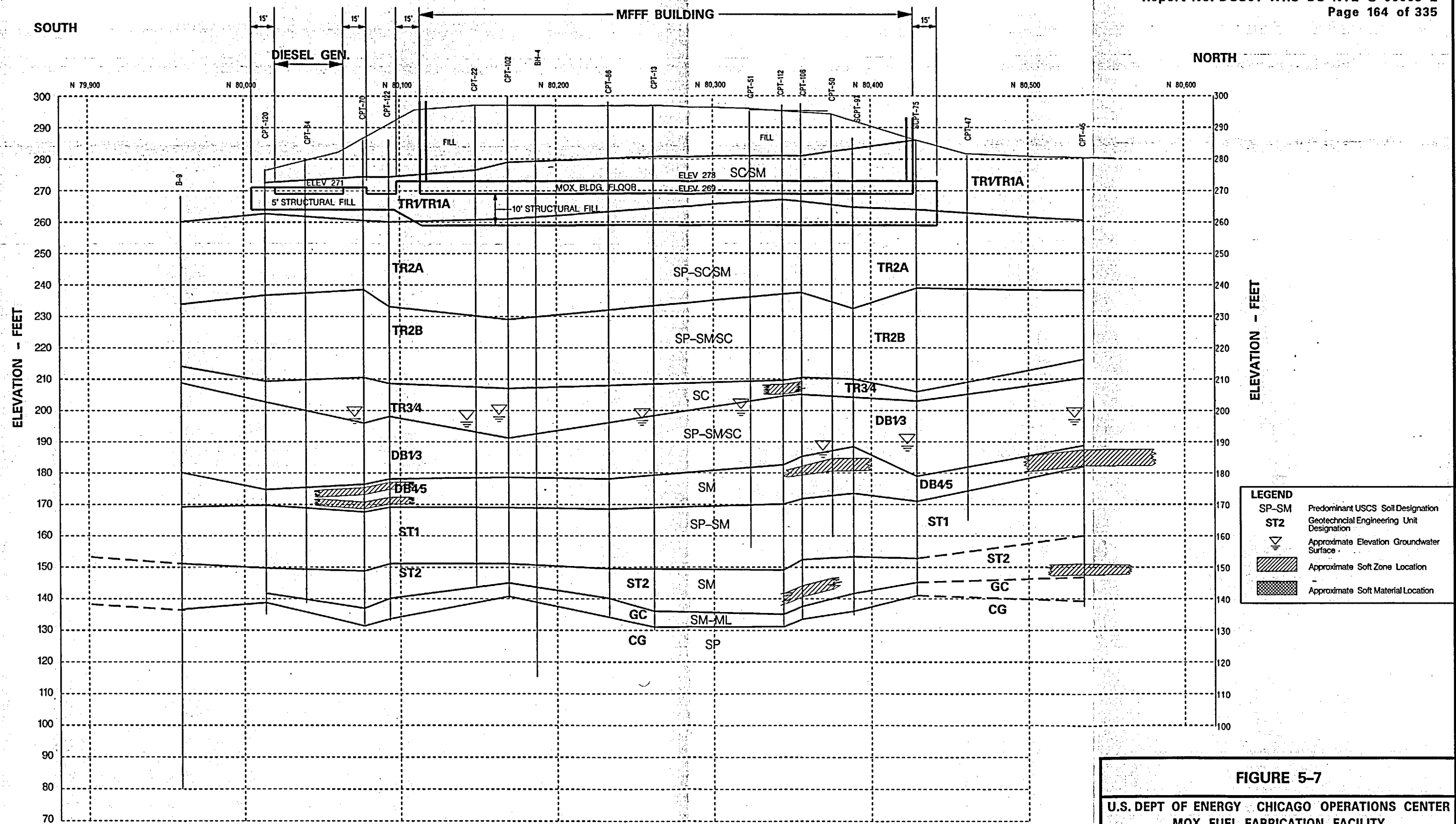
U.S. DEPT OF ENERGY CHICAGO OPERATIONS CENTER
 MOX FUEL FABRICATION FACILITY
 Contract No. DE-AC02-99CH10888

MFFF BUILDING AREA
 GEOTECHNICAL SECTION E



DUKE COGEMA STONE & WEBSTER
 08716-GSK-B-13-1





NORTH - SOUTH SECTION AT N 55,191

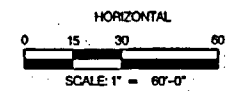


FIGURE 5-7

U.S. DEPT OF ENERGY CHICAGO OPERATIONS CENTER
MOX FUEL FABRICATION FACILITY
Contract No. DE-AC02-99CH10888

**MFFF BUILDING AREA
GEOTECHNICAL SECTION F**


DUKE COGEMA STONE & WEBSTER
08716-GSK-B-28-1